Diplomarbeit

Temporal and spatial localisation of Matrix Metalloproteinase 12 positive trophoblast cells in the development of the human placenta.

eingereicht von

Christian Peter Eyth

Geb. Dat.: 16.01.1985

zur Erlangung des akademischen Grades

Doktor der gesamten Heilkunde
(Dr. med. univ.)

an der

Medizinischen Universität Graz

ausgeführt am

Zentrum für Molekulare Medizin
Institut für Pathophysiologie und Immunologie,

unter der Anleitung von

Univ. Ass. Mag. Dr. Nassim Ghaffari Tabrizi-Wizsy
Sen. Scientist Priv.-Doz. Mag. Dr. Adelheid Kresse

Graz, am 15. September 2012 Christian P. Eyth

Eidesstattliche Erklärung

Ich erkläre ehrenwörtlich, dass ich die vorliegende Arbeit selbstständig und ohne fremde Hilfe verfasst habe, andere als die angegebenen Quellen nicht verwendet habe und die den benutzten Quellen wörtlich oder inhaltlich entnommenen Stellen als solche kenntlich gemacht habe.

Graz, am 15. September 2012 *Christian P. Eyth*

Declaration of Commitment to the Standards of Good Scientific Practice of the Medical University of Graz

As a researcher or co-worker in the area of research, I
Name: ***Christian Peter Eyth***
Institute: ***Institute for Pathophysiology and Immunology***
commit myself to adhering to the Standards of Good Scientific Practice valid at the time of my research related activities at the University.

Graz, 15th of September 2012 *Christian P. Eyth*

ACKNOWLEDGEMENTS

To write this diploma thesis would not have been possible without the unfailing help of the kind people around me. To only some of whom it is possible to give my particular mention here.

First of all, I would like to express my earnest thankfulness to my principal supervisor ***Mag. Dr. Nassim Ghaffari Tabrizi-Wizsy***, who invariably believed in my work, giving me invaluable support and guidance, encouraging me when I harboured doubts and always restored the enjoyment of my work.

Furthermore I am truly indebted and grateful to ***B. Sc. Carmen Tam-Amersdorfer*** who not only taught and inducted me into the mysteries of immunohistochemistry and in-situ hybridization, but also incessantly pushed me forward to bring out the best of me, striving for perfection in every single aspect of my work. Additionally I would like to thank ***PD Mag. Dr. Adelheid Kresse*** for good advice and her constructive criticism.

Another vital component of the success of my thesis was the excellent infrastructure and working atmosphere provided by the head of the institute, ***Prof. Dr. Anton Sadjak***, who always took time to promote my progression and set example of an efficient but familiarly style of leadership. This atmosphere also spread to ***The Team*** of the institute, which quickly affiliated me warm-hearted and ever were there on hand with help and advice if needed.

I also owe special thanks to my dear friend Michael who spent much time to review my drafts and gave me precious constructive criticism.

But at long last, I would particularly like to thank Victoria, my life companion, as well as my family, whose unequivocal and wholehearted support I always had. From an early age on, my parents encouraged me to stay inquisitive and to work always hard for my dreams. Victoria, the centre of my life, backed me up when I had to go through all the labours of the last years, keeping my motivation high, sustaining me to finish my studies at all times.

ZUSAMMENFASSUNG

Einleitung: Betrachtet man die Entwicklung der menschlichen Plazenta so ist die große Ähnlichkeit zum invasiven Verhalten maligner Tumore augenscheinlich. Im Gegensatz zum Tumor verfügt sie jedoch über ein Regulationsprogramm welches eine differenzierte Kontrolle des nahezu unbegrenzten invasiven Potentials ermöglicht und sie somit als Modell für die Tumorinvasion zunehmend in den Fokus der Wissenschaft rückt. Matrix metalloproteinasen (MMPs), zu deren Familie auch die Macrophagenelastase (MMP-12) gehört, scheinen bedeutsam für Invasion und Umbau maternalen Spiralarterien im Rahmen der Plazentaentwicklung, sowie für Wachstum, Invasion, Metastasierung und Angiogenese maligner Tumoren zu sein. Inhalt dieser Arbeit ist die Untersuchung räumlicher und zeitlicher Verteilungsmuster der MMP-12-Expression.

Material & Methoden: Vorversuche basierend auf U95A GeneChip Microarrays zeigten eine massive Überexpression in isolierten Trophoblasten des ersten Trimenons (FT), verglichen mit jenen des Geburtstermins. Mittels radioaktiver und nicht-radioaktiver In-situ Hybridisierung, sowie doppel-label Fluoreszenz-Immunhistochemie wurde der Nachweis auf mRNA- und Proteinebene im Gewebe geführt. Antikörper gegen MMP-12, HLA-G, CK-7, CD34 und CD68, sowie statistische Untersuchungen und computer-assistierte Expressionsdichtemessungen wurden zur qualitativen und quantitativen Analyse räumlicher und zeitlicher Verteilungsmuster eingesetzt.

Ergebnisse: Wir konnten nachweisen, dass die MMP-12-Expression sowohl auf mRNA- als auch auf Protein-Ebene in einer Subpopulation extravillöser, HLA-G-positiver Cytotrophoblasten stattfindet und einen Rückgang der mittleren Expressionsdichte von 0,38 und 0,35 im frühen und mittleren FT verglichen mit 0,23 im späten FT aufweist. Es konnte für plazentare Riesenzellen sowie, im Gegensatz zu vorangegangenen Publikationen, für villöse Cytotrophoblasten keine Expression nachgewiesen werden. Hohe Signaldichten fanden sich im Weiteren in Drüsen und Gefäßen der Dezidua, wobei letztere ab der 6. Schwangerschaftswoche zusätzlich ein sogenanntes *trophoblast plugging* aufwiesen.

Schlussfolgerungen: Die von uns angeführten Daten demonstrieren die deckungsgleiche Expression von MMP-12 auf mRNA- sowie Protein-Ebene und zeigen eine Abnahme der Dichte gegen Ende des ersten Trimenons. Als Grundlage für weiterführende funktionelle Assays versprechen diese Daten zukünftig tiefere Einblicke in die Mechanismen der Trophoblasteninvasion sowie der Entwicklung der menschlichen Plazenta.

ABSTRACT

Introduction: The physiological development of the human placenta shares close similarities to the invasive behaviour of a progressing malignant tumour. In contrast to the tumour, the placenta is under control of its almost unlimited invasive potential by a strict regulation program. Human placentation as a highly interesting model for controlled invasion is therefore in the focus of research, unveiling a plethora of factors acting pro-invasive as the versatile family of matrixins. Macrophage elastase (MMP-12), which was recently described in the placenta is probably involved in spiral artery remodelling, but shows also a broad range of features regarding progression, invasion, metastasis and angiogenesis in malignant tumours. The spatial and temporal localisation of this particular member is the content of this thesis.

Material & Methods: Previous data obtained from an U95A GeneChip microarray showed a highly significant upregulation of MMP-12 in isolated first trimester trophoblast (FT) compared to term trophoblast cells. Radioactive and non-radioactive in-situ hybridization as well as double-label fluorescence immunohistochemistry utilizing MMP-12 antibodies versus HLA-G, CK-7, CD34 and CD68 were used for spatial detection and identification on the RNA- as well as the protein level. Quantitative and statistical evaluation was performed by subsequent computer aided analysis of the expression density over the course of the first trimester.

Results: We showed that MMP-12 expression and translation into the protein product takes place in a subpopulation of extravillous cytotrophoblast cells (evCTB), proofed on the base of HLA-G positivity. A decrease of MMP-12 mean density was noticed from 0.38 to 0.35 at early and middle down to 0.23 at late FT. No expression was detected in placental site giant cells and, in contrast to previously published data, MMP-12 was not present in vCTB. Decidual vessels and glands exhibited unexpectedly high signal levels and furthermore showed trophoblast plugging from the 6^{th} week of pregnancy.

Conclusion: Our data showed congruent data regarding the spatial localisation on the mRNA and protein level and also a clear tendency in the decrease of signal density towards the end of the first trimester and as against term. As a foundation for conducting functional assays, these data might promise deeper insights in the mechanism of trophoblast invasion and the understanding of the development of the human placenta.

TABLE OF CONTENTS

A Foreword

From the early days of scientific research, the development of the human placenta seemed to be mysterious. The upcoming of innovative working techniques allowed disclosing some of those secrets giving deeper insights into placental function and development on a cellular as well as molecular level. But finding more and more answers, this organ became even more wondrous as the scientists had to realize that the physiological evolution of the human placenta was – at least to a certain extent – a mirror image of the growth and behaviour well known from malignant tumours.

Both, the growing human embryo and the malignant tumour, start their life originating from fundamentally one single cell that apparently falls out of the normal regulation of the human body. But whereas the tumour never will gain control about the proliferation and its invasive capabilities, the human placenta instead appears to be guided within narrow bounds. It is able to regulate the depth and extent of invasion and stops when the proximal third of the myometrium is reached (1,2). Like for all sophisticated systems, failures can occur. Under-regulation can lead to the formation of a more tumourous phenotype of trophoblast cells, setting free all its high-efficient invasive and proliferative capabilities known as for example the chorinon carcinoma. The contrary extreme would be over-regulation, leading to reduced invasiveness and diminished nutrition by the non-appearance of the spiral artery remodelling, seen related to conditions like preeclampsia, intrauterine growth retardation and second trimester miscarriage (3–5).

These similarities between malignant tumour and first trimester trophoblast cells made the latter an ideal model to investigate tumourous features. In this light several previously published reviews have shown, that matrixin expression is crucial for placental development and also has to be regarded as a main factor for tumour progression, not only mentioning invasion and ECM-degradation (6) but especially regarding proliferation, metastasis and angiogenesis (7).

This work was dedicated to unveil some of the numerous mysteries of the human placentation contributing one of the countless small building blocks on which our entire comprehension of this topic is built. Therefore a variety of methods was used to lead a logical chain of arguments for detecting and analysing the spatial expression patterns of macrophage elastase (MMP-12) in its course over the first trimester, underpinning the research results by a redundant line of argumentation whenever possible.

For a diploma thesis generally other framework conditions are assessed compared to a dissertation and a different yardstick is set down, but for both time finally becomes apparent to be the most important influence factor and the most precious resource. The obtained answers, almost mandatorily lead to the rise of even more new questions and problems, which are almost impossible to be solved in time.
But those new, open questions should not be regarded as failure but rather as an impulse and foundation for further research and to reclaim unknown scientific new land.

The author.

B Introduction

1 *The placenta*

The placenta is an essential structure for the development of life in viviparous vertebrates surrounding the unborn offspring and supporting it with various functions like gas transfer or excretion of metabolic products, just to point out two. It is principally formed as a result of the contact of maternal and foetal membranes, separating the two circulatory systems ranging from the simple folded placenta diffusa in lower primates to the much more complex villous discoidal type in humans. Its structure, development and relevance for this work will be outlined below (8).

1.1 Macromorphology and outer structure

The fully developed and delivered placenta is a disc-like shaped, flat and round to oval organ with an average diameter of 22 cm, a central thickness of 2.5 cm and an average weight of 470 g (9). However, a distinctive inter-individual variety can be observed.

The outer structure of the placenta is divided into the foetal (chorionic or amnionic) and the maternal (uterine) surface. The covering epithelium of the foetal surface, which is facing the amnionic cavity displays a shining appearance, as it is normally still intact after delivery. Underneath the chorionic plate with its centrifugally arborizing vessels can be found, starting from the – often eccentric – insertion point of the umbilical cord. Whereas the chorionic plate shows a slight opacity close to the vessels (caused by the high amount of collagen fibres), the space between is coloured either mainly dark lilac to black (as a result of the maternal blood located in the intervillous space shining through the chorionic plate), or shows opaque spots based on larger deposits of Langhans' fibrinoid (9). Shape and cord insertion resulting from the location of the implantation are functionally irrelevant (10).

In contrast to the shiny foetal surface, opacity is shown by the maternal top. This is caused by the separation process between the basal plate of the placenta and the placental bed of the uterine wall creating an artificial surface area that is not equipped with an intact epithelium (9).

The basal surface of the placenta is subdivided into 10 to 40 slightly elevated lobulations (also named cotyledons) by an irregular system of grooves (see Fig. 1). These grooves correspond to internal folds of the basal plate (the placental septa) protruding into the

intervillous space, whereas the lobes line out the localization of the position of the villous trees. The fusion of maternal and foetal parts of the placenta makes macroscopic separation impossible (9,11,12).

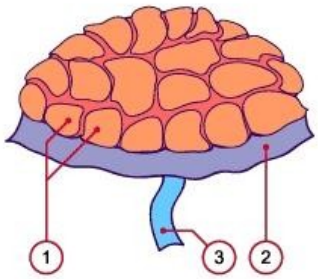

Fig. 1 – Maternal side [taken from (13)]

Fig. 2 – Foetal side [taken from (13)]

1. **Cotyledon**
2. **Amnion, cutting edge**
3. **Umbilical cord**
4. **Compact layer of the decidua, after delivery**

1.2 Micromorphology and inner structure

Working with placental tissue is often a challenge. On the one hand getting well preserved and intact human tissue is complicated because it is only available from legal abortions. Therefore it is often in a bad shape or highly degenerated. This situation deteriorates according to the increasing size of the foetal-placental unit when taken at a later stage.

On the other hand the structure and micromorphology of the human placenta is very complex and often confusing when starting to work with this kind of tissue. Therefore this chapter will give an introduction to the main components and their arrangement in this wondrous organ.

1.2.1 Definition of terminology

The fundamental structure of the placenta and its building parts is a complex and unique unit, which is described simplest by going through the different 'layers', from the foetal surface to the placental bed in the decidua as shown in Fig. 3 and Fig. 4. Hereafter a closer look onto the different types of villi and the developmental stages of the placenta will be presented to impart profound knowledge and comprehension on this topic.

1.2.2 Components of the human placenta

Amnion: A thin layer of cubical to columnar ectodermal cells, covering the chorionic plate on its foetal surface gives the delivered placenta a glossy appearance. It forms the innermost foetal membrane of the amnionic sack, which is also called caul.

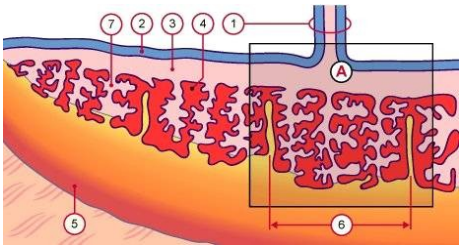

1. Umbilical cord
2. Amnion
3. Chorionic plate
4. Intervillous space
5. Basal plate
6. Cotyledon
7. Villus

Fig. 3 – Profile of a placenta around the fourth month [taken from (13)]

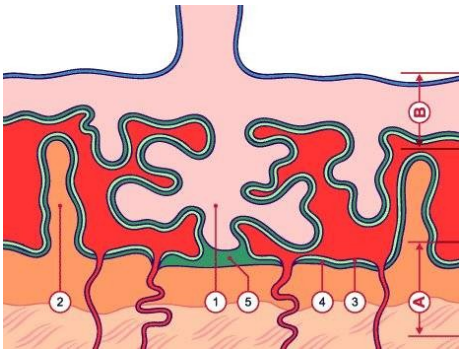

A. Basal plate and myometrium
B. Chorionic plate
1. Anchoring villus
2. Septum
3. Syncytiotrophoblast
4. Cytotrophoblast
5. Cytotrophoblast layer

Fig. 4 – Tertiary villus – enlarged segment 'A' of Fig. 3 [taken from (13)]

Chorionic plate: This stratum of mesodermal cells, located underneath the amnion is harbouring the branching umbilical vessels. From here the tree-like shaped placental villi arise and protrude into the intervillous space, which separates the chorionic from the basal plate. Both, the chorionic plate as well as the placental villi are covered by an outer syncytiotrophoblast (in direct contact with maternal blood) and an inner cytotrophoblast layer. The chorionic plate of the third trimester placenta shows several alterations compared to the early pregnancy. Two layers can be distinguished: a spongy one with numerous clefts and a compact layer of chorionic mesoderm, separates by a rudimentary basement membrane from striae, which are formed of Langhans' fibrinoid (14).

Intervillous space: Limited by the chorionic and the basal plate, the intervillous space forms a diffuse and confluent system of lacunae, surrounding the protruding villous trees. Significant maternal blood flow can be observed starting from the 13th week of pregnancy and reaches a total volume of 100 of 200 ml towards term (14). Whereas the intervillous space is wide in the first trimester, it later becomes narrow (16 to 32 µm) because of the growing placental villi with the exeption of some "subchorionic lakes" (14) close to the chorionic plate.

Maternofoetal junctional zone: During placental development foetal and maternal cells come in close contact and form a zone of mixed tissue origin. The so called maternofoetal junctional zone can be divided into one portion that stays attached to the placenta after delivery – the *basal plate* – and the remaining part, which adheres to the decidua, forming the *placental bed* (14).

Basal plate: Forms one boundary layer of the intervillous space as well as the portion of the maternofoetal junctional zone that stays attached to the delivered placenta.

Septa: These pillar-shaped structures – composed of extravillous trophoblast as well as decidual cells and lots of fibrinoid – arise from the folding of the basal plate and subdivide the intervillous space into a diffuse system of communicating lacunae.

Placental villi: They arise from the chorionic plate and form tree-like structures of 1 to 4 cm in diameter protruding into the intervillous space. Here they serve with an enlarged surface for several exchange processes.
Like the chorionic plate, the placental villi are covered by an outer continuous layer of syncytiotrophoblast cells and a discontinuous stratum of cytotrophoblast cells. The latter – also called Langerhans' cells – serve as the proliferating stem cells for the syncytio-trophoblast cell layer, which represents the maternofoetal transportation and exchange barrier. Inside, the fully developed villi are composed of connective tissue fibres and cells harbouring the foetal vessels. From early pregnancy to term the placental villi traverse different stages of development. Those are described later in chapter 1.2.3 and 1.4.1 emphasising particularly their evolution throughout the first trimester.

Anchoring villi: Beside the various types and stages of placental development, the anchoring villus takes a special position as it is connected to the basal plate through its cell columns (see Fig. 4). Anchored in the basal plate, the villous tree gets stabilized in the maternal bloodstream.

Cell columns: Emanating from the top of an anchoring villus, the cell columns do not only help to anchor the villous in the basal plate and promote longitudinal growth but they also serve as a source for extravillous trophoblast emigration, necessary for placental invasion and utero-placental artery remodelling, particularised in chapter 1.4.2 and 1.4.3.

Extravillous trophoblast cells: This term summarizes all cells with trophoblastic origin outside the placental villus. They show a wide inhomogeneity according to the various stages of differentiation and development. For instance the proliferating stem cells – also called Langerhans' cells – can be found on the basal lamina facing either the chorionic mesoderm or the villous stroma whereas non-proliferating, differentiated and highly invasive extravillous trophoblast cells have lost their contact to the basal lamina. They can be found down to the proximal third of the myometrium where they invade the maternal spiral arteries (15).

Cell islands: Spherical accumulation of extravillous trophoblast cells as still proliferating remains of primary villi that have not been excavated by villous stoma.

Decidua: In a non-pregnant mammalian uterus, the inner lining is built up by a two-layered glandular lamina, consisting of a stratum functionale and basale that undergoes periodic changes during the menstrual cycle.
Under the influence of progesterone the endometrium of the pregnant uterus gets transformed into the decidua. This includes increased secretion as well as thickness of the stratum functionale and conversion of the smaller endometrial into large, tight placed and glycogen-rich decidua cells (16). The primary function of these alterations is to build up the maternal part of the placenta and to supply the placenta-foetal unit with optimal conditions for growth and development until approximately the end of the first trimester (17,18). From this time on, the utero-placental vessels have established the maternal blood circulation in the intervillous space to sustain exchange processes and make the supply independent from histiotroph nourishment (11).

***Utero-placental vessels*:** The so-called *spiral arteries* cross the basal plate in helical turns to gain connection to the intervillous space close to the base of the anchoring villi. In contrast to the *utero-placental veins,* the arteries are largely invaded and rebuilt by intra- or endovascular trophoblast cells, a special subdivision of the extravillous cytotrophoblast. Because the adventitia as well as the media are mostly replaced by trophoblast cells, the vessel gets withdrawn of the maternal control. The veins are endothelial tubes that are only rarely invaded by trophoblast cells, which are never found in the venous lumen. Also no remodelling of these veins takes place (15).

Fibrinoid: This extra-cellular, eosinophilic substance, which is made up of fibrin, dead trophoblast cells and placental secretions, accumulates in the ageing placenta. It can easily be detected by its intense staining and differentiated on the base of its location: replacing the trophoblastic coverage of the villi it is called *perivillous fibrinoid*, whereas *the intra-villous fibrinoid* appears in the stroma.
Other fibrinoid deposits can be found below the chorionic plate (*Langhans' fibrinoid*), on the surface of the basal plate (*Rohr fibrinoid*), in the maternofoetal junctional zone (*Nitabuch fibrinoid*) and also in septa and cell islands (14). The micromorphology of the fibrinoid deposits seems to be homogeneous. In fact, it is built up of two completely different materials: *fibrin-type fibrinoid* as a cell free blood clotting product and *matrix-type fibrinoid,* which is a secretory product of the embedded trophoblast cells (14).

1.2.3 Placental villi – types and stages

These treelike-like offshoots of the chorionic plate undergo several developmental stages until they reach their full size and effectiveness in the invervillous space. The following types and stages are being distinguished and should be regarded closely concerning their microstructure.
Fundamentally, the villi are composed of an outer layer of multinucleated villous syncytio-trophoblast cells with a subjacent layer of mononucleated villous cytotrophoblast cells, sharing a basement membrane separating them from a core of connective tissue. Inside one can find connective tissue fibres, foetal vessels and *Hofbauer cells* (foetal macrophages), according to the particular developmental stages (11,19).

Primary villi: First the syncytiotrophoblast trabeculae are being invaded by cytotrophoblast cells forming a core, which is covered with a thin syncytium layer.

Secondary villi: Later foetal mesenchyme invades the primary villi developing three layers – the outermost syncytiotrophoblast with the subjacent cytotrophoblast and a mesenchyme core inside.

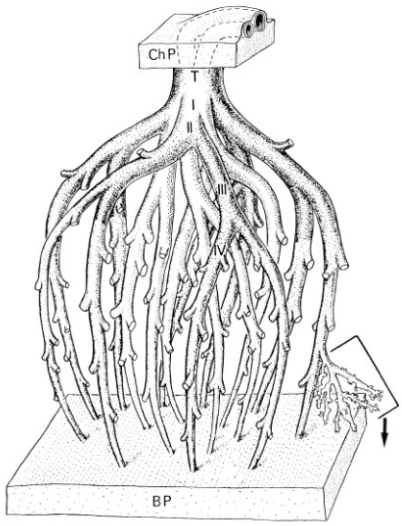

Fig. 5 – Villous tree in a term placenta [taken from (19)]

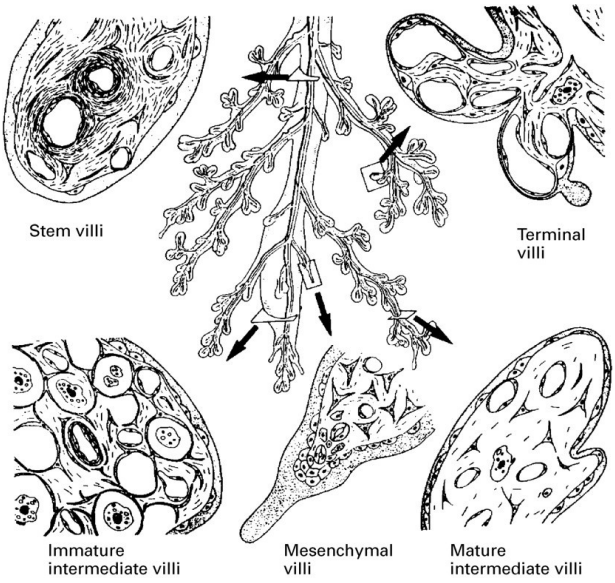

Fig. 6 – Cross section of villous tree types [taken from (20)]

Tertiary villi = mesenchymal villi: The secondary villi subsequently are invaded by foetal vessels leading to the final villous ground structure: The outside is formed by the syncytiotrophoblast with an underlying complete layer of cytotrophoblast cells placed on a basement membrane delimiting these from the mesenchyme core, traversed by the foetal vessel network. The mesenchymal villi are mainly found during the early stages of placental development (19,20).

From week seven to eight of pregnancy, these mesenchymal villi start to differentiate into the following ***four final villous types*** (20):

Immature intermediate villi: The core contains abundant oedematous mesenchyme made out of a reticularly arranged loose connective tissue, which is traversed by many matrix channels with numerous Hofbauer cells (in opposite to the mesenchymal villi) (20). They act as the forerunners of the stem villi and can easily be detected by their large diameter, the pale staining and further the absence of large foetal vessels and small amount of collagen fibres in the core. Representing the dominant population of villi in the early pregnancy, they start to decrease towards term where they only make up less than 10 per cent of the total villous volume.

Stem villi: Deriving from the mature intermediate villi, they represent the central scaffolding of the villous tree which connects it to the chorionic plate, exhibiting diameters beglefrom 80 up to several thousand micrometres (19). In their core, made up of compact stroma, they harbour at least one foetal artery and vein (or arteriole and venule) with a clear muscularly wall as well as a paravascular capillary net accompanied by the surrounding fibrous stroma. Anchoring villi are regarded as a subpopulation of the stem villi (11,19,20).

Mature intermediate villi: These slender villi with a diameter of 60 to 100 µm can be differentiated from stem villi by the absence of fibrosis and foetal stem vessels in their mesenchymal core. The stroma of the mature intermediate villi is composed of a foetal capillary network embedded in a loose connective tissue with high density of cells and low amount of fibres (11). These villi make up to 25 per cent of the villous volume in a mature placenta (20).

Terminal villi: Budding from the mature intermediate villi these grape-like side branches with a diameter of 40 – 80 µm represent, together with the afore-mentioned mature intermediate villi, the main exchange area of the third trimester placenta. They show only an incomplete or regressed cytotrophoblast layer and a loose stroma with sinusoidal dilated foetal capillaries occupying most of the villus diameter in cross sections (11,20). Terminal villi occur around the 27^{th} week of pregnancy and make up 30 to 40 per cent of the villus volume (20).

Syncytial sprout or knotting: Trophoblastic outgrowths caused by on-going syncytiotrophoblast proliferation. These are often seen in later stages of placental development and serve as the origin of newly formed villi, which later get invaded by mesenchyme and foetal vessels forming mesenchymal villi (11,19,20).

1.2.4 Villous pattern of development:

During the early stages of placental development, the mesenchymal type dominates the overall picture. Around the 7th week it differentiates into the immature intermediate type, which grows in size and transforms into the stem villi. Syncytial sprouts form the origin of side branches, generating new mesenchymal villi.

At the end of the second trimester the mesenchymal population starts to transform into the mature intermediate type serving as a scaffold for the multiple pullulating terminal villi. At term – the latter makes up the dominant subpopulation providing 50 per cent of the total exchange surface (20).

1.3 Functional aspects

The human placenta is unique as it unites all vital functions of the still immature foetal organs – apart from the musculoskeletal and central nervous system. This in the first place enables growth and development of the foetus.

To fathom most of the placental functions, an overview of the fundamental exchange mechanisms is essential. This takes place by classic membranous transport mechanisms at the surface of the mature intermediate and terminal villi outreaching an exchange area up to 12 square meters at term. Most of the substrates are exchanged through passive transport processes (by simple diffusion for non-polar and lipophilic substances or osmosis for highly polarized molecules like water), active (e.g. sodium-, potassium- or calcium-ions) or vesicular transport (for macro-molecules like immunoglobulin's) (21).

Using the mechanisms described, the placenta is able to provide gas transfer for oxygen supply and carbon dioxide removal, and therefore substitutes the breathing function of the lung. Nutritive and excretory functions replace the gastrointestinal as well as the urinary system to ensure the vital water and electrolyte together with acid-base balance and further

to supply the growing foetus with glucose (as main energy-source), amino-acids, proteins and also lipids like triglycerides or cholesterol and its derivatives (8,21).

On a large scale the placenta is involved in endocrine functions during pregnancy. These functions are conducted by the human chorion-gonadotropin (hCG) synthetized by syncytiotrophoblast cells, animating on the one hand the foetal suprarenal glands to produce dehydroepiandrosterone (DHEA) and on the other the maternal corpus luteum graviditatis to set estradiol and progestron free. At the end of the first trimester, the hormonal production is completely taken over by the syncytiotrophoblast cells (21).

During the early stages of pregnancy also the haematopoietic potency of the bone marrow and the synthetic and secretory functions of the foetal liver have to be replaced by the placenta (8).

A very important area – but largely unknown – is the immunological function of the placenta. On the one side, the foetus is actively supplied with maternal immunoglobulin (IgG) through syncytiotrophoblastic pinocytosis, providing passive maternal immunity for the first months of life (21). On the other side, the foetus as well as foetal parts of the placenta are a 'foreign tissue' to the maternal immune system. Why the anticipated excessive immunological reaction at the implantation site fails to materialise stays a marvel (21).

1.4 Development of the human placenta

1.4.1 Early development

This thesis investigates a partial aspect of the invasive process mediated by extravillous trophoblast cells taking place in the first trimester placenta. Therefore the gist of this chapter is mainly focused on the placental development. However, for a comprehensive understanding of the latter, basic knowledge of the pre-implantation and the subsequent evolution which the placenta-foetal-unit has to undergo, are essential and should be mentioned to give a broad outline for the later discussion.

Pre-implantation

This first stage of development, reaching from fertilisation of the oocyte to formation of the early blastocyst takes place in the first five days post conception. After ovulation and fertilisation in the ampulla of the fallopian tube – the zygote wanders toward the uterus passing through cell cleaves, multiplying its daughter cells. When reaching the uterus on

day four, the mulberry-like cell mass, called morula, counts roughly 30 cells, which start from this point on to take different courses of differentiation (see Fig. 7) (22).

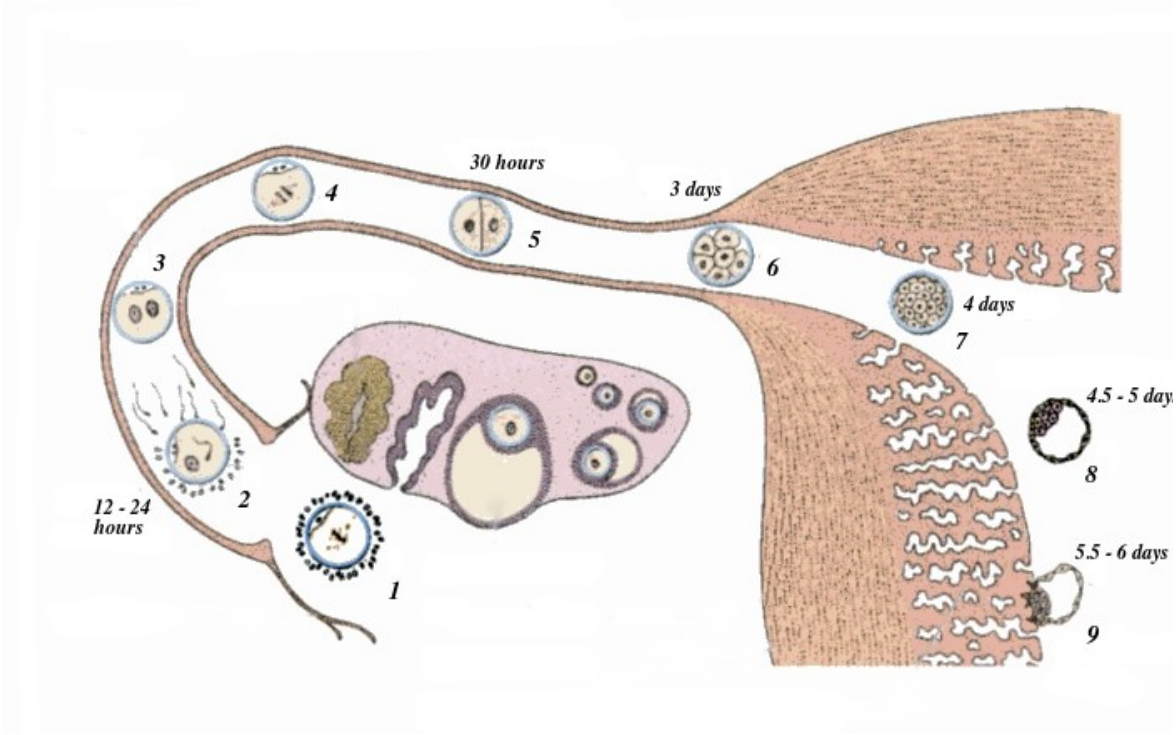

Fig. 7 – Fallopian tube, migration of the fertilised oocyte [acc. to (23), modified]

Different cell masses start to develop and can be clearly distinguished between the fourth and fifth day, forming the blastocyst made up of the inner embryoblast surrounded by trophoblast cells and the zona pelludica (see Fig. 8). Fluids secreted by the bastocyste cells form the blastocystic cavity also discriminating the polarity with the embryonic pole opposing the abembryonic one.

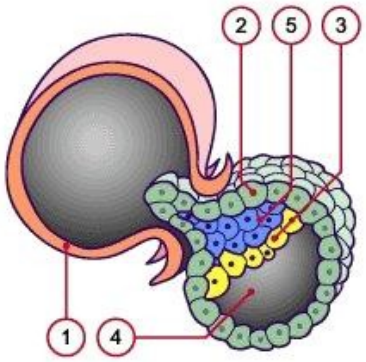

1. Zona pelludica, partially dissolved

2. Trophoblast cells

3. Hypoblast cells

4. Cavity of the blastocyst

5. Epiblast

3 and 5 = Embryoblast

Fig. 8 – Hatching blastocyst [acc. to (22), modified]

Implantation

At about the fifth to sixth day post conception (p.c.) the blastocyst gets rid of the zona pelludica – a process named hatching (see Fig. 8) – enabling the trophoblast cells to get in direct contact with the maternal decidua. This leads to proliferation and formation of a syncytium (the syncytiotrophoblast) resuming to penetrate the maternal epithelium and connective tissue of the endometrium. On day seven to eight, the blastocyst complex embeds itself into the uterine wall and gets completely covered by maternal epithelium around the ninth day post conception. The surrounding endometrial cells undergo morphological and functional changes forming the decidua (14,24). The following pre-lacunar and lacunar stages are indeed parts of the implantation, but will be shown separately as they are marked by distinct events in the foetal development.

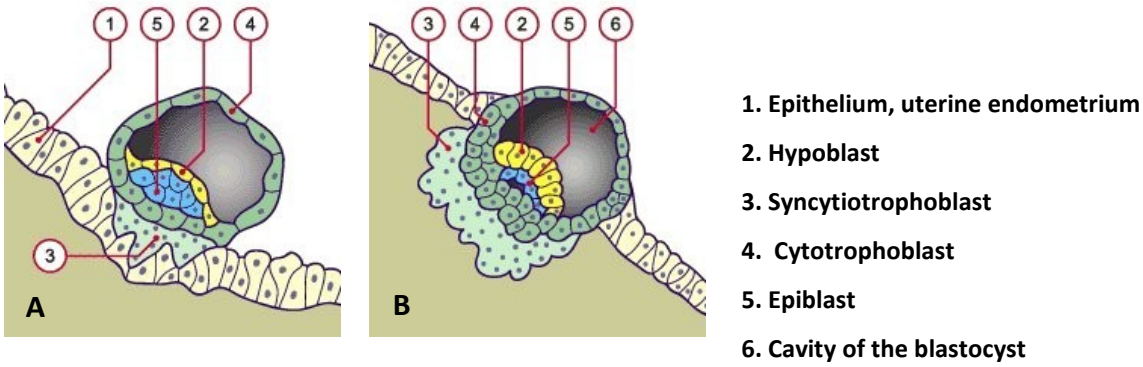

Fig. 9 – Implantation: A: Day 6 – 7; B: Day 7 – 8 [acc. to (25)]

Pre-lacunar stage

The placenta and the foetal membranes arise out of the trophoblast cells, which can be distinguished from the embryoblast around day four. During implantation, the trophoblast cells subdivide into an inner layer, forming the later cytotrophoblast cells and the outer syncytium, called syncytiotrophoblast. These latter cells are in direct contact with the endometrium and trigger its transformation into a well-perfused source of nutrition forming the later basal plate and a part of the maternofoetal junction zone (14,24).

Another function of the newly formed placental forerunner cells is the synthesis of several hormones like the aforementioned human chorionic gonadotropin (hCG), the human chorionic somatotropine (hCS) and also the human placental lactogen (hPL), which are essential for the further development and regulation of the pregnancy.

Lacunar stage

At around day 8 p.c. small vacuoles arise in the increasing syncytiotrophoblastic mass beneath the implantation pole. Quickly growing they start to merge and form a confluent system of lacunae, which is separated by trabeculae made up of remnant syncytiotrophoblast lamellae and pillars. Their appearance marks the lacunar stage lasting from day 8 to 13 p.c. (compare Fig. 10 A and B) (24,26).

As the blastocyst gets embedded deeper into the maternal decidua the thickness of the syncytiotrophoblast rises, forming more and more lacunae, which finally encase it completely. Its thickness reflects the earlier determined polarity, being thicker at the embryonic rather than at the opposite pole. This relation does not change as the thicker part is forming the later placenta and its thinner counterpart forms back to the chorion. Therefore the placenta can be seen as a highly specialised membrane.

The syncytiotrophoblast envelope of the blastocyst gets subdivided into three layers by the emergence and growth of the lacunae: the primary chorionic plate that faces the blastocystic cavity, the lacunar system with its trabeculae and finally outermost the trophoblastic shell, which is facing the endometrium (26).

Forming the inner layer, the ***primary chorionic plate*** is made up of a largely continuous stratum of single- to triple layered cytotrophoblast cells, which are covered with syncytium towards the lacunae. Around the inner surface, mesenchymal cells start to form a loose network, also called *extraembryonic mesenchyme or mesoderm* on day 14 p.c. (26), which are of non-trophoblastic origin (27,28). Underneath the primary chorionic plate the ***lacunar system*** is located. Trabeculae, made of septa or pillars that are formed of the remaining syncytiotrophoblast, separate the lacunae. Those get filled with maternal blood when small capillary vessels are eroded during the process of invasion, establishing a first slow low-pressure circulation (see Fig. 10 C and D). At around day 12 p.c., those trabeculae are invaded by cytotrophoblast cells, emerging from the primary chorionic plate. Within the next days the cytotrophoblast cells reach the outer end of the trabeculae and join together forming the ***trophoblastic shell*** (26). This process is specified below.

The lytic potency of the syncytiotrophoblast cells enables erosion of maternal tissue during the early stages of implantation. With the cytotrophoblast approaching at the bottom of the trophoblastic shell a new step in implantation and placentation starts. The then following ***trophoblast invasion*** not only allows further invasion but also makes it possible to increase and take over control of the maternal blood supply by remodelling the spiral arteries as well as anchoring the growing and developing placenta to the placental bed (26).

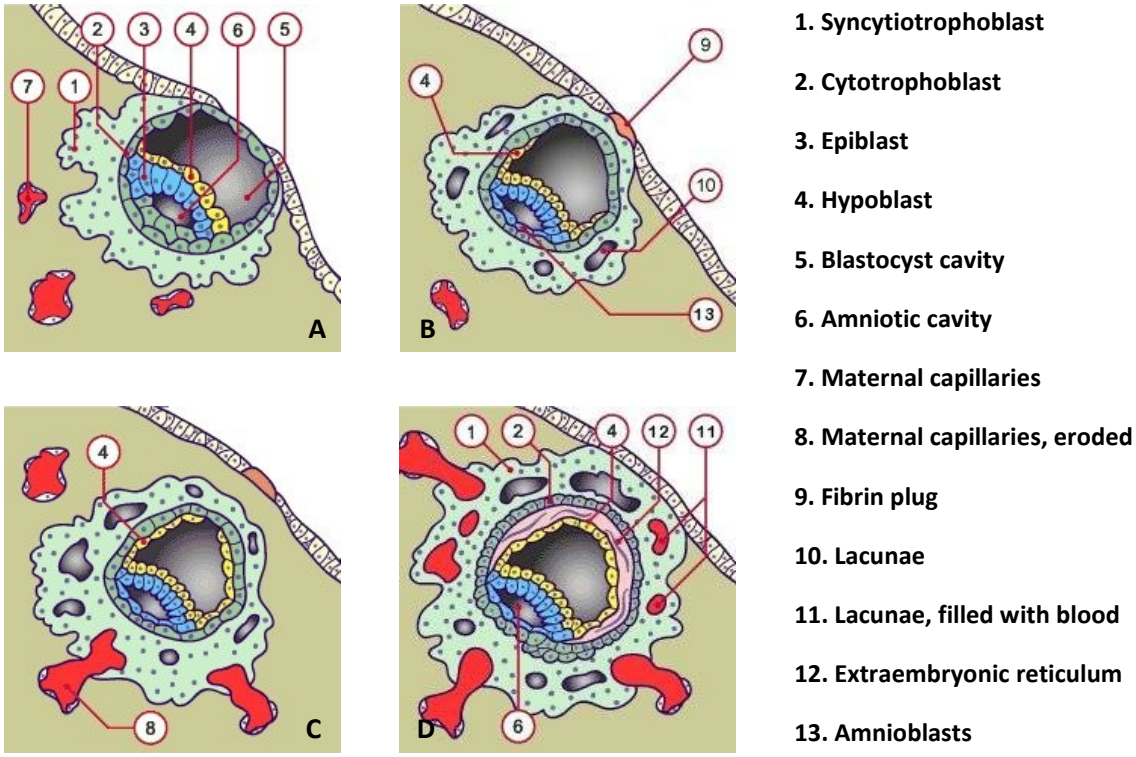

Fig. 10 – Lacunar stage of implantation
A: Day 8; B: Day 9, C: Day 9-10; D: Day 10-11 [acc. to (25), modified]

Early villous stages

When the first maternal erythrocytes start to appear in the sinusoid lacunae around day 12 p.c. (26) an increased proliferation of cytotrophoblast cells with subsequent syncytial fusion can be observed. This leads to longitudinal growth and the formation of syncytial side branches of the arising ***primary villi***. Subsequently cytotrophoblast proliferation and invasion results in further longitudinal and diametrical growth, initiating the beginning of the developmental stages demonstrated in Fig. 11 and Fig. 12 A. Ongoing proliferative activity causes further growth and branching with formation of first, primitive villous trees. Branches ending blind in the lacunae are called ***free floating villi*** in opposite to the ***anchoring villi***, which establish profound contact to the trophoblastic shell. The communicating lacunae now form a single system lined with syncytiotrophoblast cells, from this time on called the ***intervillous space*** by definition (26,29).

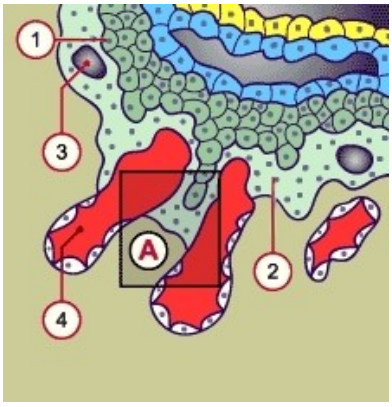

1. Cytotrophoblast

2. Syncytiotrophoblast

3. Lacunae

4. Eroded maternal vessel, feeding the linked lacunae

A. Reference segment, enlarged in Fig. 12 and Fig. 13

Fig. 11 – Lacunar stage of implantation: Day 10-11 [acc. to (29), modified]

At around day 16 the primary villi are invaded by the extraembryonic mesoderm originating from the chorionic plate transforming them into ***secondary villi*** (see Fig. 12 B) (26). Whereas the majority of the villous trees is getting invaded by villous mesenchyme, it does not reach the trophoblastic shell through the anchoring villi. From the early villous stages until the end of pregnancy these distal parts of the original trabeculae consist of cytotrophoblast cells, surrounded by a thin layer of syncytiotrophoblast, called the ***cell columns***. They promote the longitudinal growth and serve as the origin of the extravillous trophoblast cells. If the mesenchyme does not reach the tips of the free floating villi, they keep their primary villi appearance, proliferate and form the ***trophoblastic cell island*** (26).

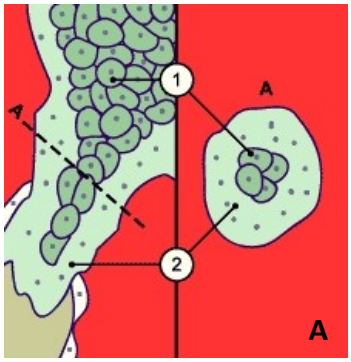

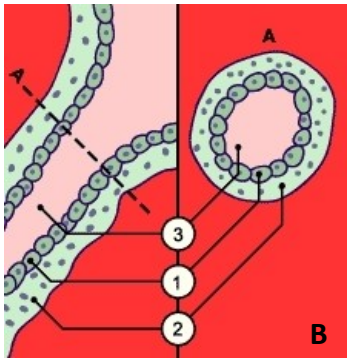

Enlarged segment A of Fig. 11

1. Cytotrophoblast

2. Syncytiotrophoblast

3. Extraembryonic mesoderm

Fig. 12 – Early stages of villous formation: A: Day 11-13; B: Day 16 [taken from (29)]

Transformation into ***tertiary villi*** takes place between day 18 and 20 when the first foetal capillary vessels start to differentiate from haematopoietic progenitor cells of the extraembryonic mesenchyme and can be obtained in the cross sections (see Fig. 13 A). From this moment on almost all villi, except of trophoblastic and villous sprouts as well as cell columns and islands, can be summarised as tertiary villi. The formation of embryonic

vessels in the villous trees enables the placenta to take up its exchange functions across the ***placental barrier***. Decrease in the diameter of the villi during their maturation and the regression of the cytotrophoblast layer are (as shown in Fig. 13 B), among other things, responsible for the reduction of the maternofoetal diffusion distance from around 50 to 100 µm down to 4 to 5 µm at term.

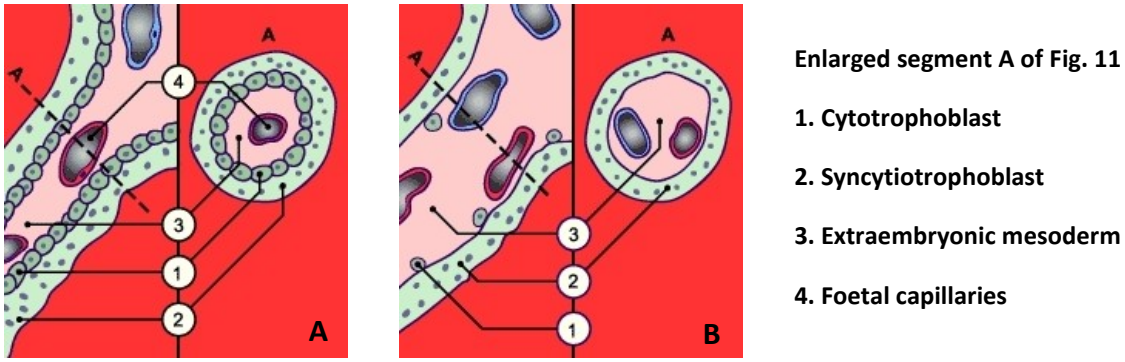

Fig. 13 – Early stages of villous formation: A: Day 21; B: 4th month to term [taken from (29)]

1.4.2 Trophoblast invasion

With proceeding growth and development of the placenta the intervillous space harbours free floating and anchored villi, which are both built up of an outer syncytiotrophoblast and inner cytotrophoblast layer. The cytotrophoblast (CTB) in the anchored villi can be divided into subpopulations with various features as well as the expression of different markers (see Fig. 14). Depending on their spatial localisation they also change their morphological appearance.

At the top of the cell columns of the anchoring villi one can differentiate between two populations of cells: **villous (vCTB)** and **extra-villous** or **interstitial (evCTB) cytotrophoblasts**. Whereas the first group is made up of immotile, polarised epithelial stem cells lying on a basal membrane the second, the evCTB, are unpolarised, motile and highly invasive.

Within the group of extravillous cytotrophoblasts a broad inhomogeneity is shown over the different stages of development. The **proximal** and still proliferating population changes shape, behaviour and expression of markers with increasing distance from the villus as its origin. This goes along with deeper invasion into the maternal decidua, down to the proximal third of the myometrium where **intermediate** and **distal** extravillous CTB's can

be observed. Those phenocopy endometrial cells and can be summarised as **endovascular trophoblast cells (enCBT).**

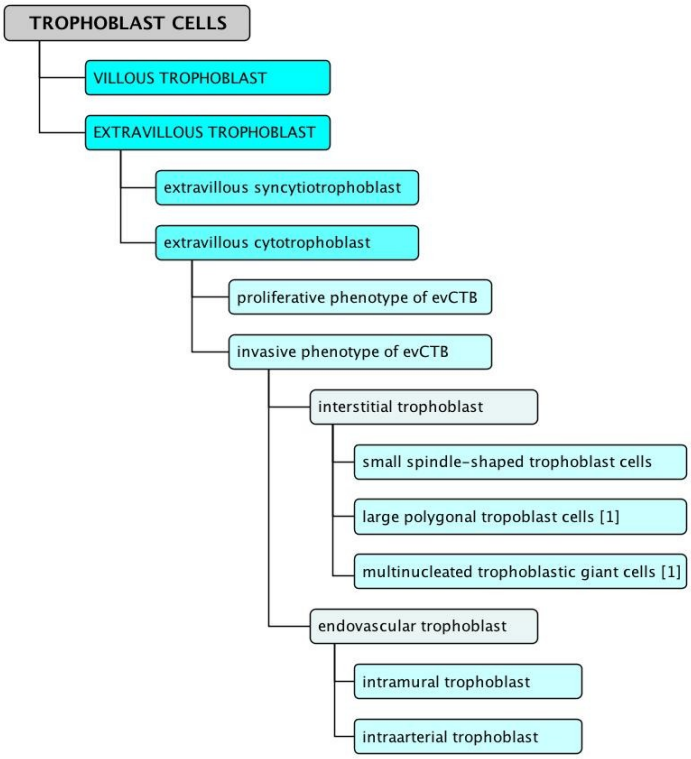

Fig. 14 – Nomenclature of trophoblast cell subtypes [acc. to (15)]
[1] Large polygonal trophoblast cells and multinucleated trophoblastic giant cells are summarized under the pathologic term **placental site giant cells** (PSGC).

The final step in trophoblast progression is the invasion of the maternal spiral, also called utero-placental arteries, starting from around the 6th week of pregnancy (15). This is a key element for understanding of the human placental development. Invasion and re- or displacement of endothelial and muscular cells enables the foetus to gain control over the maternal blood supply and adjust it to its own requirements.

The theoretical background of this process is still barely understood. The difference between human and animal placentas and the lack of experimental assays or models still conceals the true mechanism from the scientists' eyes.

In general there are two competing theories about spiral artery invasion demonstrated in Fig. 15. One group of scientists postulated an intra-luminal retrograde invasion based on findings in the rhesus monkeys. In this so called ***'extravasation theory'*** evCTB of an unknown origin gain access the maternal spiral artery and migrate retrograde inside the lumen of the vessel. They replace the endothelial lining and invade the media and

adventitia of the vessel. As in the other theory, this only takes place in utero-placental arteries, not in veins. The second group, representing the large majority of scientists, favours the postulation of an interstitial invasion and destruction of the arterial wall named the ***'intravasation theory'***. Studies with human placentas based on structural and immunohistochemical findings (15) suggest that the population of the **endovascular cytotrophoblast (enCBT)** is not an entity that has to be differentiated from the interstitial cytotrophoblast (as the first group postulates) but – in contrast – represents the developmental endstage of the latter. They invade the vessel wall from outside, replacing the media, entering the lumen where they accumulate and also replace the entire endothelial lining. This accumulation of enCBT can be so massive that it obliterates the lumen temporarily, a process called ***'plugging'***.

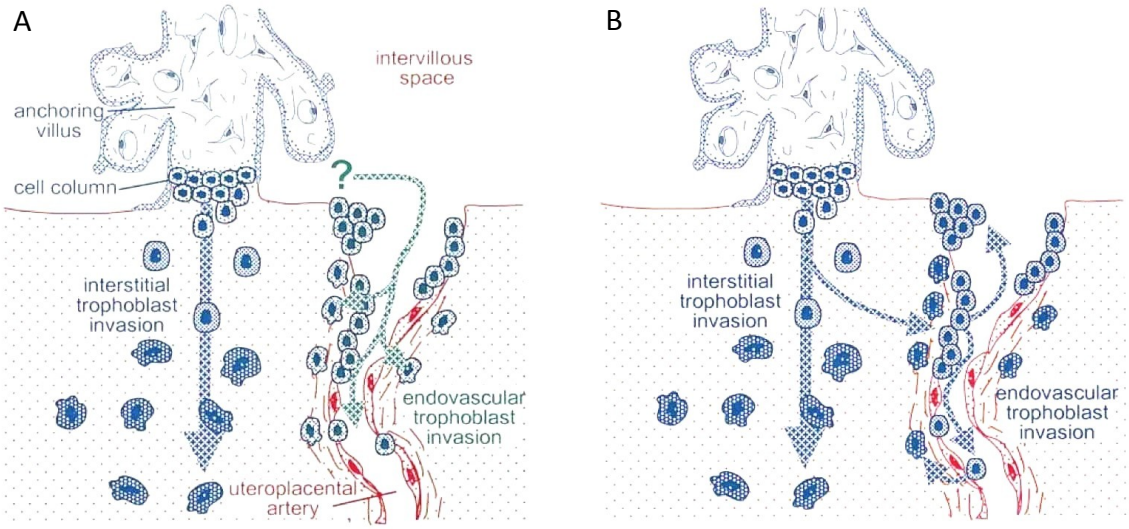

Fig. 15 – Endovascular trophoblast invasion by **A:** Extravasation **B:** Intravasation [taken from (3)]

Observations in the guinea pig placentation showed invasion of interstitial cytotrophoblast cells in the distal parts of the spiral arteries close to the intervillous space. Here they replace the media as well as the endothelium, accumulate inside the vessel and migrate retrograde to more proximal parts of the artery where they could extravasate again. Despite some indications are underpinning this hypothesis, proof unfortunately remains to be shown for this explanatory approach in human placentation (15,30).

As a marginal note the hypothesis of Kam et al should not go unmentioned. His group suggested the involvement of two different populations of trophoblast cells: inCBT are invading the adventitia and media of the vessel, whereas the second group of enCBT migrates retrograde into the lumen, accumulating and replacing the endothelial cells (31).

Differentiation of the numerous subpopulations of trophoblast cells can only be achieved by investigating expression patterns of various markers.

Category	Parameter	Villous		Extravillous			Endothelial
		vSTB	**vCTB**	**Prox.**	**Inter.**	**Distal**	**endCTB**
Proliferation markers	**Ki67**	0	1	1	0		
	PCNA	0	1	1	1	0	
Hormones	**hCG**	1	0	0	0		
	hPL	1	0	1	1	1	
Integrines	**α1β1**	0	0	0	0	1	1
	α5β1		0	0	0	1	
	α6β4	0	1	1	1	0	
	αvβ5	0	1	1	0	0	0
	αvβ3	0	0	0	0	1	1
Hypoxia markers	**HIF-1**	0	1	1	0	0	
	pVHL	0	1	1	0	0	
Histocompatibility antigens	**HLA-A, B, C**	0	0	1	1		
	HLA-G	0	0	0	1	1	
	HLA class I	0	0	0	1	1	
	HLA class II	0	0	0	1	1	
Cytoskeleton markers	**CK-7**	1	1	1	1	1	
	Vimentin	0	0	0	0	0	
Proteases and inhibitors	**MMP-1**			0	0	1	
	MMP-2			1	1	1	
	MMP-3			1	1	1	
	MMP-7	1	1	1	1	1	
	MMP-9			1	1	1	
	TIMP-1			1	1	1	
	TIMP-2			0	0	1	
	TIMP-3			1			

Tab. 1 – Relevant markers of human trophoblast cells [acc. to (32), modified]

1: presence; 0: absence.

Acting as proliferation stem cells, the proximal evCTB and vCTB are still quite similar as Ki67 and PCNA can be found in both (33). But they can be differentiated by the expression of markers like hPL or HLA-A, B and C, which are not found in vCTB (compare with Tab. 1) (32,34,35).

With deeper invasion the trophoblast cells change not only their appearance to a more fusiform type and loose their ability for proliferation, they also gain a pro-invasive set of

proteases as for example gelatinases A and B (MMP-2 and -9) (32,36). The subchapter '2.4.2 – The role of matrixins in human placentation' is addressed to look at this topic more closely with special regard to the impact of the matrixins.

To adapt to the changing environment an 'integrin-switch' takes place (37). Villous CTB and more proximal forms of extravillous trophoblast are equipped with α6β4 and αvβ5 integrin's as against α1β1, α5β1 and αvβ3 in the distal and endothelial forms. This change of receptors for cell-matrix-interaction can be observed frequently in malignant, metastasizing tumours (38,39).

1.4.3 Spiral artery remodelling

The remodelling of the utero-placental arteries is a central point in the development of the human placenta. Its missing is associated to severe pathological condition such as preeclampsia, intrauterine growth retardation (IUGR) and second trimester miscarriage through insufficient placental perfusion (4,5). However, the exact mechanism remains unclear (3).

As against erstwhile assumptions a major part of the physiological spiral artery changes takes place long before first contact with invasive trophoblast cells occurs. When the evCTB finally start their invasion, they encounter already largely altered arterial vessels.

The entirety of the physiological remodelling can be divided into three subsequent stages (15) following structural criteria:

Stage I: Trophoblast-independent vascular alterations

Initially the endothelium shows a general basophilia and vacuolations as well as a beginning lumen dilation and disorganization of smooth muscles shown in Fig. 16 A and B. That these alterations are not trophoblast-mediated was proven by the fact that not only vessels at the implantation pole were affected. Furthermore endometrial arteries in ectopic pregnancies showed the same physiological changes (40).

Stage II: Perivascular trophoblast-dependent vascular alterations

Studies in the guinea pig demonstrated that further changes appear prior to the vascular invasion, when the interstitial CBT are in close proximity to the vessel walls (as in Fig. 16 C). Deposition of fibrinoid material and reduction of smooth muscle cells are part of this

step as well as further dilation. Studies indicated that nitric oxide secretion of perivascular trophoblast cells might be the driving force behind these changes (30,41).

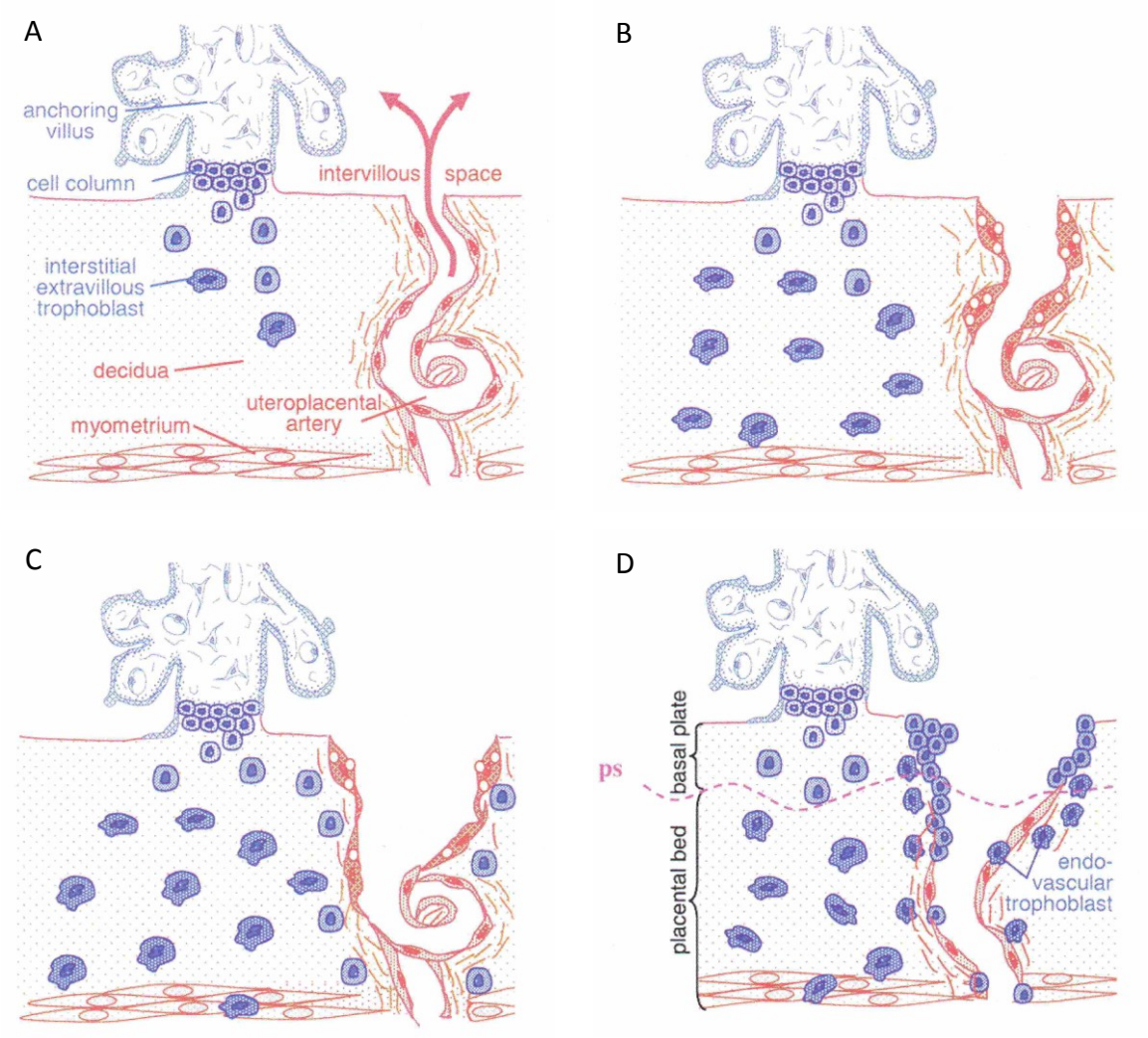

Fig. 16 – Interstitial and endovascular trophoblast invasion [taken from (15)]
A: before 6th WOP; **B:** stage I – trophoblast-independent vascular alterations; **C:** stage II – perivascular trophoblast-dependent vascular alterations; **D:** stage III – trophoblast invasion and vessel remodelling;

Stage III: Trophoblast invasion and vessel remodelling

In the final step endovascular trophoblasts invade the utero-placental arteries leading to a variety of modifications shown in Fig. 16 D. The most obvious is the further dilation up to 5 times of its original diameter. In contrast to utero-placental arteries in the myometrium measuring up to 200 µm, the altered vessels exhibit diameters of 500 to 1000 µm close to their opening into the intervillous space, which itself can be as much as 2000 µm (15).
Further invasion also is accompanied by the reduction of elastic fibres, which is mediated by the expression of matrixins such as interstitial collagenase (MMP-1), stromelysin-1

(MMP-3) or gelatinase A and B (MMP-2 and -9). Underpinning this, two major proteinase inhibitors (α_1-antitrypsin and α_1-antichymotrypsin) were only found to be expressed by endovascular but not by interstitial cytotrophoblast cells (42).

Along with the reduction of elastic fibres the elasticity is further impaired by the accumulation of the previously (in step II) described fibrinoid masses. This transforms the once flexible arterial vessels into rigid conduits.

Another effect of the trophoblast invasion is the disappearance of smooth muscle cells in the media. Older studies indicated that apoptosis might be induced by the invading cells, whereas recent investigations in the guinea pig suggested rather a dedifferentiation into myoblasts. It is assumed, that those are the base for post partial vessel reconstruction (43). This was supported by the finding of α-smooth muscle actin in human spiral arteries, which was phenotypically free of smooth muscle cells (15).

Finally the endovascular trophoblast cells reach the lumen and replace the endothelium by a mono- or polylayer even building trophoblastic plugs in some of the vessels. Surprisingly immunohistochemistry showed that some of the larger endovascular cells were factor VIII-positive but negative against hCG suggesting them to be of endothelial, rather than trophoblastic origin (44).

2 *Matrix metalloproteinases*

Matrix metalloproteinases (MMPs), also called matrixins, are a family of zinc depended endopeptidases, collectively capable of degrading almost all components of the extracellular matrix. This makes them the leading factor for the regulation of cell matrix composition (7,45). Whereas at least 23 different MMPs have been discovered in humans, more can be found in other vertebrates as well as non-vertebrates and plants.

All members of this family share a highly conserved zinc-binding site in their catalytic domain distinguishing them from other peptidases. Subfamilies can be classified by substrate specificity and domain homology (45,46).

Shortly after detection of the first MMPs, they have been linked to tumour invasion regarding their ability in degrading basement membranes – especially by MMP-2 and MMP-9 (6). Today, with enlarged understanding of the pathophysiological background in matrix degeneration and remodelling, they are associated with a broad variety of pathological conditions for example in rheumatoid arthritis, osteoarthritis, pulmonary emphysema, cardiovascular disease and cancer (7,45) as well as in basic vital procedures such as inflammation, wound healing or even embryogenesis (47,48).

This potent system of proteolytic enzymes, vital for development and maintenance of body functions, entails the risk of self-harm due to excessive activation and auto-degradation. Therefore a strict regulation system is necessary to keep it in check.

2.1 History

Matrixins have first been described by Gross and Lapière in 1962 when they tried to culture parts of tadpole tails on collagen gel and observed activity of an enzyme able to degrade native (triple helical) collagen fibres (49,50). This interstitial collagenase, which later was purified from human skin, is today known as MMP-1 (51).

In the following years other MMPs have been discovered and recognized to be involved in many normal or pathological processes. As more and more effort was put into their investigation, important steps forward in the understanding of the pathophysiological basement were taken with the recognition of MMPs being zymogens (52), their fold and structure (53,54) and the cystein switch (55). Whereas the family of matrixins first was defined by the dependence of metal ions in their catalytic domain the recognition of other similar enzymes equipped with this feature (e.g. reprolysins or serralysins) made it necessary to use DNA sequencing as a basis for the definition of this group.

In 1981 Banda et al. were able to show that a six years earlier detected elastase, secreted by stimulated murine macrophages, was a member of the matrixin subfamily (49,56,57). When cDNA cloning of the human enzyme was performed in 1996, sequencing showed that the found enzyme was the human counterpart – called MMP-12 – and data about functional aspects were put into focus of research (58).

2.2 Domain structure and function

All vertebrate matrixins, except of the membrane-type MMPs, are synthesized as pre-pro-enzymes and secreted as inactive zymogenes. In general, they show a homogeneous structure, based upon a varying composition of domain motives shown in Fig. 18.

The basic structure of all matrix metalloproteinases comprises a signal as well as a propeptide and the catalytic domain with its zinc-binding site, providing catalytic activity and stability. These are the minimal requirements for a fully functional enzyme that is epitomized in the structure of matrilysin (MMP-7), which is only composed of these three domains (59).

The other vertebrate matrixins are equipped with additional structural elements, like the c-terminal hemopexin-like domain, which can be found in all MMPs other than MMP-7 and -23. With except of MMP-21, the hemopexin-like domain is linked to the catalytic domain by a linker peptide whose exact function is yet unknown but assumed to be involved in triple helical collagen cleavage (59).

Whereas the n-terminal **signal peptide** marks the protein for secretion into the extracellular space, the **pro-peptide domain**, which is about 80 amino acids in size, holds the catalytic domain in an inactivated state. Within the latter one can find the highly conserved and unique "cysteine-switch"-sequence, PRCG(V/N)PD [1], whose cysteine interacts with the catalytic zinc-ion holding the enzyme in latency (53,59).

The centre of each matrixin enzyme is the **catalytic domain** characterized by the zinc-binding motive HExGHxxGxxHS[2], providing three histidine ligands for the catalytic zinc-ion, and a conserved methionine. Whereas the first zinc works as a catalyser for substrate processing, the second together with two or three calcium ions ensure structural stability

[1] C – cysteine, D – aspartic acid, G – glycine, N – asparagine, P – proline, R – arginine, V – valine
[2] E – glutamic acid, G – glycine, H – histidine, S – serine, x - variable

for the three-dimensional alignment of the complex. This domain with a length of about 180 amino acids shows a secondary structure of five-stranded β-sheets as well as three α-helices with bridging loops including the "met-turn" being also found in ADAMs, serralysins and astacins as a characteristic for the metzincin-superfamily (see Fig. 17) (59).

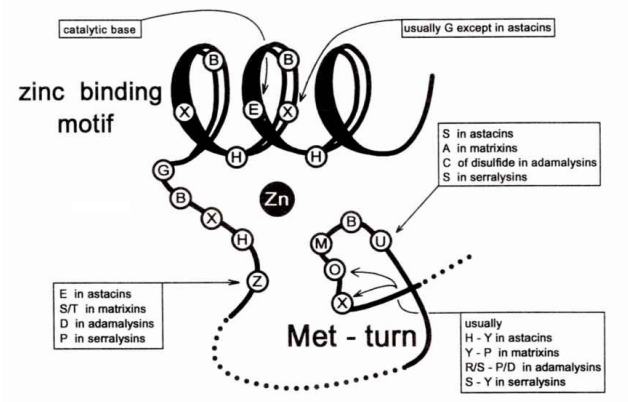

Fig. 17 – Active centre of the metzincin family [taken from (53)]

MMP-2 and 9 (gelatinase A and B) show three additional fibronectin type II domains within the catalytic domain. These are assumed to be involved in collagen- and gelatine-processing (59).

Except for MMP-7, -22 and -23, a proline-rich **linker peptide** connects the catalytic and the c-terminal **hemopexin-like domain**. This almost 210 amino acid large, ellipsoid and disc shaped structure made up of a four-bladed β-propeller pattern – each blade consisting of four anti-parallel β-strands combined with an α-helix – is absolutely vital for cleavage of triple helical collagen fibres. However, removal of this does not affect activity regarding other substrates or single collagen fibres. MMP-12 (macrophage elastase) for example, loses its hemopexin-like domain auto-catalytically shortly after activation without any interference to its elastin-degrading function (60).

Regulation of the matrixins being involved in extracellular matrix (ECM) modification and turnover needs rigorous control. Insufficient degradation would prevent cell migration and cell-matrix interaction, leading to deficiencies in development or wound healing (47,48) while excessive activation entails the risk of destruction to the extracellular matrix.

The multi-layered regulation takes place from DNA to protein level and is barely understood in wide parts.

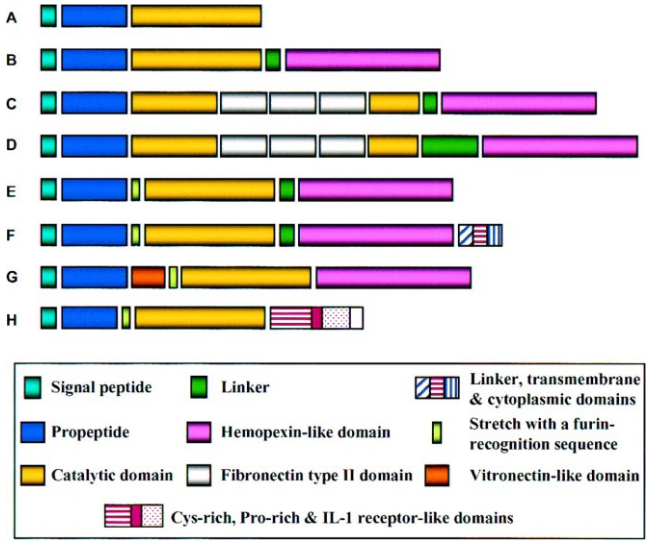

Fig. 18 – Domain arrangement of human matrixins [taken from (59)]

Protein	MMP	Composition
Collagenase 1	MMP-1	B
Gelatinase A	MMP-2	C
Stromelysin 1	MMP-3	B
Matrilysin	MMP-7	A
Collagenase 2	MMP-8	B
Gelatinase B	MMP-9	D
Stromelysin-2	MMP-10	B
Stromelysin-3	MMP-11	E
Macrophage elastase	MMP-12	B
Collagenase-3	MMP-13	B
MT1-MMP	MMP-14	F
MT2-MMP	MMP-15	F
MT3-MMP	MMP-16	F
MT4-MMP	MMP-17	F
Collagenase 4	MMP-18	B
(No trivial name)	MMP-19	B
Enamelysin	MMP-20	B
XMMP	MMP-21	G
CMMP	MMP-22	B
(No trivial name)	MMP-23	H

Tab. 2 – Domain composition [taken from (59)]

The **transcriptional regulation** is complex and can be reduced to growth-factor responsive and independent matrixins (45). Transcription of MMP-3 genes, for example, can be increased by interleukin-1β (IL-1β), tumour necrosis factor alpha (TNF-α), transforming growth factor alpha (TGF-α), epidermal growth factor (EGF), platelet-derived growth factor (PDGF), basic fibroblast growth factor (bFGF), and nerve growth factor (NGF) (45).

Changes of mRNA and protein levels up to 20-50 fold can be observed onto stimulation or repression (45). Except for immunologic cells like macrophages, which are able to store matrix metalloproteases in a larger quantity within vesicles, other cells synthesized them when they are required. Therefore their expression is normally low and gets induced when there is need for extracellular matrix remodelling (45,61).

The promotor regions of most of the matrixins show a similar arrangement of regulatory elements, which are the target for several cytokine-mediated or growth-factor related signalling pathways like the activator protein 1 (AP-1) binding site or the polyoma enhancer A binding protein-3 (PEA3) as a target for the E-twenty six (ETS) transcriptor family.

On the **protein level** several steps are necessary for **activation**. However, spatial activation and cleavage, complex formation, compartmentalization and inactivation are further utilized to gain control and limit cleavage on the necessary minimum.

Apart from MT-MMPs, the signal peptide gets cleaved after secretion into the extracellular compartment. Here the inactive zymogenes are hold in latency by the pro-peptide domain covering the catalytic centre. To activate the enzyme, disruption of the Cys-Zn^{2+}-interaction – the so called "**cysteine-switch**" – is vital and can be achieved on various ways shown in Fig. 19.

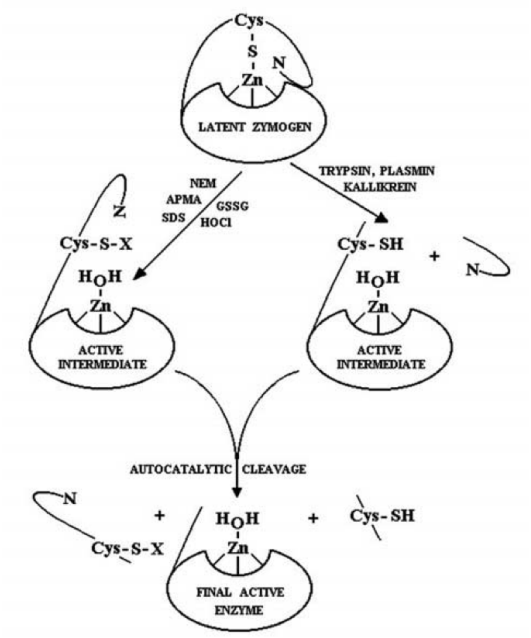

Fig. 19 – Cysteine switch mechanism and matrixin activation [taken from (45)]

In vitro chemical agents as chaotropic agents or sodium dodecyl sulphate (SDS) can expose the zinc-ion by unfolding the tertiary structure whereas other agents react directly with the sulfhydryl group of the cysteine such as hypochlorous acid (HOCl), aminophenyl mercuric acetate (APMA), N-ethylmaleimide (NEM) and oxidized glutathione (GSSG).

In vivo proteolytic enzymes, e.g. trypsin, plasmin, kallikrein or urokinase- and tissue-type plasminogen activator (uPA and tPA), are able to cleave the pro-peptide and expose the catalytic domain partially. Being activated, the metalloproteinase can now auto-catalytically cleave the (rest of the) pro-peptide domain to gain full and permanent activation (45,62).

After activation of the matrixins a complex system grants limitation of its effects as well as inactivation and clearance, holding the balance and avoiding excessive destruction.
Spatial activation is being obtained by activation of cell-surface bound factors such as urokinase-type plasminogen activator (uPA) or membrane-type matrix metalloproteinases (MT-MMPs) type 1 to 3 (MMP-14, -15 and -16) in close vicinity. Some matrixins are reliant upon distinct factors as matrilysin on proteoglycans, gelatinase B on CD44 or gelatinase A on the $\alpha_v\beta_3$- integrin. The latter also can be activated by a trimeric complex formed of pro-gelatinase A, tissue inhibitors of the metalloproteinase 2 (TIMP2) and the cell-surface bound MT1-MMP. Cell membrane located receptors for matrixin-activation trace presence and localisation of a distinct substrate and trigger the liberation of specific MMPs. This can be seen in the case of human collagenase 1 which is induced in basal keratinocytes as a response to skin injury. Disengagement from the basement membrane and contact with dermal type 1 collagen – detected by $\alpha_2\beta_1$- integrin receptors – leads to secretion of pro-collagenase 1 directed to the site of contact with subsequent activation (63,64).

Matrixin **inhibition** is provided mainly by the tissue inhibitors of metalloproteinases (TIMPs 1-4) and the inhibitors of metalloproteinases (IMPs) as well as the general proteinase inhibitor α2-macroglobulin. TIMPs are able to inhibit all active forms of matrixins by coverage and interaction with their catalytic domain as well as the hemopexin-like region. Despite their inhibiting function, especially TIMP-1 but also TIMP-2 and -3, are very potent activators for MMP-2 when forming a complex with the membrane-anchored MT1-MMP (45,52,65).
Other inhibitors are the smaller and larger inhibitors of metalloproteinase (IMPs and LIMP), the latter formed by a complex of TIMP-2 and pro-gelatinase A. LIMP is able to inhibit collagenase, gelatinase A and stromelysin as well as other MMPs. Another inhibitor is α2-macroglobulin that is able to trap proteinases utilising a bait region. Cleavage in this region by the enzymes leads to change of conformation and subsequent entrapment (66,67).
Finally **permanent clearance** of MMPs has not been investigated sufficient, but some mechanisms are known as autocatalytic cleavage and receptor associated clearance. Thrombospondin 2 (TSP2) – a protein involved in inhibition of angiogenesis, cell adhesion and migration – is able to bind e.g. latent or active MMP-2 with following endocytosis by

the LRP-scavenger receptor. Other matrixin-receptor-complexes are known to show similar activity (68,69).

2.3 Classification of MMPs

To bring order into the system of proteinases or enzymes, many different classifications are in competition. Basically one can differentiate whether the amino acid sequence or tertiary structure of important domains, respectively the active site, is regarded or otherwise focalising on the catalysed reactions. In the latter – embodied, for instance, by the enzyme commission numbers[3]– the same reaction catalysed by different enzymes is summarized under the same category.

As there are many overlapping classification systems with their pros and cons, two popular examples will be presented to sort the matrixins into entirety of enzymes.

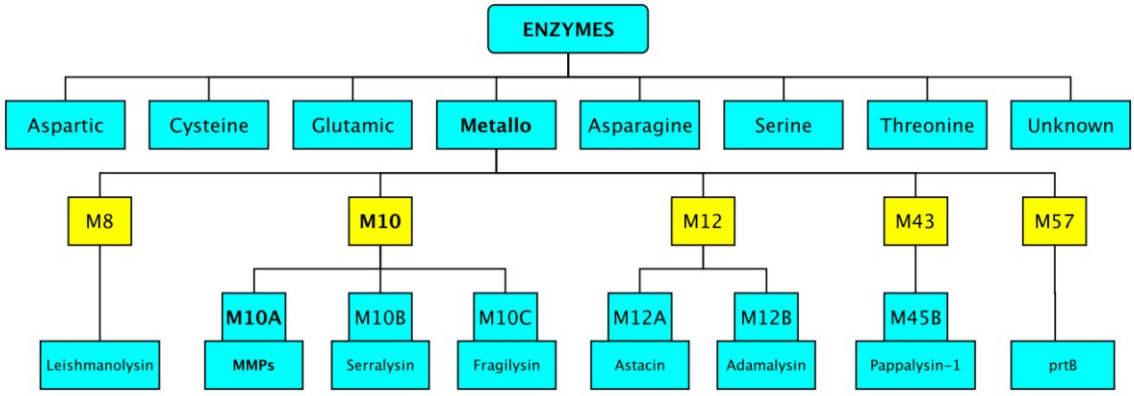

Fig. 20 – MMPs in the context of the MEROPS classification

Beginning with the umbrella term protein, the matrixins are counting to the enzymes, more precisely to the hydrolaseses as they have the ability to rupture chemical bonds by the addition of water. Using a metal ion in their active site to catalyse the digestion of peptide structures, these enzymes are called metalloproteinases and can further be divided into exo- and endopeptidases. Beside the matrilysins, the latter also includes adamalysins, serralysins or closely related enzymes.

[3] ECN: Numerical enzyme nomenclature scheme, developed in 1955 at the International Congress of Biochemistry (Brusseles) – first published in 1961.

Group	Enzyme	MMP	Substrate
Collagenases	Collagenase-1, Interstitial collagenase	MMP-1	Native collagen types (III>I>II, VII, X), gelatin, aggrecan, Link protein, entacin, tenascin, perlecan
	Collagenase-2, Neutrophil collagenase	MMP-8	Native collagen types (II>III>I, VII, X), gelatin, entactin, tenascin, aggrecan
	Collagenase-3	MMP-13	Native collagen type (I, II, III), gelatin
Gelatinases	Gelatinase A	MMP-2	Denatured collagens (gelatin), native collagen types (I, IV, V, VII, X, XI), elastin, fibroncetin, laminin-5, aggrecan, brevican, neurocan, decorin, vitronectin
	Gelatinase B	MMP-9	Denatured collagens (gelatin), native collagen types (I, IV, V, VII, X, XI), elastin, fibronectin, laminin, aggrecan, link protein, vitronectin
Stromelysins	Stromelysin-1	MMP-3	Non-triple helical regions of native collagen types (II, III, IV, V, IX, X, XI), aggrecan, laminin, fibronectin, gelatin, entactin, perlecan, decorin, tenascin, vitronectin, fibrin, fibrinogen, link protein, elastin
	Stromelysin-2	MMP-10	Gelatin type (I, III, IV, V), fibronectin, proteoglycan
	Stromelysin-3	MMP-11	Fibronectin, laminin, aggrecan
	Stromelysin-4	MMP-19	Native collagen types (IV), gelatin, laminin, fibronectin, tenascin, entactin, aggrecan, COMP, fibrin, fibrinogen
Matrilysin	Matrilysin	MMP-7	Non-helical segents of native collagen types (IV, V, IX, X, XI), fibronectin, laminin, gelatin, aggrecan, entactin, tenascin, vitronectin, fbrin, fibrinogen
		MMP-26	Native collagen types (IV), gelatin, fibronectin, fibrin, fibrinogen, vitronectin
Membrane-type MMPs	MT1-MMP	MMP-14	Native collagen types (I, II, III), gelatin, fibronectin, vitronectin, aggrecan
	MT2-MMP	MMP-15	Proteoglycan
	MT3-MMP	MMP-16	Nativ type collagen (III), fibronectin
	MT4-MMP	MMP-17	Gelatin, fibrin, fibrinogen
	MT5-MMP	MMP-24	Fibronectin, proteoglycans, gelatin
	MT6-MMP, Leukolysin	MMP-25	Native collagen types (IV), gelatin, fibronectin, proteoglycans (DSPG, CSPG), Laminin-1, Fibrin, fibrinogen
Other	Metalloelastase	MMP-12	Elastin, fibronectin, laminin, proteoglycan, fibrin, fibrinogen, myelin basic protein
	Enamelysin	MMP-20	Amelogenin, COMP, aggrecan
		MMP-21	No substrate known
		MMP-23A	No substrate known
		MMP-23B	No substrate known
		MMP-27	Fibronectin, laminin, collagen.
	Epsilysin	MMP-28	Casein

Tab. 3 – Matrixin substrates [acc. to (70), modified]

COMP – cartilage oligomeric matrix protein; CSPG – chondroitin sulphate proteoglycan; DSPG2 – decorin;

To achieve an overview of the different kinds of proteinases this first classification system might appear to be sufficient, but it is not when seeking for a more subtle system implying domain-structure similarities and evolutionary aspects.

An up to date on-line database for peptidase, their substrates and inhibitors is provided under the name MEROPS[4]. Similarities at the tertiary as well as primary structural levels are the base for this hierarchical classification system shown in Fig. 20.

In the first line MEROPS divides the peptidases into actually seven[5] groups, well defined by the consistency of their catalytic centre, either by the functional amino acid or a metal complex. Each group is marked by the first letter. Families are formed within these groups by significant sequence homology, especially regarding the catalytic unit, and identified by unique numbers. Further division into subfamilies can be performed if evidence for evolutionary divergence within a family is shown, which is then marked by another letter (e.g M10A for MMPs).

Families and sub-families can be further assembled into clans linked by a special sequence or structural motif vital for the enzymes' functions. Within the group of metallopeptidases (M), the most frequent metal ion is zinc. The zinc-binding motif HExxH is therefore uniting the families within the clan MA, which are also called the zincins. Some of the families within the clan MA are equipped with another histidine residue as well as a so-called met-turn. They form the metzincin sub-clan MA(M), which is defined by the motif HExxHxxGxxH[6] (71,72).

2.4 Role in tissue remodelling and invasion

All processes involving growth, reorganisation and invasion of cells in larger, eukaryote organisms require degradation of extracellular matrix components. Whereas strictly controlled in physiological processes as embryological development or wound healing, overexpression of several matrixins can be observed in malignant tumours (52). Numerous studies have shown a correlation between the alteration of expression patterns and poor prognosis. For example is the overexpression of MMP-12 in patients with hepatocellular carcinoma related to a more aggressive behaviour with early tumour recurrence and poor overall survival (73).

[4] MEROPS: http://merops.sanger.ac.uk; First published by Rawlings & Barret (1993), provided and funded by the Wellcome Trust Sanger Institute, Hinxton, Cambridgeshire, UK.

[5] Eight, if "unknown" enzymes are included.

[6] E – glutamic acid, G – glycine, H – histidine, x - variable

Below this key aspect will be viewed under the light of tumour invasion and the invasive behaviour of extravillous trophoblast cells during the development of the human placenta.

2.4.1 The role of matrixins in tumour development

Development and progression of malignant tumours is a complex, multi-step process that involves local proliferation, angiogenesis, migration and invasion as well as the ability to spread to a secondary site (7). Early after their discovery, the matrixins were linked to tumour progression, e.g. allowing the tumour cells to degrade and penetrate basement membranes, which is still seen to be an important prognostic factor for many tumours (6).
In the following years more MMPs were discovered and their importance as prognostic markers for tumour outcome acknowledged. While the first theories assumed, that matrixin-overexpression is only provided by tumour cells, following studies showed the involvement of stromal cells of the host. This was observed for example in breast cancer where the levels of MMP-1, -2, -3, -9, -11, -12 and -13 were elevated (74,75).
Whereas overexpression of matrixins was always thought to be vital for tumour progression at the primary and secondary site, recent studies showed that some matrixins might act in an anti-tumourigenic or guarding role (7,76,77).

In what follows the role and possible influence of MMP-expression regarding the different steps of cancer progression is described.

<u>Tumour proliferation</u>

A review published by Martin et al (7) summarised a plethora of studies investigating the influence of matrixins on tumour growth at the primary and secondary site with pro- as well as anti-tumourigenic abilities.
Promoting influence was shown in one study using B16F10 melanoma cells, overexpressing the MMP inhibitor TIMP-1, being injected into the vascular system of chicken chorioallantoic mebranes (CAMs). Contrary to expectations, no failure in extravasation but a significant reduction in cell growth at the secondary site resulted compared to the control group (78).
As an alternative, matrixins are also able to promote tumour growth by cleavage of proteoglycans as perlecan and decorin. These constituents of the extracellular matrix are

able to bind fibroblast growth factor (FGF) and transforming growth factor beta (TGF-β), which are released when being cleaved by collagenase-1 and stromelysin-1 (for perlecan) or gelatinase-A, stromelysin-1 and matrilysin (for decorin) (79,80).
Other studies showed the induced progression of MCF-7 breast adenocarcinoma cells and DU-145 prostate adenocarcinoma cells by degradation of the insulin-like growth factor binding protein-1 (IGFBP-1) through stromelysin-3 and gelatinase-B. The latter is controlled by an autocrine loop involving the secretion of insulin-like growth factors, insulin-like growth factor binding proteins and gelatinase-B (81,82).
Further there have been indications that indirect influence on proliferation might occur due to alterations of the ECM-constitution e.g. by expression of the αvβ6-integrin (83).
A controversial issue is the effect of matrilysin on the apoptosis of cancer cells. Its ability to liberate soluble Fas ligand (sFasL) from the cell membrane showed a time dependant result. In matrilysin-null mice a decrease of the apoptotic index of more than 60 per cent was observed, whereas cell culture assays showed varying results depending on the exposure time. Subsequent investigation of this inconsistency indicated a selection mechanism for tumour cells with reduced sensitivity to apoptosis (84–87).

In contrast to these tumour-promoting properties, there were also studies pointing out anti-tumourigenic effects for some matrixins.
An interesting study performed with collagenase-2-deficient male knockout mice demonstrated an increased number of papilloma and a decreased latency period after treatment with the chemical carcinogenesis protocol using DMBA+TPA. This effect did not appear in female mice unless ovaries were removed or the anti-estrogen Tamoxifen applied. Interestingly, the opposite effect was shown for collagenase-1-deficient mice. Here rather pro-tumourigenic results like acanthosis, hyperkeratosis and epidermal hyperplasia were observed as well as acceleration in tumour incidence and increased tumour numbers (88,89).
A bivalent appearance can be recorded for stromelysin-1. Reports about this member of the matrixin family were showing both, protective as well as pro-tumourigenic effects in mammary gland tissue and breast cancer studies.
Whereas MMP-3 knockout mice exhibited a fast initial growth rate, enhanced proliferation and undifferentiated appearance on various chemical carcinogenesis procedures, other transgenic mice, expressing the activated form of stromelysin-1 showed had 30 per cent less mammary tumours onto DMBA-treatment compared to the wild type (90,91). Further

studies with Sp-1 cell lines showed protective effects and promotion of cellular differentiation when MMP-3 was upregulated (92).

On the other hand, there was also proof of tumour-promoting effects of this member of the matrixin family in mammary carcinogenesis: a tetracycline regulated, stromelysin-1 overexpressing phenotypically normal mammary cell line was injected into the fat pads of mice. With the presence of tetracycline blocking the expression, the cells that formed, differentiated glandular structures, whereas without tetracycline small tumours were found (93).

Further it has been published that MMP-3 is able to increase levels of cellular reactive oxygen species (ROS) leading to oxidative damage and genomic instability in breast cancer (94).

Remarkable was the effect of metalloelastase that altered depending on the cells expressing it. A study investigating progression of squamous cell carcinoma from the vulva showed that metalloelastase expression in tumour cells was associated with low differentiation and a more aggressive histology. Whereas expression in tumour associated macrophages correlated with well-differentiated histology, rather grad I than III, and a better outcome (95).

Angiogenesis

For each growing tumour the generation of new blood vessels is a very important step providing nutrients, oxygen and a possible route for metastatic dissemination. The great number of studies conducted, showed the two faces of matrixins on this issue (7).

Whereas matrix metalloproteinases first were thought to be conductive for the formation of new vessel by degrading the surrounding ECM, it was later recognized that their sphere of influence also included cleavage of substrates generating anti-angiogenic agents as endostatin, tumstatin and angiostatin (96). The latter, for example can be generated from plasminogen by stromelysin-1, matrilysin, gelatinase-B and macrophage elastase (97–100).

Well-investigated was gelatinase-B that also showed pro- and anti-angiogenetic effects. On the one side it was able to generate angiostatin as well as tumstatin. The last named was derived from type IV collagen and reduced vessel formation through an αvβ3-inegrin dependant mechanism. Several studies in gelatinase-B- or α1-null mice confirmed this observation (101,102). On the other side it showed pro-tumourigenic properties, directly triggering the ‘angiogenic switch’ by solubilisation of vascular endothelial growth factor

(VEGF) and the recruitment of pericytes promoting formation of new blood vessel networks (103,104). Those effects were only observed from stromal derived gelatinase-B.
The majority of the available data about macrophage elastase suggested both, protective and anti-angiogenic effects. Together with the aforementioned matrixins, it was responsible for the generation of angiostatin (99). Lung metastasis models using MMP-12 deficient transgenic mice showed an increase in development of metastases but no difference regarding the number of micrometastases compared to the wild-type. Expression of macrophage elastase was also associated with reduced micro-vessel density and confined to tumour-associated macrophages (105). In a similar study also using Lewis lung carcinoma (LLC) the MMP-12 deficient mice presented with the same number of metastases but a 2-fold increased amount of tumours with a diameter measuring more than 2 millimetres (106). While the stromal expression of MMP-12 in host macrophages led to protective effects, expression in squamous cell carcinoma and non-small cell lung carcinoma lead to a more aggressive phenotype and a poor prognosis (95,107,108).

Invasion and metastasis

Evidence for involvement of matrixins in the process of invasion and metastasis was early shown by the ability of gelatinase A and B to degrade type IV collage, a major component of the basement membrane, being crucial for tumour progression (6). Subsequent studies unveiled their broad involvement as pro-invasive agents, which were often expressed at the invasive edge of tumours not only involved in the turnover of ECM-components (109). Studies utilising recombinant TIMP-1 in B16F10 cells or TIMP-1 overexpression led to reduced lung metastasis (110–112). Conversely tests with gelatinase A and B deficient mice resulted in the same result (113,114).

Protective effects were observed for neutrophil collagenase (MMP-8) that was upregulated in a human breast cancer cell line. Overexpression was associated with inhibition of the metastatic capabilities, which were highly developed in its counterpart originating from the same parental line but with 20-fold lower MMP-8 levels. These effects were reversible by overexpression of the neutrophil collagenase in the metastatic and knockdown in the non-metastatic line (115,116). Sharing type I collagen as a main substrate, membrane-type 1 matrix metalloproteinase was rather pro-invasive and –metastatic as opposed to the aforementioned neutrophil collagenase. It has shown its invasive capabilities in three-

dimensional collagen gels, chicken chorinoallantoic membrane assays and in vivo by increased progression and invasion of cervical carcinoma (117–119).

Gelatinase B – known as a key player in angiogenesis – had also influence on invasion. MMP-9-null mice had a reduced incidence of tumours with diminished keratinocyte hyperproliferation but also a higher graded and more aggressive phenotype. Notably, even leading to an increased number of tumours, MMP-9 seemed to show protective effects driven from stromal inflammatory cells (120).

Other metastasis models, using MMP-9 deficient mice and Lewis lung carcinoma cells, were drawing a different picture: here a reduction of lung tumours of 81 per cent was observed and was also related to stromal inflammatory cells. In this study MMP-9 seemed to increase tumour cell survival by its anti-apoptotic properties (121).

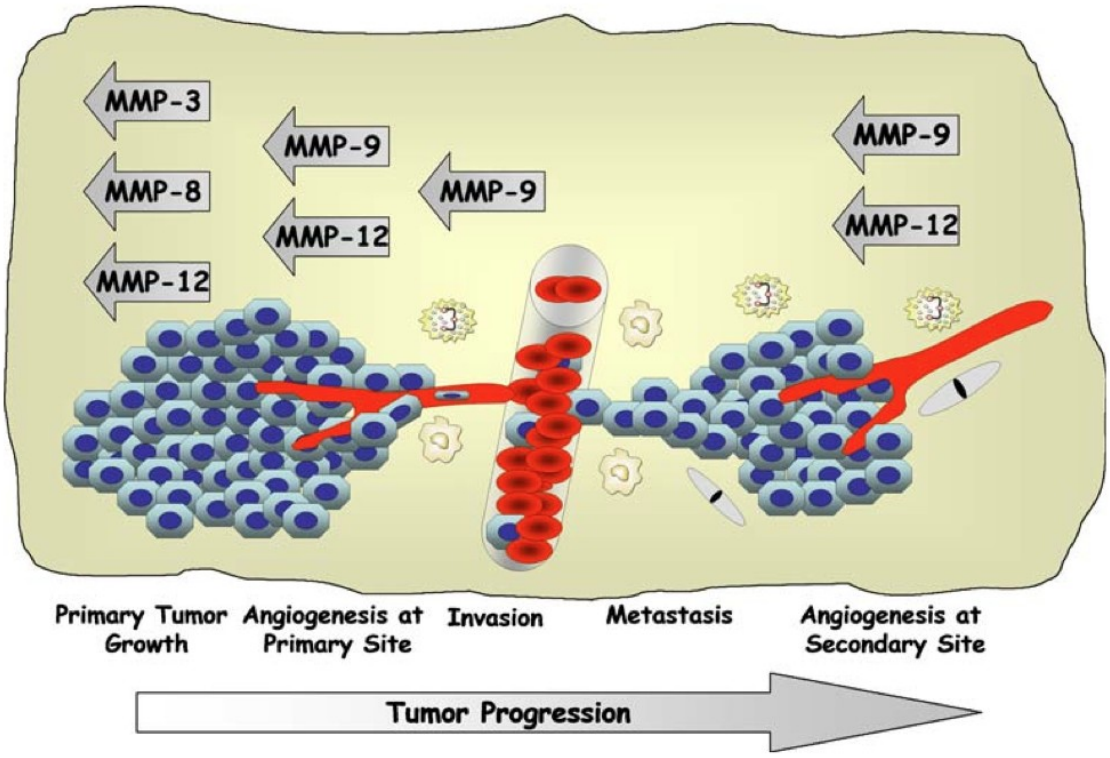

Fig. 21 – Influence of matrixins on tumour progression [taken from (7)]

2.4.2 The role of matrixins in human placentation

The implantation of the embryo and the subsequent trophoblast invasion (specified in subchapter '1.4.2 – Trophoblast invasion') is a mesmerizing and unique process forwarded by the maternal decidualisation and the enormous invasive potential of the embryo. There are many similarities between trophoblast and tumour invasion as both are utilising the same cellular and molecular processes as e.g. expression or repression of specific patterns of molecules crucial for cell adhesion, secretion of ECM-digesting proteases and acquisition of a sufficient blood supply. Further increased telomerase activity, proto-oncogene product expression and also evading the response of the immune system should not go unmentioned (1). Although the behaviour of the invasive phenotype of tumour and trophoblast cells seems to be resembling, the latter are rigorously regulated and show a strict temporal as well as spatial limitation: under physiological circumstances invasion occurs in the first trimester with a peak around the 12^{th} week of pregnancy and does not penetrate beyond the proximal third of the myometrium (1,2).

The 'pseudo tumour-like' appearance of the trophoblast cells created them to be an ideal model to investigate tumour invasion. As this work emphasises the importance of matrix metalloproteinases for implantation and trophoblast invasion – further reference can be obtained from numerous reviews on this topic (1,2,38).

Crucial for tumour as well as for invasive trophoblast cells is the ability to loosen contact to neighbouring cells and the basement membrane to make their way through the surrounding extracellular matrix and to break into the circulation (1,6,122).

The three pillars, most important for this process, are the molecules of the extracellular matrix (such as collagen, laminin or fibronectin), their receptors (as the integrins) and finally the proteases (such as the matrixins), which are able to degrade this matrix (1,122).

A plethora of studies indicated that matrix metalloproteinases are not only degrading ECM to open a way for cell movement and ingrowing vessels. Instead they are directly promoting proliferation by liberating growth factors from proteoglycans (79,80) or show anti- and pro-angiogenic properties in tumours. Cleavage of substrates can generate either agents as endostatin, tumstatin or angiostatin – or the pro-angiogenic counterpart VEGF to count only a few (7,96–100). This makes them being key players not only in tumour progression but also in placental development. That cytotrophoblast and endometrial cells are a source of matrix metalloproteinase expression and secretion was shown in vitro by

several studies (123,124). The following matrixins have been detected in the human placenta:

The expression of ***collagenase-1*** (MMP-1) in invasive trophoblast cells is not surprising regarding their ability to degrade – among other substrates – type I and III collagen, the most frequent found in the human endometrium (15,36). Increasing MMP-1 activity was shown onto in-vitro stimulation with type I collagen (125).

Gelatinase A (MMP-2) and ***gelatinase B*** (MMP-9), which are both known as type IV collagenases are able to degrade the essential element of basement membranes. Whereas MMP-2 only was found in the invasive phenotype (126,127) – MMP-9 expression was present at the proliferating edges of the extravillous trophoblast, down-regulated during early invasion and up-regulated again in the deeper stages (15,36,128). For both, the highest mRNA levels were found within the first 12 weeks of pregnancy, decreasing towards term (129). In vitro studies utilizing TIMP-1 and -2 as well as specific antibodies led to complete inhibition of MMP-9-mediated cytotrophoblast invasion, whereas inhibition of the plasminogen activator system only had a partial effect of 20-40 per cent emphasising the importance of this matrixin (130).

Stromelysin-1 (MMP-3) shows a weak expression in the proximal layer of proliferating cells. Similar to MMP-9 it is being downregulated in the early stages of invasion and gets upregulated again later (15,36).

Both, ***stromelysin-3*** (MMP-11) and ***matrilysin*** (MMP-7) were shown to be expressed by invasive trophoblast cells and, for the latter, also in the decidua (15,131,132).

In 2010 Aplin & Harris detected the presence of ***metalloelastase*** (MMP-12) as a key mediator for elastolysis during spiral artery remodelling. To permit permanent luminal extension of the altered utero-placental arteries, degeneration of elastic fibres is essential, which are found in the 'internal elastic lamina' (IEL) and the musculo-elastic media of myometrial artery segments. Gene expression profiling and brightfield immunohistochemistry showed that MMP-12 was expressed in interstitial and endovascular CTBs of the placental bed and, notably, also in the vascular smooth muscle cells (VSMCs) of the remodelling spiral arteries. Stimulable by perfusion with CTB-conditioned medium, the influence of soluble factors (released by CTBs) on the VSMCs was assumed, promoting cooperatively degeneration (133).

Decomposition products of the elastin metabolism as the 'elastin-derived peptides' (EDP) might be involved in the regulation of a positive-feedback mechanism, which is further

increasing the expression of MMP-12. Approximately 60 to 70 % of the total elastase activity is provided by membrane-associated metalloelastase, whereas the remaining proportion most likely is mediated by MMP-2, and -9. Both are capable of degrading elastic fibres and are expressed by trophoblast cells (133,134).

MT1/2-MMP (MMP14/15) were found in proliferating as well as invasive trophoblast cells (15,135). Showing a similar distribution pattern as gelatinase A, MT1-MMP might play a role for the activation of pro-gelatinase A (136).

Regulation of matrixin expression in the context of trophoblast invasion seems to be mediated by a large number of agents such as hormones, cytokines and growth factors. Despite the fact that most of the regulatory mechanisms are poorly understood, in vitro studies were indicating both, auto- and paracrine regulation, originating from trophoblast and endometrial cell populations (2).

Most important, and well investigated, are the tissue inhibitors of metalloproteinases (TIMPs). The general marixin-inhibitor ***TIMP-1*** and the rather MMP-2-specific ***TIMP-2*** were found to be expressed by decidual and extravillous trophoblast cells (15,128,130,137). These results also showed the presence of TIMP-2 in the walls of decidual arterioles suggesting its importance for spiral artery invasion and remodelling (137). Further ***TIMP-3***, known as an inhibitor for MMP-9 and MT1-MMP, has also found to be expressed by invasive trophoblast cells (138). Whereas TIMP-1 and -3 are reducing activity of their targets – TIMP-2 is involved in the activation of pro-gelatinase A, forming a trimeric complex with MT1-MMP (65).

Other factors like the constitution of the extracellular matrix have a direct pro-invasive influence on trophoblast cells regarding the expression of specific matrixins (139). For instance, type I collagen had a remarkable stimulatory effect on the secretion of gelatinase by cytotrophoblast cells in vitro (125).

Furthermore, hormones such as progesterone and human chorionic gonadotropine are supposed to have autocrine regulatory effects on invasive progression, as they are secreted in large amounts by first trimester cytotrophoblast cells (2). Whereas progesterone decreases the secretion of gelatinase B by an unknown process – hCG acts contrary and takes specific influence on its upregulation (2,140,141). In ectopic pregnancies hCG levels correlated positively with the depth of invasion (142).

There was a plethora of literature indicating the importance of growth factors and cyto-kines for the regulation of matrixin secretion in the light of trophoblast invasion. The most

important were Interleukin-1 and 6 (IL-1, -6), tumour necrosis factor (TNF), epidermal growth factor (EGF), transforming growth factor (TGF), leukaemia inhibitory factor (LIF), insulin-like growth factor binding protein-1 (IGFBP-1) and insulin-like growth factor II (IGF II) (2,141).

3 *Aims of the study*

The physiological development of the human placenta shares close similarities to the invasive behaviour of a progressing malignant tumour. In contrast to the tumour, the placenta is under control of its almost unlimited invasive potential by a strict regulation program. Human placentation as a highly interesting model for controlled invasion is therefore in the focus of research, unveiling a plethora of factors acting pro-invasive as the versatile family of matrixins. Macrophage elastase (MMP-12), which was recently described in the placenta is probably involved in spiral artery remodelling, but shows also a broad range of features regarding progression, invasion, metastasis and angiogenesis in malignant tumours. The spatial and temporal localisation of this particular member is the content of this thesis.

C Material & Methods

1 *Case selection*

Human tissue containing placenta villi and decidua were obtained from elective vaginal terminations of first-trimester pregnancies (gestational age see Tab. 4) and term placenta after delivery, both at the Hospital for gynaecology and obstetrics at LKH University Hospital Graz. Following macroscopic preparation the collected tissues were either immediately frozen in liquid nitrogen or fixed overnight in 4 % paraformaldehyde (PFA) at 4°C (for PFA production see Protocol 8 in the appendix).

Only 16 of the 22 cases were applicable for this study as some of the tissue samples were inadequate, degenerated or generally non-reactive to our immunofluorescence staining. The Human Research Ethics Committee of the Medical University of Graz approved all procedures involving human tissue in this work. All women gave informed consent for collection and investigational use of tissues.

	Gestational age	**Total**	**Taken**
early first trimester	***6 weeks***	4	3
	7 weeks	2	2
	8 weeks	5	5
middle first trimester	***8-9 weeks***	2	1
	9 weeks	3	1
	9-10 weeks	1	1
	10 weeks	1	0
late first trimester	***11 weeks***	3	2
	12 weeks	1	1
total		***22***	***16***

Tab. 4 – Case selection

2 *RNA isolation, purification and assessment*

To isolate and purify total RNA from frozen tissue the TRI reagent® RT kit (Molecular Research Center Inc., Cincinnati, OH, USA) was used according to the manufacturer's instructions (see Protocol 1).

Homogenization: In this first step RNA was liberated together with other building blocks of the cell by lysation of a 50 to 100 mg piece of tissue. This is performed chemically by the addition of 1 to 2 ml TRI reagent, containing guanidinthiocyanat, as well as mechanically using the Ultraturrax mixer three times for 10 seconds. Intermediate cooling on ice was necessary to preserve the RNA.

The second main component of TRI reagent, the organic solvent phenol, was used to bind the DNA in an acidic milieu, subsequently enabling the RNA to get separated from the latter as well as from the cellular proteins.

A major problem working with RNA was its vulnerability against ribonucleases (RNAses), able to cleave the desired molecule. To inactivate these ubiquitous occurring enzymes several agents including diethylpyrocarbonat (DEPC) or guanidinthiocyanat, which is an component of TRI reagent, can be utilised. Working under an exhaust hood was required as guanidinthiocyanat and phenol were both toxic and volatile.

RNA extraction: After 5 minutes of incubation at room temperature 100 µl of bromchlorpropan (BCP) were added to increase the phase separation that was initiated with phenol in the first step. After another 10 minutes of incubation and 15 minutes of centrifugation at 12.000 g, three distinct phases became visible. The supreme aqueous phase contained the desired RNA followed by a whitish interphase and the reddish organic phase, which both comprised DNA and degraded cellular proteins.

To minimize DNA contamination all centrifugation steps in this protocol were conducted at 4°C using a ***Sigma 3 K 15 laboratory centrifuge*** (Sigma Laborzentrifugen GmbH, Osterode am Harz, Germany).

RNA precipitation: Hereafter the upper aqueous phase was transferred into a new eppendorf tube. Addition of 500 µl ice-cold isopropanol led to precipitation of the RNA. Followed by another 10 minutes of incubation the RNA got concentrated in a pellet by 8 minutes of centrifugation at 12.000 g.

RNA wash: Residual salt ions, which were able to promote RNA degradation and impede the storage process, were removed by an ethanol-washing step. Therefore the supernatant was poured off and 1 ml ice-cold 75% ethanol added to the pellet that was subsequent ly centrifuged at 7.500 g for 5 minutes.

RNA solubilisation: To get the RNA pellet ready for further utilisation or storage, the ethanol supernatant was removed and the pellet briefly air-dried. Avoidance of desiccation was important to enable re-solubilisation. Therefore 100 µl bi-distilled DEPC water, free of ions or RNAse contamination, were added and the RNA gently dissolved for 10 to 15 minutes at 55°C on the heating block.
For quantification and quality assessment the RNA was temporarily put on ice and later stored at -80°C to prevent from degeneration.

Spectroscopic RNA quantification

To proof the quantity of the isolated and purified RNA an analysis was performed using the ***NanoDrop ND-1000 spectrophotometer*** (PEQLAB Biotechnology GmbH, Erlangen, Germany). Beside the quantification also the grade of purification could be assessed by the quotient of the absorption of 260 nm versus 280 nm. The target value was around 2.0 for pure RNA. Contamination with protein, phenol or other substances with an absorption maximum close to 280 nm was presumed, for the appearance of significantly decreased ratios (143).
To conduct a measurement first of all a blank was set with 2µl of the used solvent (in this case: DEPC water). After cleaning the measurement pedestal with fuzz-free tissue, the RNA quantification was conducted in 2µl measuring units. Data was collected and assessed through ***Microsoft Excel*** (Microsoft Corporation, USA) to obtain a target dilution of 100 ng/µl.

Electrophoretic RNA quality assessment

The previously fabricated 1 % agarose gel (0.5 g agarose with 50 ml TAE 1x) with 1 µl ethidium bromide was placed in TAE buffer. Each 5 µl of sample or control RNA were added with 2 µl loading buffer 6x and 5 µl of bi-distilled DEPC water and subsequently placed in the slots of the agarose gel.
While a voltage of 80 V was applied to the gel for 20 minutes the negative charge, caused by the numerous phosphate groups, dragged the RNA molecules towards the anode. The

porous gel exerted resistance against larger molecules and separated them by size. Well preserved RNA displayed two circumscribed bands of ribosomal 18S and 28S RNA. Degraded RNA was discernable by a fuzzy streak of small to large fragments. Finally the separated samples had to be visualized and documented by the ***ChemiDoc XRS translumi-nometer*** (Bio-Rad Laboratories GmbH, Munich, Germany).

At all times, working with the highly carcinogenic agent ethidium bromide had to be performed under high safety conditions in a separated laboratory.

Step	***Description and Time***
Prearrangement	centrifuge on 4°C heating block on 55°C cast mini-gel box with ice
Homogenization	50 – 100 mg tissue with 1-2 ml TRI reagent homogenise – 3x10 sec – temporarily on ice fill homogenizate into eppendorf tubes incubate at room temperature for 5 min
RNA extraction	add 100 µl BCP – shake gently 20x incubate at RT for 10 min centrifuge, 15 min, 12.000 g, 4°C
RNA precipitation	pipet upper phase in new tube 500 µl isopropanol – shake gently 20x incubate at RT for 10 min centrifuge, 8 min, 12.000 g, 4°C
RNA wash	remove supernatant add 1 ml ice-cold 75 % EtOH centrifuge, 5 min, 7.500 g, 4°C
RNA solubilisation	remove EtOH supernatant centrifuge shortly and remove remaining fluid air-dry RNA pellet briefly (avoid desiccation!) add 100 µl RNAse free water dissolve for 10-15 min at 55°C RNA interim storage on ice

Protocol 1 – RNA Isolation

3 *Chip microarray expression profiling*

To identify genes involved in trophoblast invasion, messenger RNA expression of highly (first trimester) and poorly (term placenta) invasive trophoblast cells was compared in a large-scale gene expression profiling using a ***U95A GeneChip microarray*** (Affymetrix, Santa Clara, California, USA). Therefore four populations of isolated trophoblast cells – each two for first trimester and at term – were analysed at the Scripps Research Institute's Affymetrix Array Core facility (144) according to the manufacturer's protocols (145).

4 *Polymerase chain reaction*

The chip array showed overexpression of several genes, including MMP-12, comparing their expression in first and term placenta. Implying a much higher state of MMP-12 activity in early stages of development, we decided to investigate first the temporal and subsequently the spatial localization over the course of the first trimester.

Detection of MMP-12 on the level of RNA was achieved by semi-quantitative reverse transcriptase PCR followed and complemented by in-situ hybridisation (ISH).

RefSeq No.	Gene ID	Gene name		Primers	Size (bp)
NM_002426	MMP-12	Macrophage elastase	fw rv	CACCTGACATGAACCGTGA GCAGAGAGGCGAAATGTGT	393
NM_000989	L30	Homo sapiens ribosomal protein L30	fw rv	GAAGTACGTCCTGGGGTACAA GTCAGAGTCACCTGGATCAAT	238

Tab. 5 – PCR primers for comparing first trimester and term placenta
Legend: fw – forward primer, rv – reverse primer

The same level of hygiene as in the previously working steps was necessary to prevent denaturation of the RNA to achieve high quality output.

First the "master-mix" for the Qiagen one-step PCR kit (Qiagen, Hilden, Germany) had to be evaluated for a total of 10 reactions including MMP-12 (each two samples for first trimester and term placenta), the ribosomal protein L30 as a positive and water as a negative control. To preserve the RNA, the master-mix was pre-fabricated containing the reagents and primers shown in Tab. 5 and Tab. 6. After the mix had been distributed into the PCR-tubes, 2 µl of the RNA earlier isolated and diluted to 100 ng/µl, were added. The last PCR tube was used for the negative control to eliminate influence of the pipet inaccuracy.

Reagent	*Single Volume*	*Total volume*
DEPC ddH_2O	15 µl	150 µl
Buffer 5x	5 µl	50 µl
dNTP-Mix	1 µl	10 µl
5' primer	0.5 µl	5 µl
3' primer	0.5 µl	5 µl
Enzyme mix	1 µl	10 µl
Total volume	**23 µl**	**230 µl**

Tab. 6 – Master-mix for one-step RT PCR

Subsequently the prepared mixture was put into the PTC-200 Thermocycler (GMI Inc., Ramsey, MI, USA) and the standard protocol RT25 was executed (see Tab. 7).

One-step polymerase chain reaction was build up of three stages: in the *first* one the mixture was heated up to 50°C to initiate the reverse transcription. 30 minutes later the total RNA sample was converted into strands of complementary DNA (cDNA). The temperature then was raised to 95°C to disable the reverse transcriptase, activate the Taq DNA-polymerase and un-pair the cDNA strands (as in the denaturation step shown below). The *second* stage included 25 cycles of three repeating steps: denaturation, annealing and elongation. In the first ***denaturation step*** the temperature was raised up to 94°C for 30 seconds to separate the cDNA strands from each other. In the subsequent ***annealing step*** cooling to 60°C for another 30 seconds allowed the primers to bind to the cDNA strands. The temperature optimum for Taq polymerase was 72°C, which was provided within the ***elongation step*** for 60 seconds. This cycle was then repeated 25 times before the final elongation, the *last* phase, was executed at 72°C for 10 minutes.

The amplified final product was then cooled down to 4°C until the samples were taken out and the programme manually stopped.

Time	*Temperature*	*Cycles*	*Step*
30 min	50°C	1	Reverse transcription
15 min	95°C	1	Initial PCR-activation
30 sec	94°C	25	Denaturation
30 sec	60°C		Annealing
60 sec	72°C		Elongation
10 min	72°C	1	Final elongation

Tab. 7 – PCR program RT25 for PTC-200 Thermocycler

Electrophoretic cDNA quality assessment

As for the RNA an agarose gel was prefabricated. This time a 1.5 % gel was used (2.25 g agarose and 150 ml TAE 1x) with 3 µl ethidium bromide, placed in TAE buffer.

For each 25 µl sample 3µl loading buffer 6x was added and placed in the slots. To measure the product's size a 100 kb standard was used. Water was used as negative control. Electrophoresis time was 70 minutes with a voltage of 150 V.

Hereafter the gel had been visualized and documented by the ***ChemiDoc XRS translumi-nometer*** (Bio-Rad Laboratories GmbH, Munich, Germany) and the PCR-products were cut out and stored in eppendorf tubes at -20°C.

5 *Tissue processing and sectioning*

To investigate the changes in the expression pattern of invasive trophoblast cells not only in vitro but also regarding their spatial localization histological working techniques such as in-situ hybridization or immunofluorescence double-labelling were required.

Therefore the collected tissue samples were fixed overnight in 4 % paraformaldehyde (PFA) at 4°C (compare Protocol 8). According to a modified version of the UCSF paraffin embedding protocol for small tissue shown in Tab. 8, the tissue samples passed through dehydration in an ascending ethyl alcohol series, followed by two toluene steps and subsequent immersion of infiltration and embedding paraffin.

As living tissue generally comprises a high percentage of water, paraffin – a hydrophobic agent – would not have been able to infiltrate. The water was therefore removed by bathing the samples in progressively ascending concentrations of alcohol, which itself was

removed by organic solvents such as xylene or toluene. These were highly hydrophobic and able to dissolve long chained hydrocarbons. Differences in the constitution of #6 and #9 paraffin (Richard-Allan Scientific paraffin – Thermo Fisher Scientific: Microm International GmbH, Walldorf, Germany) had a bearing on their properties giving the first a better ability for infiltration and advantages regarding the later production of thin sections for the latter. For embedding the ***MICROM AP280-1, -2 and -3 embedding array*** (Thermo Fisher Scientific: MICROM International GmbH, Walldorf Germany) was used.

Reagent		***Time***
Ethanol	75 %	60 min
	95 %	60 min
	95 %	30 min
	100 %	60 min
	100 %	30 min
Toluene		60 min
Toluene		30 min
Paraffin	#6	60 min
Paraffin	#9	60 min

Tab. 8 – Paraffin embedding [acc. to (146), modified]

After this procedure the blocks were cut in 5µm sections using a ***MICROM HM 335 E microtome*** (MICROM International GmbH, Walldorf, Germany) and placed on ***Superfrost Plus slides*** (Thermo scientific, Gerhard Menzel GmbH, Braunschweig, Germany). A haematoxylin eosin stain was done for histo-morphological quality assessment according to the standard guide shown in Protocol 2.

Step		*Description*	*Time*
Xylene I		*Deparaffinises section*	2 min
Xylene II			2 min
Ethanol	100 %	*Removes xylene*	2 min
	100 %		2 min
	95 %	*Adds water*	2 min
	95 %		2 min
	75 %		2 min
Aqua dest		*Hydrates tissue*	2 min
Hematoxylin		*Stains nuclei: 1-5 min*	2 min [R]
Rinse in H_2O		*Until water remains clear*	2 min
Acid ethanol	0.5 %	*Background decolourisation*	1-5 sec
Rinse in H_2O			2 min
Scott's H_2O		*Until section appears to be blue: 1-5 min*	2 min [R]
Rinse in H_2O		*Several changes*	3 min
Ethanol	75 %		2 min [R]
Eosin		*Depending on desired brightness: 1-30 sec*	20 sec [R]
Ethanol	95 %	*Removes excess eosin*	1 min
	95 %		1 min
	95 %		1 min
	100 %	*Dehydrates tissue*	2 min
	100 %		2 min
Xylene I		*Removes ethanol*	2 min
Xylene II			2 min
Coverslip		*Histomount 2 gtt*	

Protocol 2 – Routine H.E. stain for paraffin sections
[R] = recommended

6 *In-situ hybridisation*

To investigate the spatial localisation of MMP-12 gene expression over the course of the first trimester in-situ hybridization was the method of choice. In general, it allows detecting well-defined mRNA sequences in tissue sections, cultured cells or even whole organisms by hybridizing the complementary strand of the probe to the target sequence. With a sensitivity of 10-20 copies of mRNA per cell this method gives a paramount sensitivity up to single cell resolution (147) but requires profound knowledge and experience to handle it.

As there are countless different ways and protocols to perform in-situ hybridization it is important to focus on the main aspects distinguishing them: the type of probe and its labelling. The probe is embodied by a sequence of nucleotide bases complementary to the desired target mRNA exhibiting a length from 20 – 40 up to more than 1000 base pairs (bp). In the main four different types of probes are used and described below.

Oligonucleotide probes are very popular synthetically produced probes, which are commercially available. With a size of only 40 to 50 bp they can easily penetrate cells or tissues and are also easy to handle as they are resistant against ribonucleases. Being single stranded no denaturation step has to be performed. Synthetic automated production allows producing large quantities of the same high quality, providing commensurableness.

As a disadvantage they are less sensitive, more expensive and designing the probe's sequence can be tricky (147).

Single stranded DNA probes are produced by reverse transcription of RNA or PCR using single antisense primers only, subsequent to the fabrication of the desired cDNA sequence in a first PCR run. Compared to oligonucleotide probes they are larger in size measuring 200 to 500 bp but showing the same good manageability.

Unfavourably their production is time and resource consuming, needs to be performed by seasoned expert professionals and is therefore expensive (147).

Double stranded DNA probes can be fabricated either using bacterial plasmids for replication or by PCR. Both methods have their pros and cons, whereas the latter provides a highly pure sample it is also very expensive compared to the replication in bacteria. That method, by contrast, needs several steps to amplify the desired sequence, lyse the bacteria

and excise the sequence with restriction enzymes. But it also makes it possible to achieve large quantities with a smaller budget.
The biggest disadvantage of this probe is the need for denaturation as the double stranded probes have to melt before binding to the target sequence. It is also less sensitive due to the tendency of DNA-DNA rehybridisation (147).

RNA probes, also called riboprobes, are still the most widely used probes as they feature some convincing advantages. They are produced either through RNA polymerase-catalysed mRNA transcription, or by in vitro transcription subsequently to the linearization of plasmid DNA using RNA polymerases of bacteriophage origin.
The advantage of the RNA-RNA hybrids feature high thermostability making them resistant to ribonuclease-digestion, and can be used to remove excessive RNA, which has not hybridized to reduce background staining.
Otherwise this is also their downside as they are highly sensitive to RNAses in the non-hybridized state, making uncompromisingly sterile working conditions a basic requirement for success. The need for well-experienced professionals limitates this method (147).

There are at large two different ways of labelling probes: either radioactive or hapten-based.
Classically radioactive isotopes such as ***^{3}Hydroxygen, ^{35}Sulfur*** or ***^{32}Phosphate*** (^{3}H, ^{35}S, ^{32}P) are used if high resolution is required. Which one is used depends amongst other things of the specific question. Subcellular resolution and years of storability are features of ^{3}H with a half-life of 12 years and therefore the need of several weeks of exposure. ^{35}S however has a half-life of only 87 days limiting its shelf life but leading to faster results (normally within one week – but longer for weak signals). The resolution is within the diameter of one cell, thus still excellent compared to non-radioactive labels. ^{32}P featured with a 14-day half-life and a poorer resolution is therefore only mentioned for the sake of completeness. Visualization is achieved by exposing a photographic film or emulsion with subsequent development (148).
The disadvantage of radioactive labelled probes is the need for a special equipped laboratory with special trained expert staff. It is expensive and time consuming but still the gold standard if high accuracy and sensitivity is requested.

Easier and safer to handle are the non-radioactive, hapten-based labels. The most common are ***biotin***, which is detected by avidin or streptavidin as well as ***digoxigenin*** (DIG), which can be detected by antibodies. These probes can be stored at -20°C for 1 to 2 years.
While fluorescing labels can be observed directly, however DIG requires an intermediate step with anti-DIG-antibodies linked to an amplifier such as peroxidase or alkaline phosphatase. This enzyme can convert the substrate 5-bromo-4-chloro-3-indolyl phosphate (BCPI) in the presence of the oxidant nitro blue tetrazolium (NBT) into a blue precipitate. Biotin can either be detected by anti-biotin-antibodies or by (strept-) avidin also conjugated to direct visual labels or amplifiers (149).

Considering in-situ probes the difference between ***sense*** and ***antisense*** is important. RNA that can be translated into a protein sequence is called sense. As hybridization requires a complementary strand to bind to the desired (sense) mRNA within the investigated tissue, only an antisense-strand can be used as a probe. As a control for specificity one should test slides with antisense and sense probes. The first is binding to mRNA by sequence specific hybridization and to non-specific targets by chemical interactions. The sense probe only to non-specific targets. If the sense is negative, the antisense signal must be specific for the target mRNA.

In some cases ***permeabilisation*** can be a problem for the large probes as cell membranes or proteins surrounding the target mRNA might bar the way. To solve this problem some protocols make use of 0.2M ***hydrochloric acid*** or detergents such as ***Triton X-100*** or ***sodium deodecyl sulphate*** (SDS). In other protocols the non-specific ***proteinase K*** is used to remove target-surrounding proteins, but it always has to be used with caution to preserve integrity of the sample.

6.1 Preparatory work

MMP-12 cDNA, generated using the primers shown in Tab. 9, was the starting template for subsequent steps in ISH-probe synthesis.

RefSeq No.	Gene ID	Gene name		Primers	Size (bp)
NM_002426	MMP-12	Macrophage elastase	fw rv	ACACATTTCGCCTCTCTGCT CCTTCAGCCAGAAGAACCTG	192

Tab. 9 – PCR primers for MMP-12 cDNA template synthesis
Legend: fw – forward primer, rv – reverse primer

6.2 Radioactive ISH

To detect the presence and localisation of MMP-12 mRNA the most sensitive method, using ^{35}S-labelled riboprobes, was applied first.

To synthesize the probes, ^{35}S-UTP (NEN New England Nuclear Corp. GmbH, Perkin Elmer Life and Analytic Sciences, Vienna, Austria) with an activity of 1.200 Ci/mmol[7] (respectively 44,40 TBq/mmol) was used.

In-situ hybridization was executed according to the S35 protocol (see Protocol 3) on the base of a manual published by Josiah N. Wilcox (Genentech Inc. San Francisco, CA, USA). The slides were developed as shown in Protocol 4 at eight weeks of exposure.

All procedures, interacting with radioactive agents, have kindly been performed by B. Sc. Carmen Tam-Amersdorfer. Due to security regulations permission to those restricted areas is only granted to specially trained and authorised expert staff.

[7] Curie [Ci] is a still used non-Si unit, defined as 1 Ci = 3.7 x 10^{10} decays per second. It is applicable to measurement and expression of the quantity of a radioactive material.

Step	*Description*	*Time*
Deparaffinisation	Xylene (two times)	2x 10 min
Remove xylene	Ethanol 100 % (two times)	2x 5 min
Add water	Ethanol 95 % / Saline	2 min
	Ethanol 85 % / Saline	2 min
	Ethanol 60 % / Saline	2 min
	Ethanol 30 % / Saline	1 min
Hydrate Tissue	Saline	1 min
Washing	PBS 1x at RT	30 sec
Fixation	PFA 4 % at 4°C	10 min
Washing	SSC 0.5x at RT	5 min
Deproteination	Proteinase K solution 1 µg/ml in RNAse buffer	10 min
Washing	SSC 0.5x at RT	10 min
Post fixation	PFA 4%	3 min
Washing	SSC 0.5x at RT	5 min
Prehybridisation	Remove excess liquid around sections Position slides in wet-box (Box-buffer) Cover sections with *100 µl rHB2* Incubation at 56°C	 1 h
Hybridization mix	For each 100 µl prehybridisation buffer: 2.0 µl probe (300k cpm/µl in TE) and 1.0 µl tRNA (50 mg/ml stock)	
Hybridization	Heat up to 95°C Put on ice and add 17.0 *µl rHB2* 20 µl hybridization mix to each 100 µl of prehybridisation solution; coverslip Incubation at 55 – 58°C	3 min Overnight
Washing	SSC 2x at RT (two times)	2x 10 min
Digestion	Immerse in RNAse A solution (10 mg/ml) at RT **<u>CAUTION: use filter tips – do not contaminate pipet!!</u>**	30 min
Washing	SSC 2x at RT (two times)	2x 10 min
	SSC 0.1x at 60°C	2 h
	SSC 0.5x at RT (two times)	2x 10 min
Dehydration	Ethanol 50 % / Ammonium acetate 0.3 M	1x 2 min
	Ethanol 70 % / Ammonium acetate 0.3 M	1x 2 min
	Ethanol 90 % / Ammonium acetate 0.3 M	1x 2 min
Drying	In fume hood	2 hrs
Autoradiography	Dip in Kodak NTB2 nuclear emulsion, Diluted 1:1 with water	
	Dry in the dark at room temperature	Overnight
Exposure	In the dark at 4°C with desiccant	1-8 weeks

Protocol 3 – ^{35}S-riboprobe protocol for radioactive ISH

Step	*Description*	*Time*
Development	Kodak D19, diluted 1:1 with cold water	3 min
	Water stop	20 sec
	Kodak fixer, full strength	3 min
	Water (three times)	3x 5 min
	Counterstaining	

Protocol 4 – Development of radioactive ISH using Kodak NTB2 emulsion

6.3 Non-radioactive ISH

After the presence of MMP-12 mRNA was detected by radioactive in-situ hybridization, the additional samples had to be tested. As radioactive ISH was a very reliable but also cost- and time-intensive method, preference was given to the use of DIG-labelled probes. Using the previously synthesised probes the hybridization was performed on the first day according to Protocol 5. On the second day *sheep anti-Dig-antibodies, Fab fragments* (Roche Applied Science, Mannheim, Germany) were applied for signal detection with NBT/BCIP and counterstained with Methyl Green as described in Protocol 6.

Pictures of radioactive and non-radioactive ISH were taken using the ***Motic BA310 trinocular microscope***, equipped with a ***Moticam Pro 285 B scientific CCD camera*** and processed with the image capturing and analysis software ***Motic Images Advanced 3.2*** (all three: Motic Deutschland GmbH, Germany).

Step	*Description*	*Time*
Day 1 – Preparation and hybridization		
Deparaffinization	Xylene (two times)	2x 10 min
Remove xylene	Ethanol 100 % (two times)	2x 5 min
Add water	Ethanol 95 % / Saline	2 min
	Ethanol 85 % / Saline	2 min
	Ethanol 60 % / Saline	2 min
	Ethanol 30 % / Saline	1 min
Hydrate Tissue	Saline	1 min
Washing	PBS 1x at RT	30 sec
Fixation	PFA 4 % at 4°C	10 min
Washing	SSC 0.5x at RT	5 min
Deproteination	Proteinase K solution 1 µg/ml in RNAse buffer	10 min
Washing	SSC 0.5x at RT	10 min
Post fixation	PFA 4%	3 min
Washing	SSC 0.5x at RT	5 min
Prehybridization	Remove excess liquid around sections Position slides in wet-box (Box-buffer) Cover sections with *100 µl DIG hybridization solution* Incubation at 55°C	 1 h
Hybridization mix	Calculate dilution Add probe	
Hybridization	Heat up to 95°C Put on ice and remove excess liquid from slides Add 100 µl of hybridization mix; coverslip Incubation at 55 – 58°C	5 min Overnight

Protocol 5 – ISH DIG-protocol, Day 1

Step	*Description*	*Time*
Day 2 – DIG-antibodies and detection		
Washing	SSC 2x at RT (two times)	2x 10 min
Digestion	Immerse in RNAse A solution (10 mg/ml) at RT **CAUTION: use filter tips – do not contaminate pipet!!**	30 min
Washing	SSC 2x at RT (two times)	2x 10 min
	SSC 0.1x at 60°C	2 h
	SSC 0.5x at RT (two times)	2x 10 min
Incubation	Buffer #1 (TRIS pH 7.5, NaCl)	10 min
Block	Normal sheep serum at RT Buffer #1 2 µl, Triton-X-100 6 µl, Normal sheep serum 40 µl (diluted 1:50)	20 min
Anti-DIG-Ab	At RT Buffer #1 2 µl, Triton-X-100 6 µl, Normal sheep serum 20 µl (diluted 1:50), Anti-DIG-Antibodies (AP-Fab) 4 µl (dilute 1:500)	2 h
Washing	Rinse in Buffer #1 (two times)	2x 10 min
Washing	Rinse in Buffer #3 (TRIS pH 9.5, NaCl, $MgCl_2$)	2 min
Staining	NBT 60 µl, BCIP 3.5 µl, Levamisole 20 µl in 20 ml Buffer #3 Incubation at RT in the dark	30 min – overnight
Stop reaction	Buffer #4 (TRIS pH 8.0, EDTA)	2 – 4 min
Washing	Rinse in water	
Counterstain	Methyl Green	3 min
Washing	Rinse in distilled water	
Finish	Coverslip with Kaiser Gelatine	

Protocol 6 – ISH DIG-protocol, Day 2

7 *Immunofluorescence double staining*

Radioactive and non-radioactive in-situ hybridization showed the presence and localization of MMP-12 mRNA in first trimester and term placenta. To furnish proof of the ***translation*** from messenger RNA into protein in situ, immunohistochemical working techniques were necessary.

Generally investigation, not only of the presence, but also of the ***origin*** on a cellular level necessitates detecting different markers with a high resolution on the same section. Working techniques for parallel detection in standard bright field immunohistochemistry have been described, but these methods are more complicated. Easier to handle and better for later analysis is the ***double-label fluorescence immunohistochemistry***.

This multicolour method either uses primary antibodies labelled with fluorescent dye in a ***direct*** method, or the fluorescence of labelled secondary against the primary antibodies in the ***indirect*** method. For detection of weak signals as they can be found with MMP-12 the second was the method of choice providing adequate signal amplification.

Working with more than one primary antibody necessitates careful considerations about their choice and constitution. To avoid cross-reactions when the secondary antibodies are applied it is recommended to use primary antibodies of different species in the first line (150). If primary antibodies of different species are not available, it is possible to use different IgG subtypes or even different haptenylations if they are of the same species and subtype (151).

The advantages of the direct method are the need for fewer reagents and working steps as well as lower background for the price of a weaker signal. Furthermore it allows the parallel detection of up to seven different antigens at the same time (152).

In return unlabelled primary antibodies as well as labelled secondary antibodies targeting for immunoglobulins of foreign species are normally easier to acquire and cheaper, as they are produced in much larger quantities.

As primary antibodies we used *monoclonal rabbit anti-human MMP-12* (hinge region, ab38935; Abcam plc, Cambridge, MA, USA) and *monoclonal mouse anti-human HLA-G* (clone: MEM-G/1; BioVendor GmbH, Heidelberg, Germany) as a marker for invasive trophoblasts. The dilution was 1:1.500 for MMP-12 and 1:2.000 for HLA-G.

When further experiments had to be performed at a later stage, the original MMP-12 (hinge region) ran out and had to be replaced by *polyclonal rabbit anti-human MMP-12*

(carboxyterminal end, ab66157: Abcam plc, Cambridge, MA, USA) diluted 1:750. Markings have been placed in the results part to clearly differentiate images obtaining the different clones.

The secondary antibodies were *goat anti-rabbit* labelled with Dylight488 and *goat anti-mouse* conjugated with Cy3 (both: Jackson ImmunoResearch Laboratories INC, West Grove, PA, USA), either concentrated 1:800. As a counterstain for cell nuclei 4',6-diamidino-2-phenylindole (DAPI – Invitrogen, Life Technologies, Grand Island, NY, USA), binding to A-T rich regions of the DNA, was used in a concentration of 1:100.

Primary antibodies			***Secondary antibodies***			***Ex [nm]***	***Em [nm]***	***Colour***
Target	***Species***	***Dilution***	***Species***	***Dilution***	***Dye***			
MMP-12 (a)	Rb vs. H	1:1500	G vs. Rb	1:800	Dylite488	493	518	Green
MMP-12 (b)	Rb vs. H	1:750	G vs. Rb	1:800	Dylite488	493	518	Green
HLA-G	M vs. H	1:2.000	G vs. M	1:800	Cy3	550	570	Red
CD34	M vs. H	1:200	G vs. M	1:800	Cy3	550	570	Red
CD68	M vs. H	1:250	G vs. M	1:800	Cy3	550	570	Red
CK-7	M vs. H	1:10.000	G vs. M	1:800	Cy3	550	570	Red

Cell nucleus stain

Target	***Dilution***	***Dye***			
DNA	1:100	DAPI	358	461	Blue

Tab. 10 – Antibodies and cell nucleus stain for fluorescent IHC
Legend: hinge region (a), carboxyterminal end (b), excitation (Ex), emission (Em), goat (G), human (H), mouse (M), rabbit (Rb);

Beside *HLA-G* (MEM-G/1) for invasive trophoblast cells, a set of other antibodies was used for further differentiation. Do determine whether the positive signals were derived from Hofbauer cells (which are a known source of elastase activity) *CD68* – a classical marker for macrophages – was targeted with *monoclonal mouse anti-human CD68* (clone: PG-M1) antibodies. Further, distinction of vessel-derived MMP-12 activity was gained by the use of *monoclonal mouse anti-human CD34 Class II* (clone: QBEnd-10) and *monoclonal mouse anti-human cytokeratin-7* (clone: OV-TL 12/30) antibodies. Whereas the first is primarily found on capillary endothelial cells and often used as an alternative for the *von Willebrand Factor*, the second is located on larger vessels as well as glandular ducts. Antibodies against CD68, CD34 and CK-7 were all produced by Dako (DakoCyto-

mation, Glostrup, Denmark). An overview of the antibodies used and the nucleus stain is summarised in Tab. 10.

The two-day protocol for double-label immunofluorescence is listed in Protocol 7. Starting with deparaffinization and hydratization on day one, subsequent heating in a sodium-citrate-buffer was performed for ***antigen retrieval***. In general formalin degenerates proteins and alters their conformation during the process of fixation. Breaking of the methylene bridge cross-links by heat [8] or proteolytic enzyme digestion [9] (e.g. with proteinase K, trypsin or pepsin) allows the proteins to change back close to their tertiary conformation. This allows better access to the epitopes and increases the signal-to-background ratio in formalin-fixed paraffin-embedded tissues (FFPE) (153,154).
In our protocol the sections were heated in sodium-citrate-buffer (pH 6.0) in a microwave oven set to 'medium' for a total of 10 minutes (2x 4 min and 1x 2 min). Decreasing levels of buffer had been refilled at the pauses. After the slides had cooled down to room temperature a washing step in TBST was performed. This buffer mixed of Tris, KCl, NaCl and Tween 20 (a polysorbate surfactant) acts as a detergent, ***reducing non-specific antibody binding***. Blocking with H_2O_2 after bringing up a circular hydrophobic barrier around the sections was performed for 12 minutes followed by another washing in TBST. Finally the primary antibody-mix of anti-MMP-12 and anti-HLA-G was applied and incubated overnight in a wet chamber at 4°C (153).
The second day started with a TBST wash and subsequent application of the secondary antibody-mix for 30 minutes. Followed by another TBST washing step the DAPI cell nuclei stain was applied and incubated for 20 minutes. After final washing the slides were covered with ***Vectashield mounting medium*** (Vector Laboratories, Burlingame, CA, USA). All buffers used can be referred to appendix "J – Buffers and Protocols".

Fluorescent pictures were taken with the ***Leica DM4000B trinocular microscope***, equipped with a ***Leica DFC300 FX digital camera*** and processed with the image capturing software ***Leica Application Suit, Version 3.6.0*** (all three: Leica Microsystems Ltd., Heerbrugg, Switzerland).

[8] HIER – heat-induced epitope retrieval
[9] PIER – proteolytic-induced epitope retrieval

Step	*Description*	*Time*
Day 1 – Preparation and primary antibody		
Deparaffinisation	Xylene (two times)	2x 5 min
Remove xylene	Ethanol 100 % (two times)	2x 5 min
Add water	Ethanol 95 % / Saline	5 min
	Ethanol 60 % / Saline	5 min
Antigen retrieval	Sodium-citrate-buffer (pH 6.0)	2x 4 min
	Microwave: medium	1x 2 min
Cooling down	To room temperature	20-40 min
Washing	In Tris-buffered saline Tween-20 (TBST)	5 min
Peroxidase-Block	Circle section with PAP-pen	
	H_2O_2-onto section	12 min
Washing	In TBST	5 min
Primary antibody	Cover circled area with 115 µl primary antibody	
	Incubate at 4°C	Overnight
Day 2 – Secondary antibody		
Washing	In TBST	5 min
Secondary antibody	Cover circled area with 115 µl secondary antibody	
	Incubate at RT	30 min
Washing	In TBST	5 min
DAPI	Cover circled area with 115 µl secondary antibody	
	Incubate at RT	20 min
Washing	In TBST	5 min
Coverslip	Add Vectashield drop-wise	

Protocol 7 – Immunofluorescence double staining

8 *Picture analysis and statistical evaluation*

Analysing MMP-12 expression on the protein level qualitatively was enabled by the investigation of signal patterns within the cell columns.

Quantification was much more complicated in comparison to a cell suspension for example, placental tissue was extremely inhomogeneous. Cell columns and villi were orientated in an irregular three-dimensional pattern when they were embedded and cut. The cutting edges therefore could run in different planes in space with subsequent incomparability of the results from two different sections – even from two different areas within a single section.

Instead of counting total numbers for inter-individual comparison, ratios were taken. Here the total number of counted cells was negligible as only their relation to the total cell count as reference constancy was regarded. As all the MMP-12-positive cells seemed to be a subpopulation of invasive cytotrophoblast cells, therefore HLA-G was a valuable marker outlining the reference cell population.

To analyse the density of MMP-12-positive cells they were counted within the total of all HLA-G positive cells of the observed cell column. The following formula shows the ratio R by division of the number of MMP-12 positive cells through the number of invasive trophoblast cells.

$$R = \frac{n_{MMP\text{-}12\text{-}pos}}{n_{HLA\text{-}G\text{-}pos}}$$

Counting the desired signals in merged double-label immunofluorescent images was complicated for both, the human eye as well as a computer program. To enable computer assisted counting the different coloured layers green, red and blue separated by band pass filters were segregated and analysed separately.

The indirectly Cy3 marked HLA-G positive cells acted as a landmark to narrow down the desired area containing invasive trophoblast cells. Within this region of interest (ROI) Dylight488-marked MMP-12-positive cells as well as DAPI-stained cell nuclei were captured and counted using ***Motic Images Advanced 3.2*** (Motic Deutschland GmbH, Germany).

To reduce the high error rate of the software used directly on fluorescent images, they had to be labelled manually. For this purpose each target cell in each image was separately marked by a colour dot using the open source software ***GIMP*** (Open Source, GNU

General Public License, Version 3). To reduce false positive counts it was necessary to choose a colour, which was not represented in the corresponding colour histogram. Further error rate reduction was gained by the utilization of a colour dot with a minimal size of *'(15)'*. The so prepared images (as in Fig. 22 E and F) were loaded in Motic Images Advanced and counted as described below.

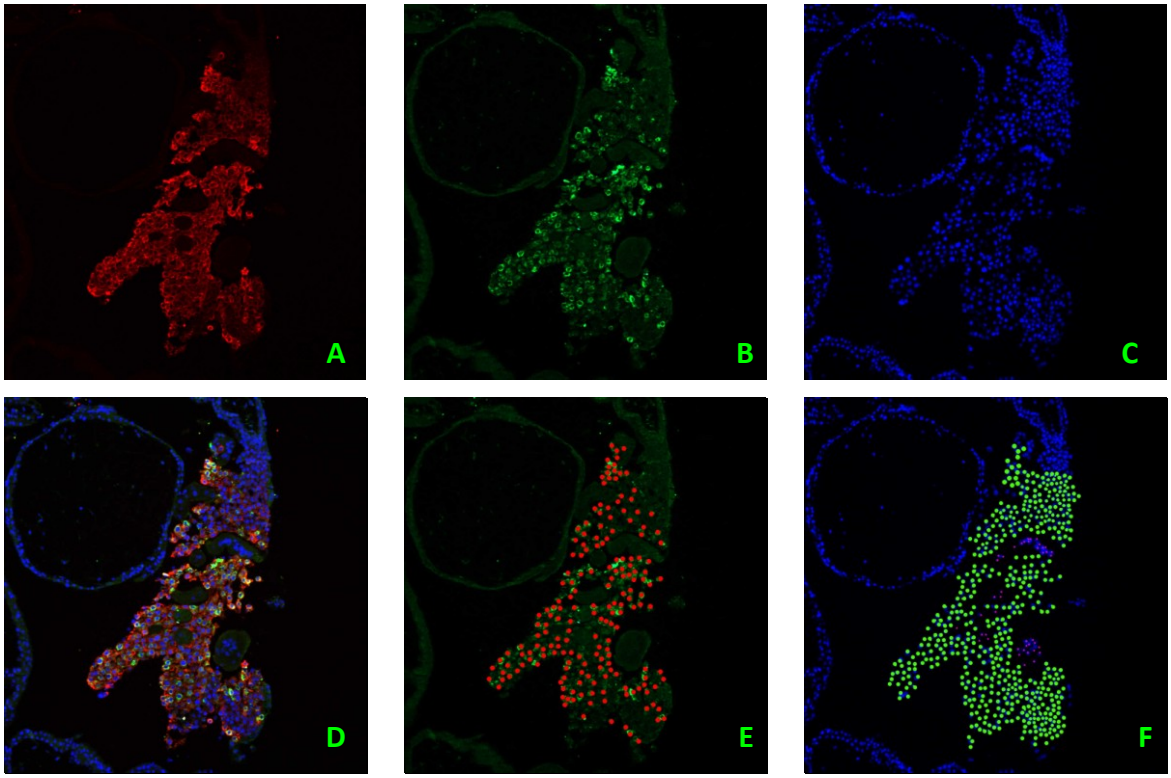

Fig. 22 – Double-label IF-images after marking: 8/007-1, placenta 8th WOP **(200x)**
A-F: Cell column marked with fluorescent IHC, different layers; **A:** HLA-G (Cy3); B: MMP-12 (Dylight488); **C:** Cell nuclei (DAPI); **D:** merged image of A-C; **E:** Positive MMP-12-signals marked with red dots; **F:** Cell nuclei of invasive CTB marked with yellow dots; **E, F:** only the signals and cell nuclei within the HLA-G positive area are marked and therefore counted.

Motic Images Advanced 3.2 is a software package to analyse and assemble microscopic images in multiple ways. For this study it was only used to gather and count the previously marked signals. The detailed description of this process is covered below.

Fig. 23 and Fig. 24 show the upper and lower bars of the working screen. All commands to run the process can be selected by the buttons, shown and described within the instruction in Fig. 25 to Fig. 28.

Fig. 23 – Screenshot: Motic Images Advanced, upper bar

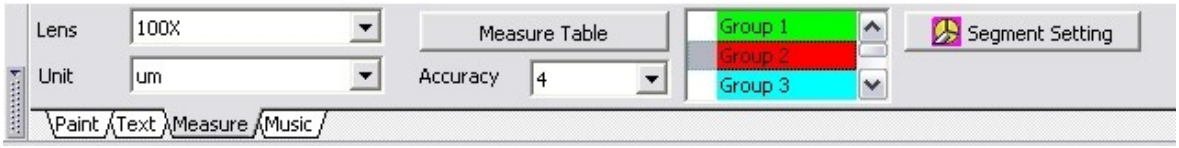

Fig. 24 – Screenshot: Motic Images Advanced, lower bar

1. Selection of target area
2. Mark selection
3. Enlarge selection
4. Reduce noise, fill holes
5. Measure selection

Fig. 25 – Important buttons and settings

In Fig. 26 the working screen of the program is shown with an already loaded image of the green fluorescence image-layer. A selection of all loaded pictures is present on the right side. In the present one the positive signals have been marked with red dots. Violet dots mark the undesired regions, delimiting them from the area of interest.

To define this area for automated processing (as already shown in the image) it has to be limited using the “selection button” No. 1 in Fig. 25.

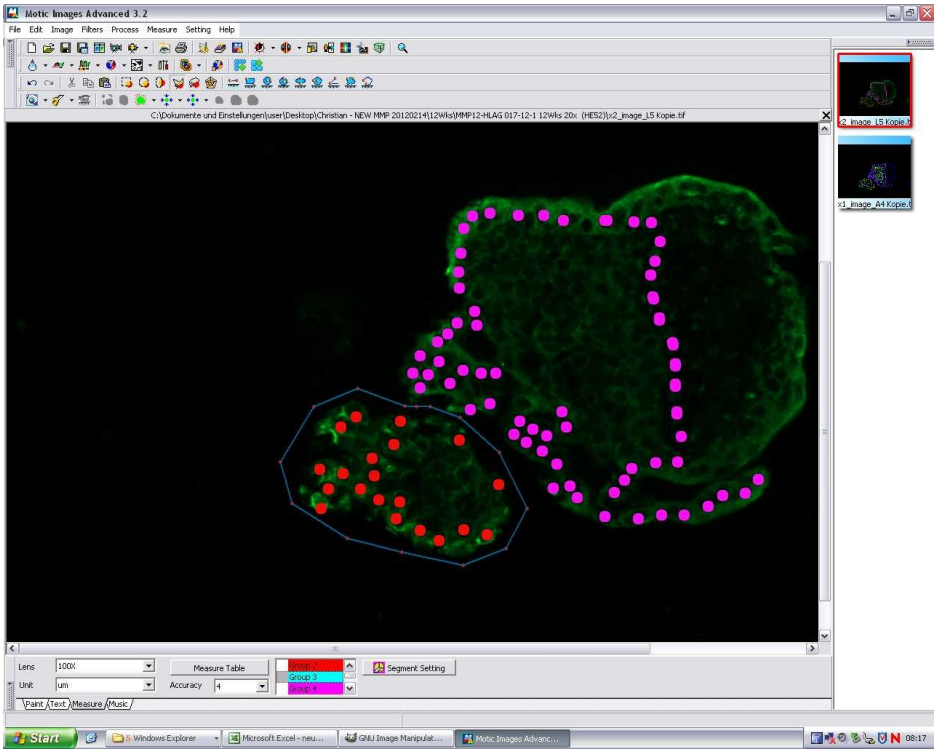

Fig. 26 – Screenshot: Working screen

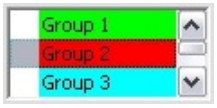

Before the signals can be marked in the now limited area of interest allocation to a group and marking paint has to be performed.

Fig. 27 – Group selection

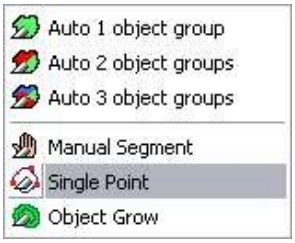

The button No. 2 (see Fig. 25) releases the drop-down menu shown in Fig. 28.

To capture the colour dots the "single point"-setting in the drop-down menu highlighted in grey has to be chosen.

Fig. 28 – Screenshot: Drop-down menu: mark selection

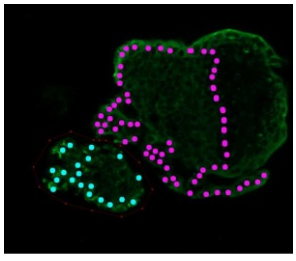

All successfully detected dots are then marked in the group-corresponding marking paint. They change from red to turquoise in this example.

Fig. 29 – Screenshot: Selection tagged with marking paint

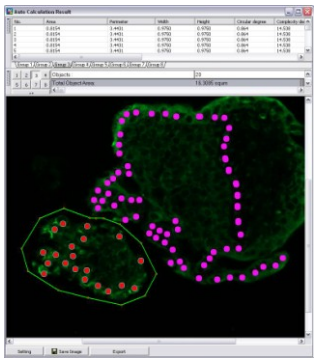

Button No. 4 (see Fig. 25) reduces noise caused by inadequate colour detection and can be supplemented with button No. 3, which enlarges the size of the group mark. The latter should not be used if the signals are in close vicinity as this may lead to reduced sensitivity. 'Measure table' (button No. 5 in Fig. 25) starts counting of the detected colour dots and creates a table for the data output for the marked groups.

Fig. 30 – Screenshot: Data output after measurement

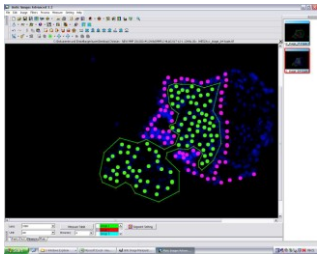

The same procedure is then repeated for the DAPI stained image layer. Starting with narrowing down the area of interest, selecting the group and colour followed by single point selection.

Fig. 31 – Screenshot: Area of interest – DAPI

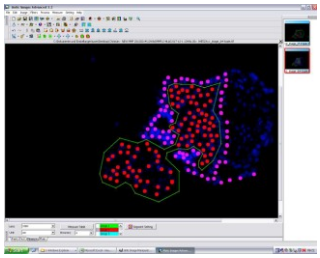

Hereafter the detected colour dots are tagged with the group-corresponding marking paint. Red is usually used for DAPI image layers, as this creates virtually no background.

Fig. 32 – Screenshot: Selection tagged with marking paint

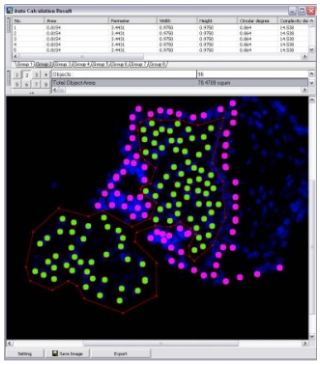

Subsequent to noise reduction and adjustment as previously described the signals are counted and the output collected in a Microsoft Excel sheet.

Fig. 33 – Screenshot: Data output for DAPI

This process was manually repeated for all images and the collected output was calculated to achieve ratios for the different samples and stages.

D Results

1 *Chip microarray*

Comparison of highly (first trimester) and poorly (term placenta) invasive trophoblast cells showed 220 invasion or migration-related genes. For MMP-12 a decrease of 89.58 fold was observed comparing messenger RNA-expression of the two measure points (shown in Tab. 11).

Gene	*First trimester placenta*	*Term placenta*	*Expression ratio*
MMP-12	10767.30 [A]	120.20 [A]	**89.58** [B]

Tab. 11 – Chip microarray data for mRNA expression of MMP-12
A: absolute measurements, arbitrary parameters; **B:** relative relationship between first trimester and term placenta measurements, no parameter;

2 *Polymerase chain reaction*

Subsequently to the chip array, which hint at the potential differences regarding the expression of MMP-12 in first trimester and term placenta, a semiquantitative RT-PCR was performed. In Fig. 34 A the 100 bp standard on the left is adjacent to four placental samples, each two of the first trimester (FTP) and of term (TP), as well as water representing the negative control on the right edge. In contrast to the term placenta, the first trimester samples displayed well-circumscribed bands of very similar intensity and a product size of around 400 bp, matching the expected 393 bp of the desired product. The negative control also showed no signal.

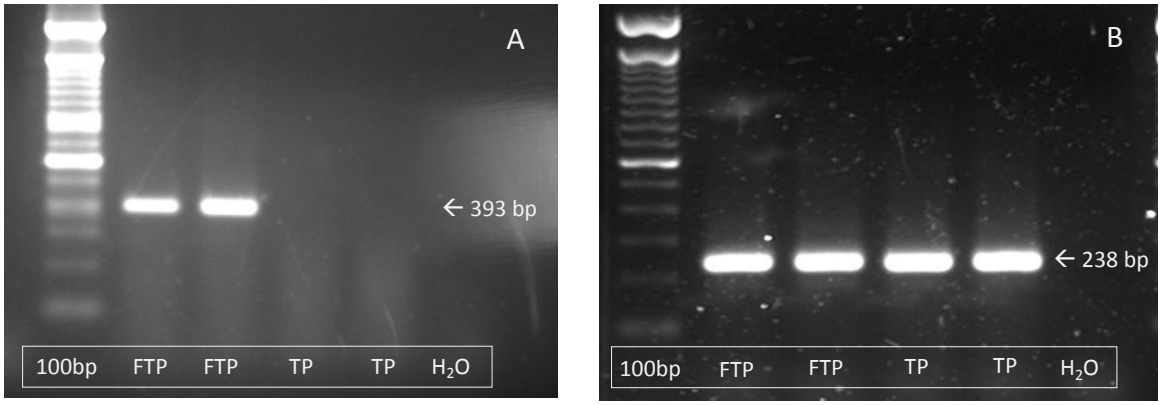

Fig. 34 – Gel electrophoresis for MMP-12 and L30 PCR-products; A: MMP-12, **B:** L30
Legend: FTP: first trimester placenta, TP: term placenta;

In Fig. 34 B the results for L30 as the positive control is summarized. All four individuals showed identical bands, matching the expected size of 238 bp. Again, water as the negative control was placed in the right outer well, and showed no signal.

3 *Images and image analysis*

GeneChip microarray analysis and polymerase chain reaction had shown the presence of MMP-12 in placental tissue and its varying expression over time with increased levels at first trimester and a large decrease towards term. In the following step mRNA expression was analysed with in-situ hybridization to gather information about its spatial localization. To prove not only expression but also the translation into the final protein product as well as to quantify its temporal change during the first trimester, double label fluorescent immunohistochemistry was used.

To understand the various levels of detection and their analysis, images from in-situ hybridization and immunofluorescence are presented below. Tab. 12 gives a summary of the abbreviations and symbols used to explain the illustrations.

STB	Syncytiotrophoblast
vCTB	Villous Cytotrophoblast
evCTB	Extravillous cytotrophoblast
CC	Cell column
PSGC	Placental site giant cells
E	Erythrocytes
D	Decidua
EM	Extraembryonic mesenchyme
TB	Trophoblast plugging
UPA	Utero-placental artery
UPV	Utero-placental vein
VL	Vessel lumen
⇨	S35 autoradiography
⇨	Dig-NBT/BVIP

Tab. 12 – Legend for abbreviations in images

4 *In-situ hybridisation*

4.1 Radioactive ISH

In Fig. 35 to Fig. 37 images of radioactive labelled ISH-probes against MMP-12 mRNA were taken as bright- and darkfield images after 8 weeks of exposure, grouped according to their stage (6, 8 and 11 wks.).

Silver granules within the pictures (examples marked by fascinated arrows as shown in Tab. 12) indicated positive signals of extravillous trophoblast cells (evCTB) in the cell columns (CC). Furthermore syncytiotrophoblast (STB) and cytotrophoblast cells (CTB) as well as placental site giant cells (PSGC), were all negative for MMP-12. In the course over time the signal seemed to decrease, so basically only background was observed at 11 weeks of pregnancy (compare Fig. 37).

Differentiation between specific and nonspecific binding was proofed on the base of anti-sense (A, B) as well as sense-control (C,D) probes and shown in Fig. 36.

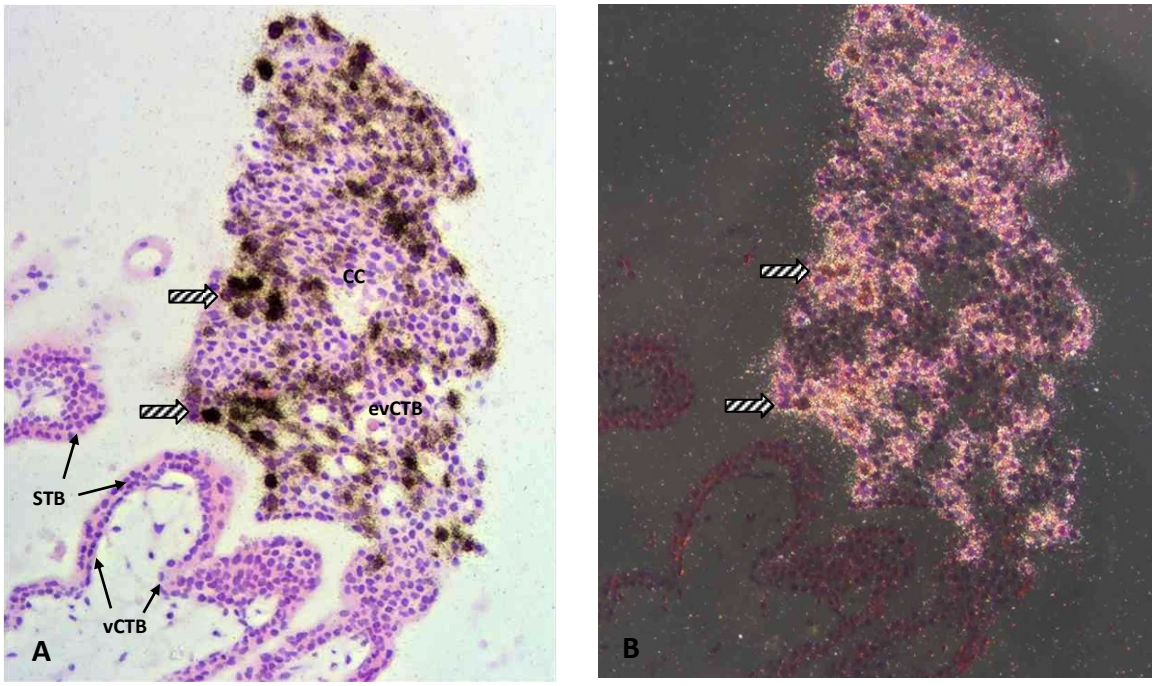

Fig. 35 – ^{35}S labelled ISH probe for MMP-12 mRNA (anti-sense), placenta 6/021-1, 6th WOP (200x)
Exposure time: 8 wks.; **A:** Brightfield; **B:** Darkfield
Symbols: villous/extravillous cytotrophoblast (v/evCTB), syncytiotrophoblast (STB), erythrocytes (E), decidua (D), cell column (CC), placental site giant cells (PSGC), fascinated arrows (positive dig signal);

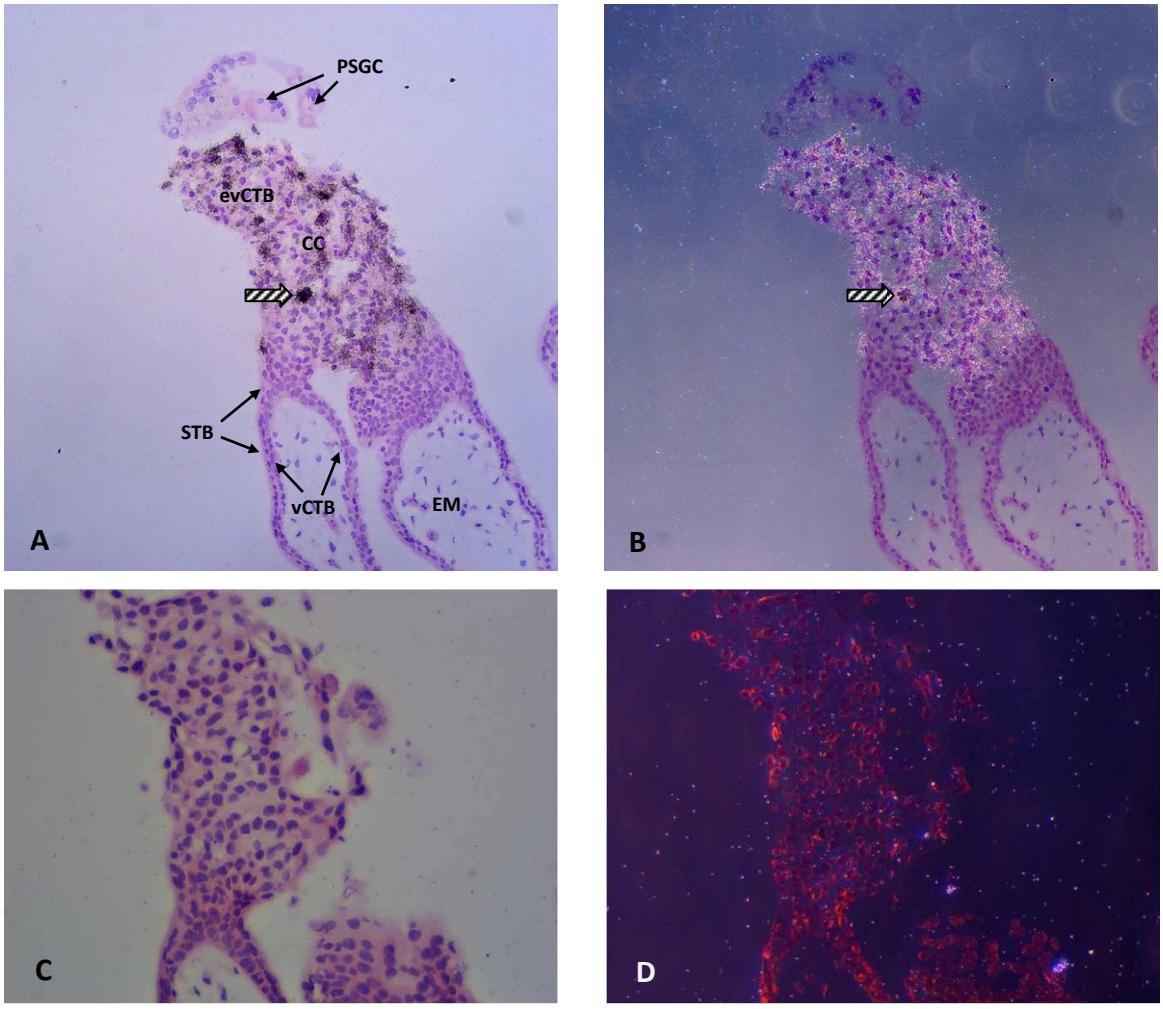

Fig. 36 – ^{35}S labelled ISH probe for MMP-12 mRNA, placenta 8/010-1, 8th WOP (200x)
Exposure time: 8 wks.; **A, C:** Brightfield; **B, D:** Darkfield; **A, B:** Anti-sense; **C, D:** *Sense-control*
Symbols: villous/extravillous cytotrophoblast (v/evCTB), syncytiotrophoblast (STB), erythrocytes (E), cell column (CC), placental site giant cells (PSGC), fascinated arrows (positive dig signal);

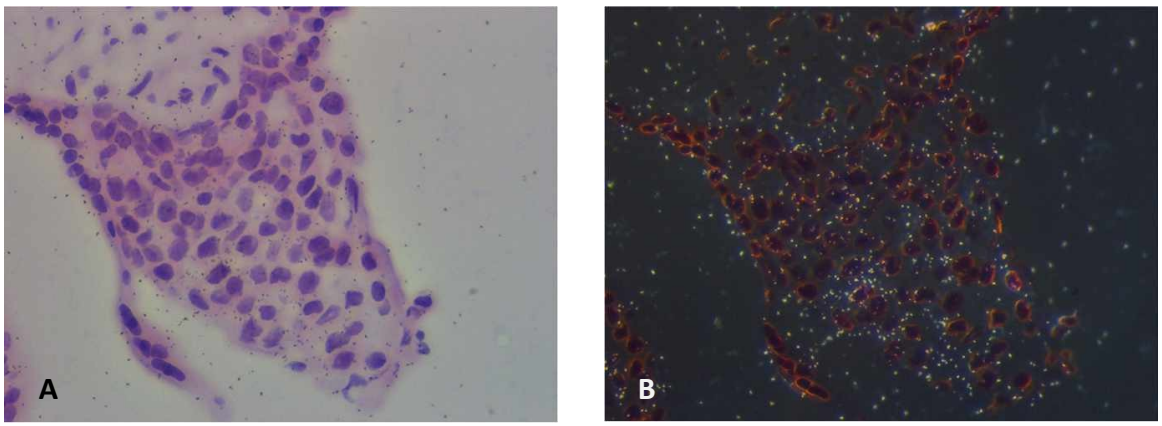

Fig. 37 – ^{35}S labelled ISH probe for MMP-12 mRNA (anti-sense), placenta 11/015-2, 11th WOP (400x)
Exposure time: 8 wks.; **A:** Brightfield; **B:** Darkfield

4.2 Non-radioactive ISH

The images shown in Fig. 38 to Fig. 41 are examples for non-radioactive, Dig-labelled in-situ hybridization aiming for MMP-12 mRNA. Placenta and decidua tissue samples of the weeks 6, 7, 8, 9-10, 10 and 11 had been used. Distinction against nonspecific binding was proven on the base of comparing anti-sense and sense-control probes as shown in Fig. 41.

Positive signals were marked by longitudinally striated arrows within the extravillous trophoblast cells (evCTB). Examples for syncytiotrophoblast (STB), cytotrophoblast (CTB) and placental site giant cells (PSGC) were indicated by the corresponding abbreviation. Some images displayed small amounts of erythrocytes (E).

Decreasing of MMP-12 signals was observed, but not as significant as in the radioactive ISH. The detection of MMP-12 in decidual vessels was a remarkable finding and shown in Fig. 50 A and B as well as in Fig. 51 B.

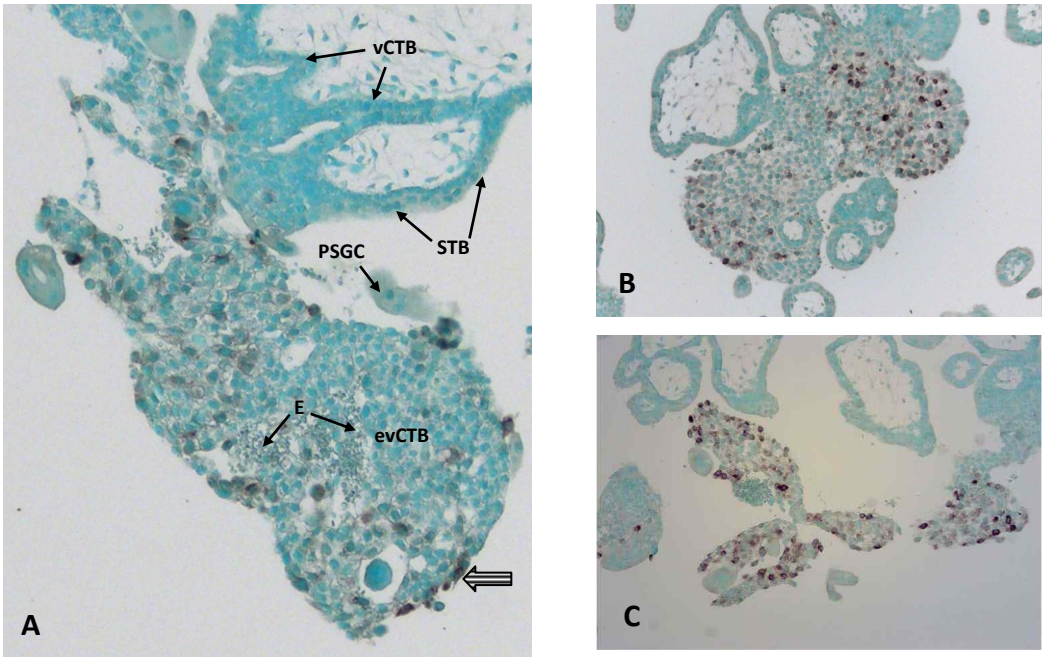

Fig. 38 – DIG-labelled ISH probe for MMP-12 mRNA, placenta 6th WOP (200x)
A: 6/001-1; **B:** 6/020-1; **C:** 6/021-1;
Symbols: villous/extravillous cytotrophoblast (v/evCTB), syncytiotrophoblast (STB), erythrocytes (E), decidua (D), cell column (CC), placental site giant cells (PSGC), striated arrows (positive dig signal);

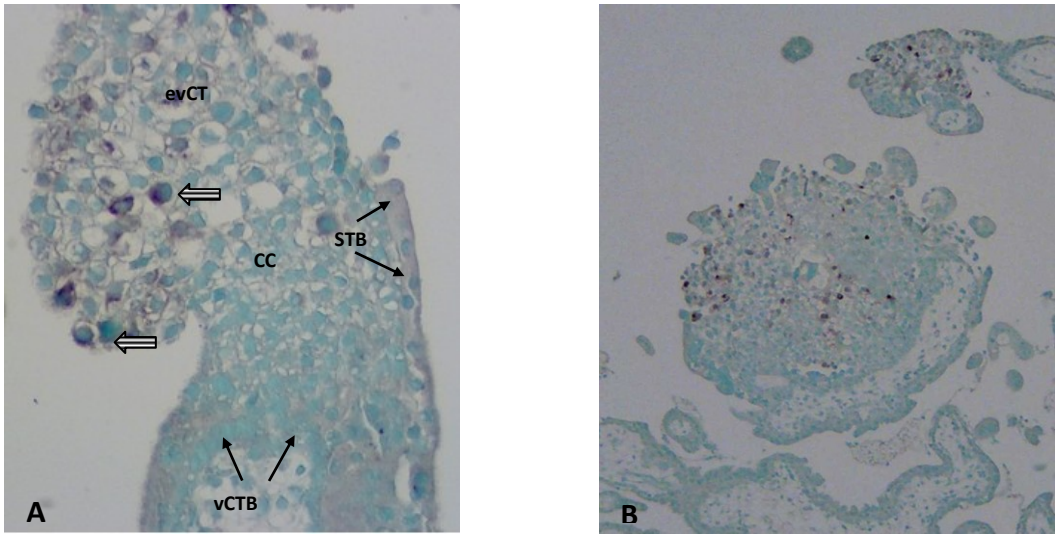

Fig. 39 – DIG-labelled ISH probe for MMP-12 mRNA, placenta (200x/400x)
A: 7/022-1, 7th WOP; **B:** 8/012-2, 8th WOP;

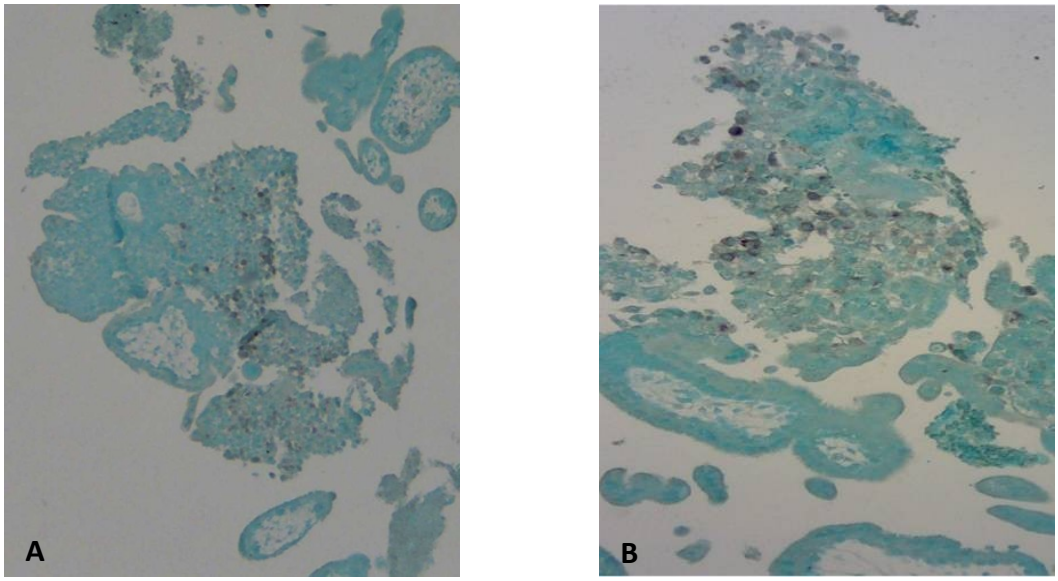

Fig. 40 – DIG labelled ISH probe for MMP-12 mRNA, placenta (200x)
A: 10/023-1, 10th WOP; **B:** 11/016-1, 11th WOP;

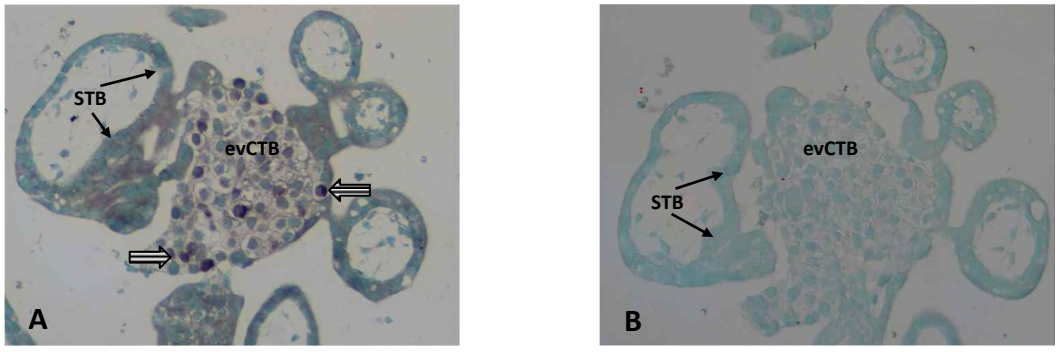

Fig. 41 – DIG-labelled ISH probe for MMP-12 mRNA, placenta (400x)
A, B: 6/026-1, 6th WOP; **A:** anti-sense, **B:** sense-control;
Symbols: villous/extravillous cytotrophoblast (v/evCTB), syncytiotrophoblast (STB), erythrocytes (E), decidua (D), cell column (CC), placental site giant cells (PSGC), striated arrows (positive dig signal);

5 *Double label fluorescent immunohistochemistry*

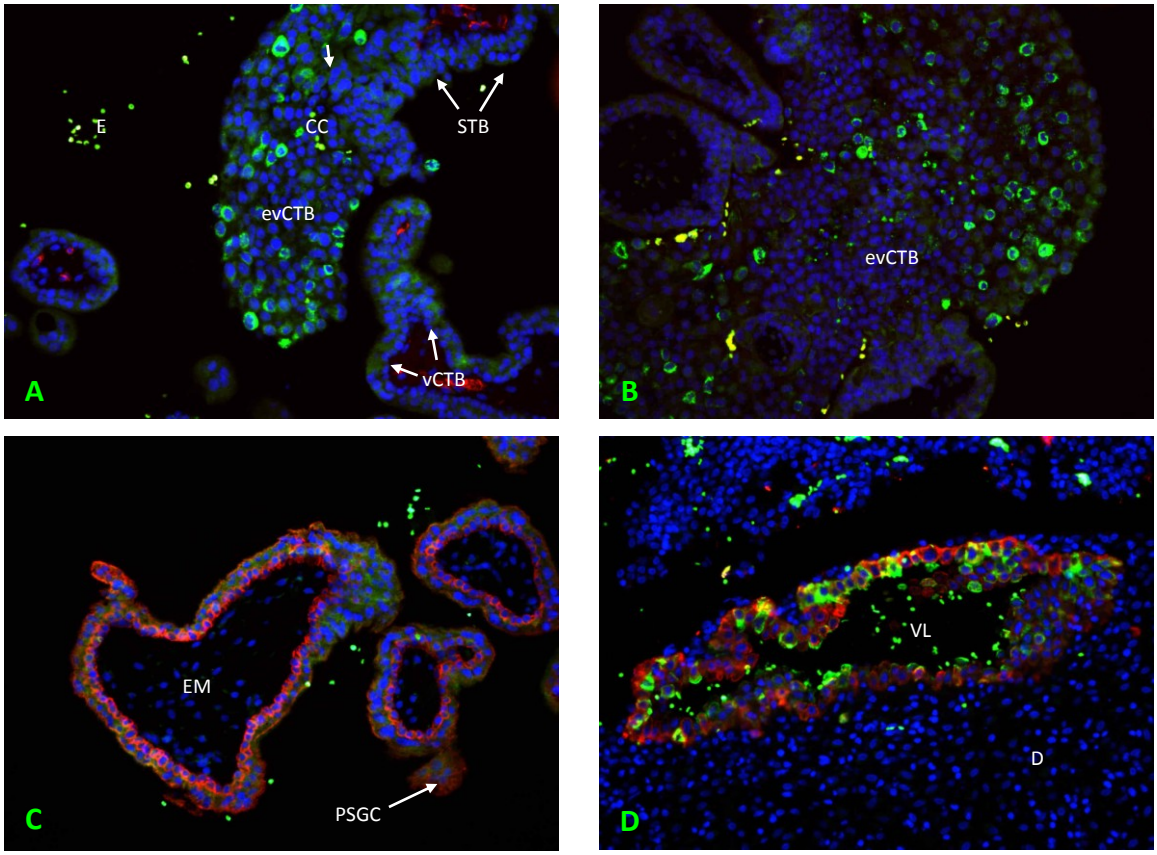

Fig. 42 – Other targets than HLA-G
A: CD34 (red), MMP-12^{HR} (green); B: CD68 (red), MMP-12^{HR} (green); C, D: CK-7 (red), MMP-12^{HR} (green); For all images displaying MMP-12^{HR} the clone ab38935 (hinge region) was used. **Symbols:** villous/extra-villous cytotrophoblast (v/evCTB), syncytiotrophoblast (STB), erythrocytes (E), decidua (D), cell column (CC), placental site giant cells (PSGC), extraembryonic mesenchyme (EM), vessel lumen (VL);

For detection of the translated protein of MMP-12 within the placental and decidual samples, the previously described double-label fluorescent immunohistochemistry was used. To acquire information about the origin of the MMP-12 expressing cells they were overlaid together with antibodies against CD34, CD68, CK-7 and HLA-G. Secondary antibodies against MMP-12^{HR} were always labelled green using Dylight 488, whereas the counter-target was marked red with Cy3. The cell nuclei were stained blue using DAPI as a standard feature.

While Fig. 43 to Fig. 47 list examples for HLA-G positive sections which were used for quantitative analysis in a later step, Fig. 42 shows CD34, CD68 and CK-7 as different counter-targets. CD34, a marker for capillary endothelial cells, which was taken as an alternative for the rat anti-human vWF antibody, showed only weak signals within the

mesenchyme in Fig. 42 A, but no match with the MMP-12^{HR} positive cells. The macrophage standard marker CD68 was completely negative in the tested cell columns (Fig. 42 B). Cyto-keratin-7 (CK-7), a cytoskeletal marker often found in blood vessels and glandular ducts, was detected in villous but not in extravillous trophoblast cells (Fig. 42 C). Very interesting is the fact that MMP-12 positive cells were matching the highly CK-7 positive signals in endothelial cells found in utero-placental vessels within decidua sections (see Fig. 42 D).

MMP-12^{HR} positive cells within the HLA-G positive extravillous trophoblasts (evCTB) of the cell columns (CC) were displayed in the following images (Fig.43 to Fig. 47).

Furthermore placental villi with syncytio- and cytotrophoblast cells (STB and CTB) as well as the placental site giant cells (PSGC) with their elusively high background staining for the green Dylight488 dye (without a positive signal in ISH) were shown. The latter had to be considered for later quantitative image analysis. Another highly positive signal especially for green dye was given by erythrocytes (E), which interacted with every fluorescent dye but could easily be separated by their small size.

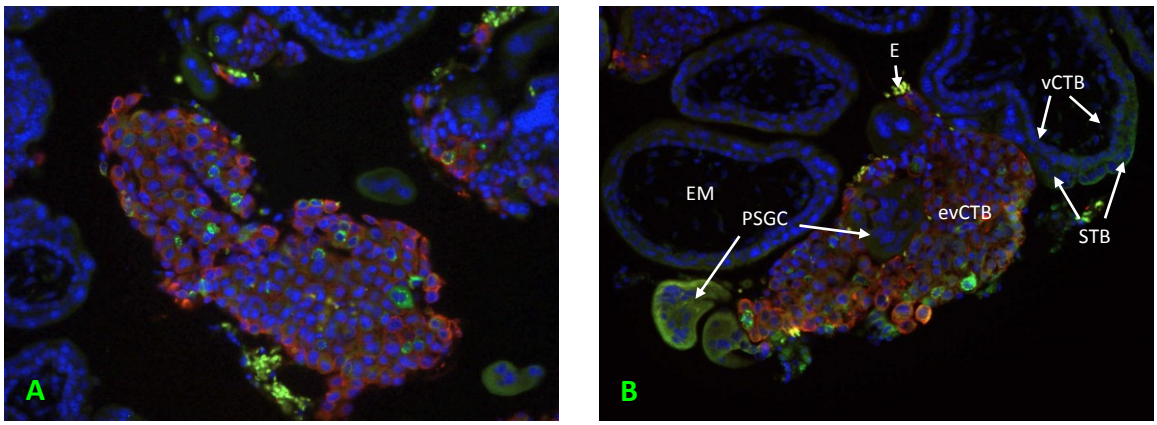

Fig. 43 – Double-label fluorescent IHC, placenta 6th WOP (200x)

A, B: 6/002-1; **HLA-G (red), MMP-12^{HR} (green), DAPI (blue);** For all images displaying MMP-12^{HR} the clone ab38935 (hinge region) was used. **Symbols:** villous/extravillous cytotrophoblast (v/evCTB), syncytiotrophoblast (STB), erythrocytes (E), decidua (D), cell column (CC), placental site giant cells (PSGC), extraembryonic mesenchyme (EM);

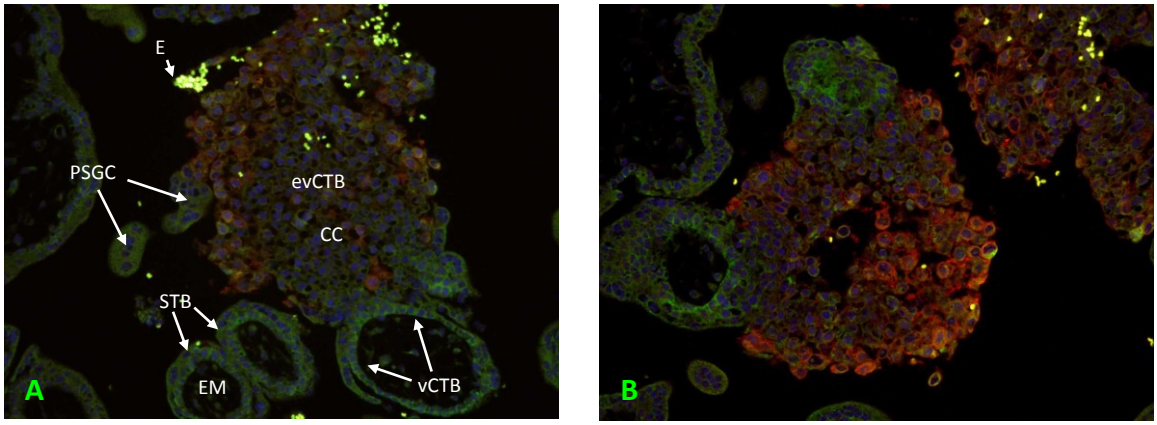

Fig. 44 – Double-label fluorescent IHC, placenta 7th WOP (200x)
A, B: 7/005-1; **HLA-G (red), MMP-12^{HR} (green), DAPI (blue);**

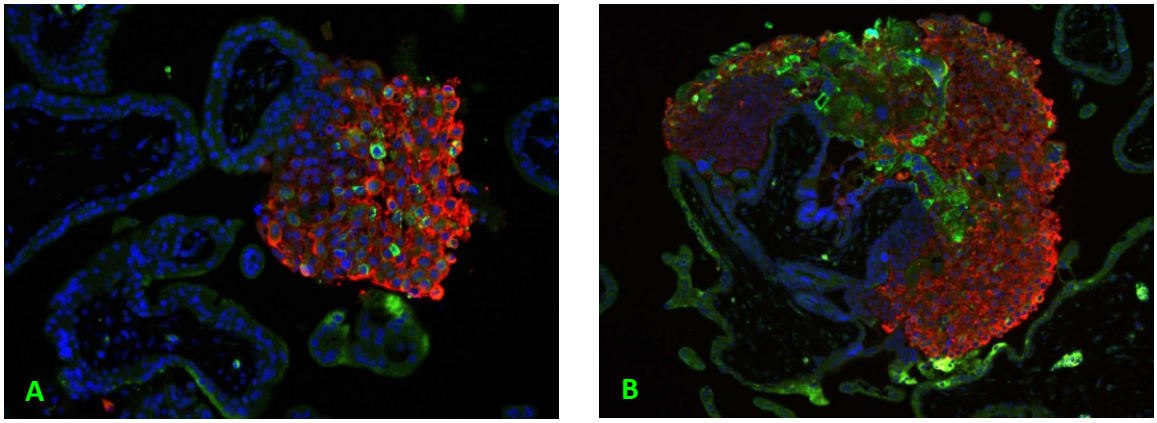

Fig. 45 – Double-label fluorescent IHC, placenta 8th WOP (200x)
A, B: 8/008-1; **HLA-G (red), MMP-12^{HR} (green), DAPI (blue);**

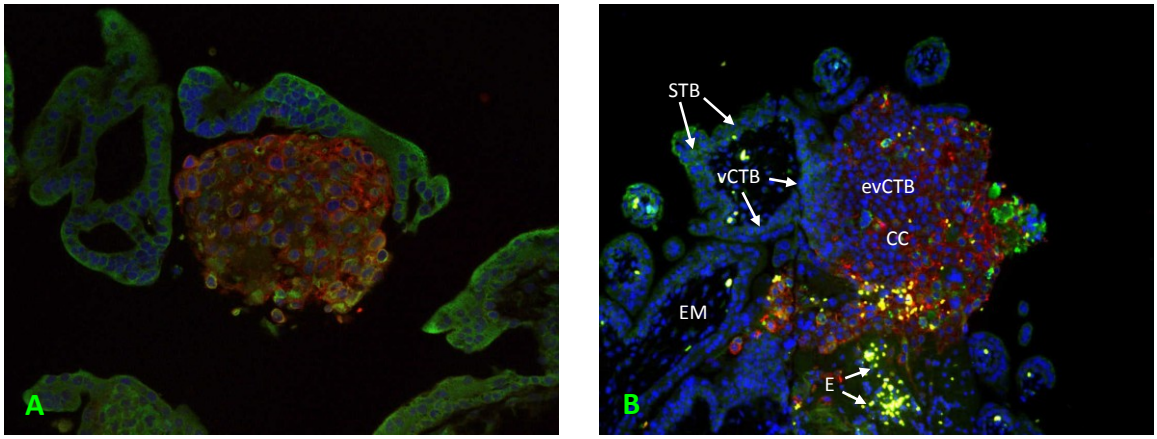

Fig. 46 – Double-label fluorescent IHC, placenta (200x)
A: 9/014-2, 9th WOP; **B:** 11/016-1, 11th WOP; **HLA-G (red), MMP-12^{HR} (green), DAPI (blue);** For all images displaying MMP-12^{HR} the clone ab38935 (hinge region) was used. **Symbols (for all shown images):** villous/extravillous cyto-trophoblast (v/evCTB), syncytiotrophoblast (STB), erythrocytes (E, cell column (CC), extraembryonic mesenchyme (EM), placental site giant cells (PSGC);

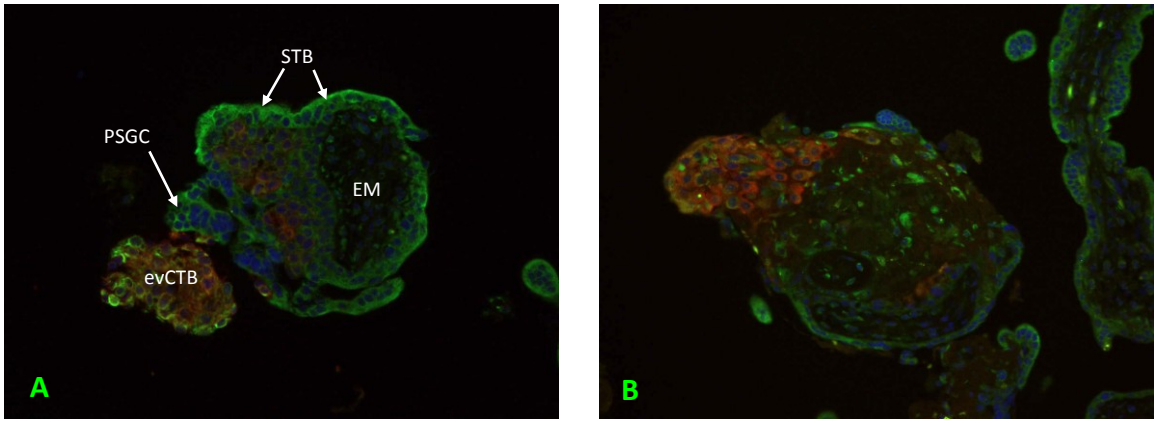

Fig. 47 – Double-label fluorescent IHC, placenta 12th WOP (200x)
A, B: 12/017-1; **HLA-G (red), MMP-12^{HR} (green), DAPI (blue);** For all images displaying MMP-12^{HR} the clone ab38935 (hinge region) was used. **Symbols (for all shown images):** villous/extravillous cytotrophoblast (v/evCTB), syncytiotrophoblast (STB), erythrocytes (E), decidua (D), cell column (CC), extraembryonic mesenchyme (EM), placental site giant cells (PSGC);

In Fig. 48 images of decidual vessels as well as decidual glands are shown, which exhibited partially strong signals for MMP-12 and HLA-G co-expression. Unfortunately the signal-to-background-ratio was inferior, as due to the previously explained fact that the polyclonal MMP-12^{CE} (ab66157, carboxyterminal end) antibody had to be used for this pass, showing a poorer performance compared to the principally used monoclonal MMP-12^{HR} (ab38935, hinge region) clone.

Utero-placental arteries (UPA), clearly recognisable by their prominent media, were displayed in Fig. 48 C and D showing a mass of endovascular cells plugging the vascular lumen. These cells were highly positive for MMP-12 and made a differentiation to the endothelial cells impossible. Within the level of the smooth muscular cells forming the media, as well as in close vicinity to the vessels immunopositivity for MMP-12 was noticed. Those, as well as the plugging cell population showed a congruent expression of HLA-G.

Analysis of the other vessel-like or glandular formations was more complex and not entirely possible as invaded and remodelled spiral arteries are known to lose their media, grow in size and exhibit cubical cells instead of the flat endothelial cells rather resembling glandular ducts (17). Unidentified luminal structures are therefore named as ‘vessels’ and not closer specified in this thesis.

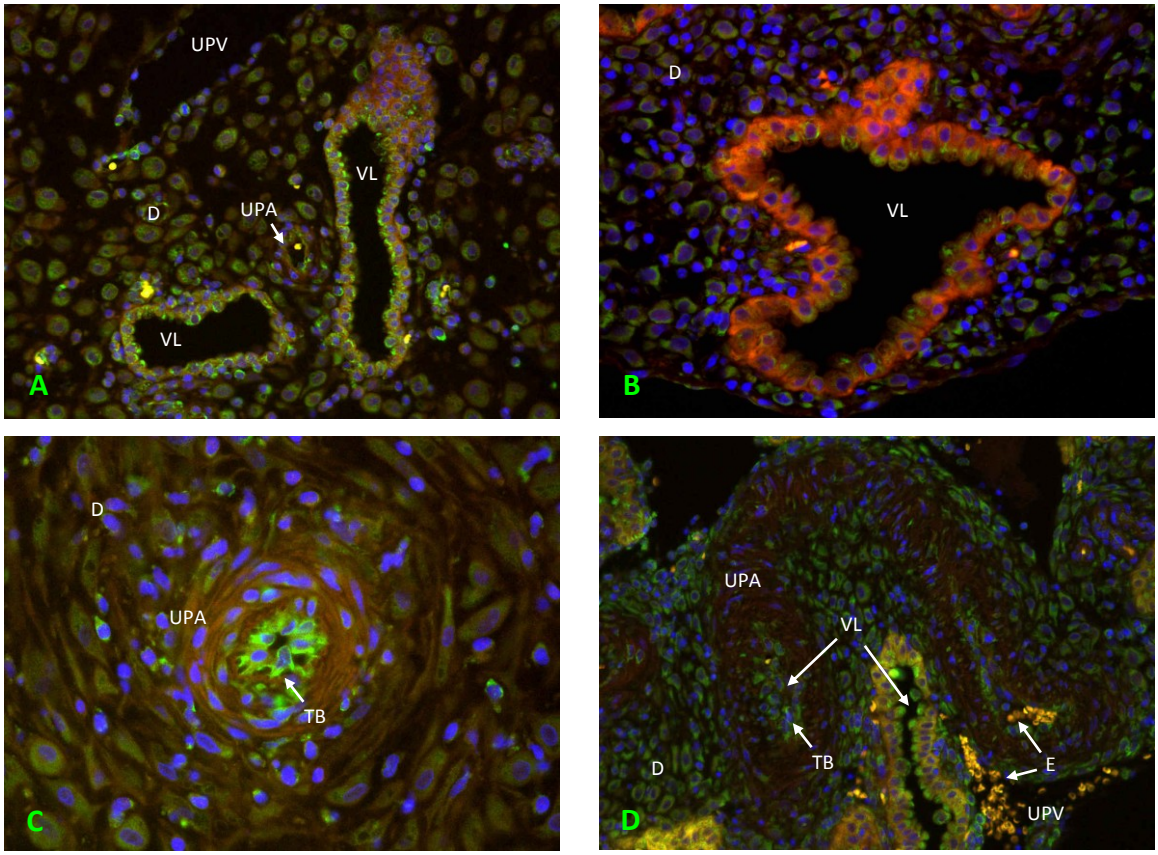

Fig. 48 – Double-label fluorescent IHC, decidua 6th and 9th WOP (200/400x)

A, C: 6/026-1; **B, D:** 9-10/025-1; **HLA-G (red), MMP-12^{CE} (green), DAPI (blue);** For all images displaying MMP-12^{CE} the clone ab66157 (carboxyterminal end) was used. **Symbols:** villous/extravillous cytotrophoblast (v/evCTB), syncytiotrophoblast (STB), erythrocytes (E), decidua (D), cell column (CC), placental site giant cells (PSGC), extraembryonic mesenchyme (EM), vessel lumen (VL); utero-placental artery (UPA), utero-placental vein (UPV), trophoblast plugging (TB);

As shown in Fig. 48 A, B and D those unidentified vessels showed a large but compressed or even star-shaped lumen with intense congruent positivity for MMP-12 (CE) and HLA-G. The staining was even more intense as in the neighbouring spiral arteries when taken as a reference value (compare Fig. 48 A and D). All cells counted among the population which represented the inner layer were isocubical to columnar or even round in the case of detachment. Utero-placental veins were observed in Fig. 48 A and D exhibiting a flat endothelium without increased staining for MMP-12 and some erythrocytes (in Fig. 48 D).

A difference in the general colourability between the various images independent from the used clones was discernible. This was traced back to the fact that placental tissues of different individuals showed wide varieties concerning their general response to staining. Furthermore the MMP-12 antibodies are difficult to handle, making it complicated to

obtain a sufficient signal intensity compared to background. Minimal variations naturally occurring within each pass – normally barely noticeable, if easy-to-handle antibodies such as HLA-G were used – lead to significant differences in the output for the MMP-12 antigen detection.

5.1 Qualitative analysis

Picture comparison on the different levels of detection, as done in Fig. 49 and Fig. 50, was used to validate the previous observations. Only matching signals on in-situ hybridisation and double-label fluorescence immunohistochemistry – representing the RNA- and protein-level – were count as positive signals in the following discussion.

In Fig. 49 the matching couples were brought in direct contrast to compare similarities in the distribution of MMP-12 expression. On the RNA level (compare A, B, C, G and H) positive signals were only noticed within some extravillous trophoblast cells of the cells columns – not in villous syncytio- or cytotrophoblast cells and also never in placenta site giant cells. The appearance of MMP-12 positive cells within the cell columns was random, not following any visible spatial order like i.e. an invasion frontier. An exception had to be made for the decidua, where some weak signals were present within the stroma and also alongside the level of the endothelium within the utero-placental vessels (see Fig. 50 A)

On the protein level (compare Fig. 49 D, E, F, I and J) matching signals represented by the green dye were noticed within the population of extravillous trophoblast cells exhibiting red fluorescence. Slight differences in the location were due to the distance between some of the sections of the same block of tissue. Green staining of varying intensity was observed for villous syncytio- and cytotrophoblast cell populations as well as for placental site giant cells. As for all fluorescent dyes – erythrocytes were always highly positive.

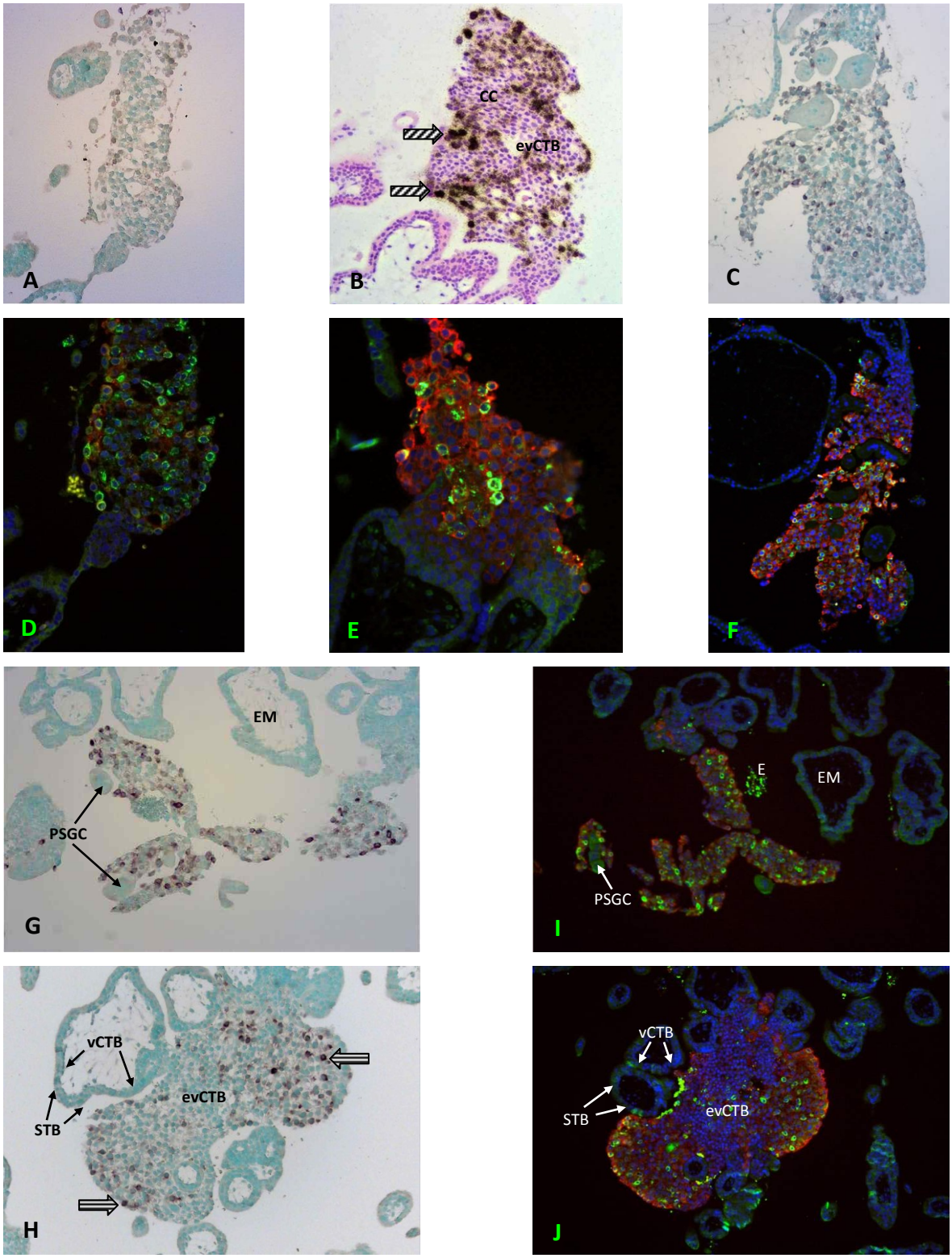

Fig. 49 – Comparison of S35-/Dig-ISH and double-label fluorescent IHC, placenta (200x)
A, C, G, H: DIG-ISH; **B:** S35-ISH; **D, E, F, I, J:** fluorescent IHC – ***HLA-G (red), MMP-12^{HR} (green), DAPI (blue);*** *6th WOP:* **B, E:** 6/021-1; **G, I:** 6/021-1; **H, J:** 6/020-1; *7th WOP:* **A, D:** 7/004-1; *8th WOP:* **C, F:** 8/007-1; All IHC images: MMP-12^{HR} clone ab38935 (hinge region). **Symbols:** villous/extravillous cytotrophoblast (v/evCTB), syncytiotrophoblast (STB), erythrocytes (E), decidua (D), cell column (CC), extraembryonic mesenchyme (EM), placental site giant cells (PSGC), fascinated arrows (pos. S35 signal), striated arrows (pos. Dig signal).

To interpret the images in Fig. 50 it has to be mentioned again that the differentiation between remodelled spiral arteries, utero-placental veins or decidual glands (cut close to their opening into the intervillous space) was sophisticated. Not clearly identified structures were therefore just summarised under the term 'vessel'.

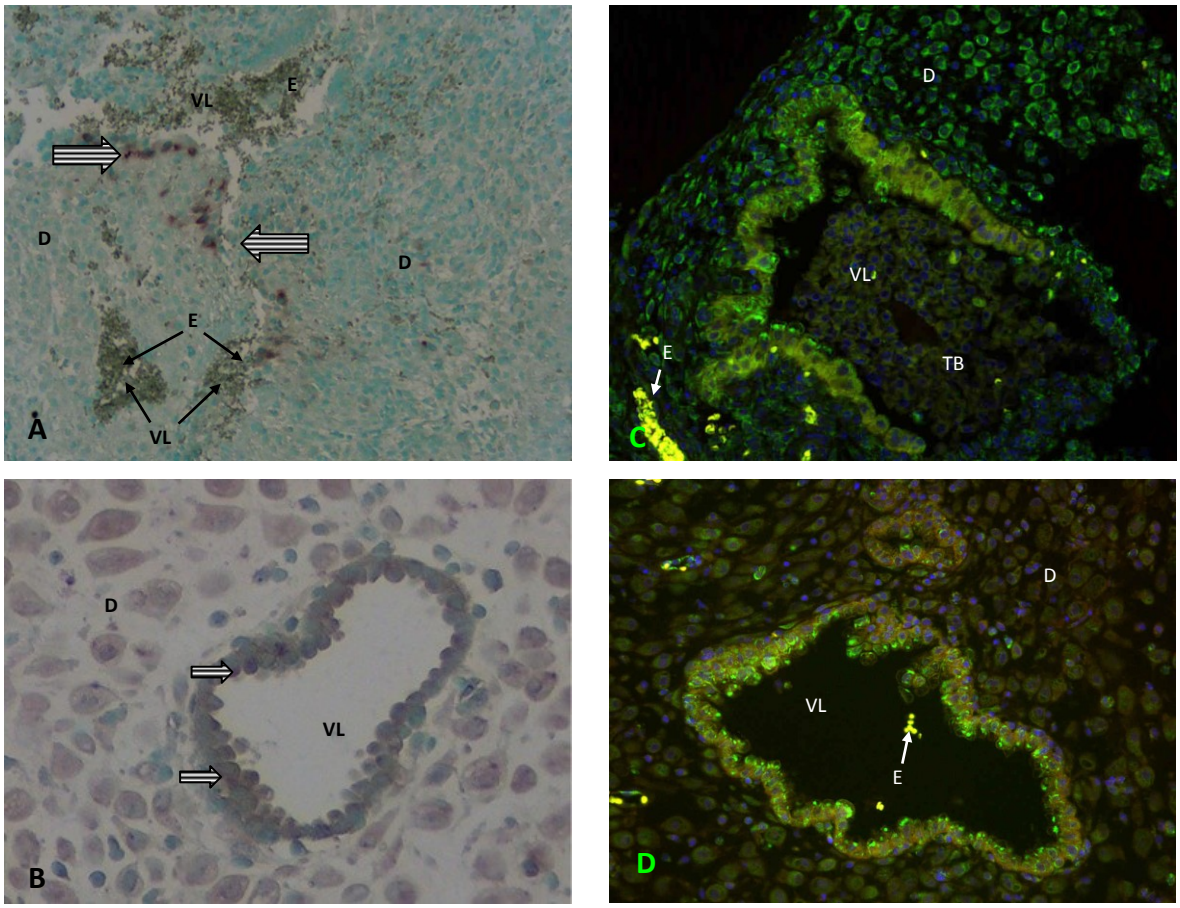

Fig. 50 – Comparison of Dig-ISH and double-label fluorescent IHC, decidua (200/400x)
A: 9-10/025-1, Dig-ISH; **B:** 6/026-1, Dig-ISH; **C:** 9-10/025-1, fluorescent IHC; **D:** 6/026-1, fluorescent IHC; **A, C:** 9-10th WOP; **B, D:** 6th WOP; For all images displaying MMP-12^{CE} the clone ab66157 (carboxyterminal end) was used. **Symbols:** decidua (D), erythrocytes (E), trophoblast plugging (TB), vessel lumen (VL), striated arrows (pos. Dig signal); **HLA-G (red), MMP-12^{CE} (green), DAPI (blue).**

The in Fig. 50 A presented vessels exhibited large amounts of erythrocytes as against in Fig. 50 C and D where only some few were shown. Striated arrows mark the positive signals which were detected for MMP-12 mRNA along the endothelial lining and very weak in the neighbouring decidual stroma. The vessel shown in Fig. 50 B also displayed a number if highly MMP-12 mRNA-positive cells (examples marked by striated arrows), of these some seemed to detach into the lumen.

A congruent picture was drawn by the immunofluorescence images showing large vessels with a folded endothelial lining made up of isocubical to columnar, highly MMP-12 and

HLA-G positive cells (Fig. 50 C and D). Only traces of erythrocytes were shown in their lumen whereas the small surrounding blood vessels were filled with larger quantities. As an interesting feature a large-sized plug of cells with a very weak MMP-12 immunopositivity was almost occluding the lumen in Fig. 50 C.

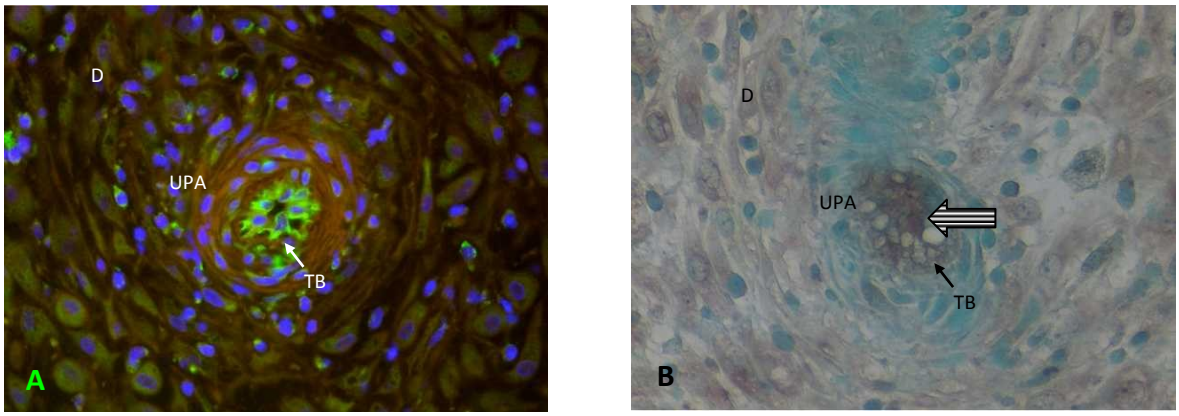

Fig. 51 – Comparison of double-label fluorescent IHC and Dig-ISH, 6 /026-1, placenta 6th (400x)
A: 6/026-1, fluorescent IHC; **B:** 6/026-1, Dig-ISH; **Symbols:** decidua (D), trophoblast plugging (TB), vessel lumen (VL), utero-placental artery (UPA); striated arrows (pos. Dig signal); **HLA-G (red), MMP-12^{CE} (green), DAPI (blue);** For all images displaying MMP-12^{CE} the clone ab66157 (carboxyterminal end) was used.

The matching pair of an utero-placental artery in Fig. 51 proved the presence of MMP-12 on the RNA as well as the protein level. In the immunofluorescence image A a spiral artery with a clearly outlined media exhibited massive trophoblast plugging resembling the mirror image B where the plug was highly positive for the Dig anti-MMP-12 probe. The second picture also showed, that the artery was not only cut in the orthograde plane but also alongside, demonstrated by the stronger uptake of the counterstain by the smooth vascular muscles, which appearing blue in the upper part of the picture.

5.2 Quantitative analysis

Case No.	*WOP*	*HLA-G*	*MMP-12*	*Ratio*
6/001-1/01	6 wks.	90	18	**0,20**
6/001-1/02	6 wks.	612	129	**0,21**
6/001-2/01	6 wks.	454	88	**0,19**
6/001-2/02	6 wks.	814	249	**0,31**
6/002-1/01	6 wks.	452	97	**0,21**
6/002-1/02	6 wks.	291	69	**0,24**
6/002-1/03	6 wks.	304	66	**0,22**
6/002-1/04	6 wks.	327	72	**0,22**
6/002-1/05	6 wks.	512	121	**0,24**
6/002-1/06	6 wks.	199	86	**0,43**
6/002-1/10	6 wks.	79	21	**0,27**
6/002-3/02	6 wks.	203	43	**0,21**
6/002-3/03	6 wks.	450	94	**0,21**
6/002-3/04	6 wks.	504	157	**0,31**
6/003-1/01	6 wks.	176	57	**0,32**
7/004-1/01	7 wks.	168	81	**0,48**
7/004-1/02	7 wks.	246	143	**0,58**
7/004-1/03	7 wks.	227	117	**0,52**
7/004-1/04	7 wks.	241	124	**0,51**
7/004-1/05	7 wks.	122	60	**0,49**
7/004-1/06	7 wks.	103	90	**0,87**
7/004-1/07	7 wks.	172	87	**0,51**
7/005-1/01	7 wks.	322	201	**0,62**
7/005-1/02	7 wks.	168	122	**0,73**
7/005-1/03	7 wks.	56	35	**0,63**
7/005-1/04	7 wks.	66	45	**0,68**
7/005-1/05	7 wks.	76	53	**0,70**
7/005-1/06	7 wks.	184	88	**0,48**
7/005-1/07	7 wks.	271	133	**0,49**
7/005-1/08	7 wks.	193	77	**0,40**
7/005-1/09	7 wks.	251	110	**0,44**
7/005-1/10	7 wks.	270	91	**0,34**
7/005-1/11	7 wks.	152	55	**0,36**
8/006-1/01	8 wks.	100	62	**0,62**
8/007-1/01	8 wks.	530	188	**0,35**
8/008-1/01	8 wks.	478	130	**0,27**
8/008-2/01	8 wks.	413	132	**0,32**
8/006-2/01	8 wks.	80	27	**0,34**
8/010-1/01	8 wks.	173	54	**0,31**
8/012-1/01	8 wks.	105	34	**0,32**
8/012-2/01	8 wks.	165	30	**0,18**
8/012-1/02	8 wks.	308	154	**0,50**
8-9/013-1/01	8-9 wks.	65	16	**0,25**
8-9/013-1/02	8-9 wks.	62	24	**0,39**
9/014-1/01	9 wks.	80	41	**0,51**
9/014-1/02	9 wks.	448	224	**0,50**
9/014-2/03	9 wks.	75	23	**0,31**
9/014-1/04	9 wks.	404	94	**0,23**
9/014-2/05	9 wks.	120	28	**0,23**
9/014-1/06	9 wks.	217	115	**0,53**
9/014-2/07	9 wks.	63	34	**0,54**
11/016-1/01	11 wks.	143	24	**0,17**
11/016-1/02	11 wks.	443	154	**0,35**
11/016-1/03	11 wks.	499	66	**0,13**
11/016-1/04	11 wks.	94	7	**0,07**
11/016-1/05	11 wks.	70	5	**0,07**
12/017-1/01	12 wks.	96	20	**0,21**
12/017-1/02	12 wks.	67	21	**0,31**
12/017-1/03	12 wks.	49	20	**0,41**

Tab. 13 – Analysis of the MMP-12 vs. HLA-G ratio in dl fluorescence IHC

In Tab. 13 ratios of all single measurements of the different samples and sites were listed in ascending order following their gestational age. The ratios had been assessed by the method explained in chapter 'C8 – Picture analysis and statistical evaluation'. Many samples from different individuals had been collected and analysed in the early and middle, however only two were listed for the late first trimester. This originated in the source of the samples as legal abortions, which were rare in later stages and therefore hard to get. Additionally those late-staged tissues were often of a bad quality, showing only little areas that were suitable for analysis.

When grouped by early, middle and late first trimester[10] as in Fig. 52 as well as the corresponding Tab. 14 a negligible increase of the median from 0.32 to 0.33 with a significant subsequent decrease to 0.23 in the late stage was observed. Moreover the early stage featured a broad dispersion of values within the range of the 0.25 and 0.75 percentile compared to the other stages was present.

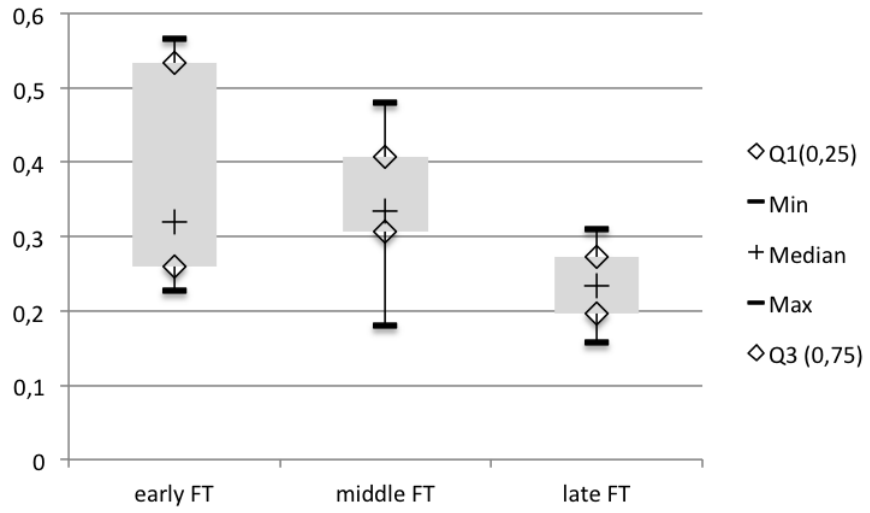

Fig. 52 – Analysis of MMP-12 signals by groups
Early FT: 6 to 7 wks.; **middle FT:** 8 to 10 wks.; **late FT:** 11 to 12 wks.

	early FT	*middle FT*	*late FT*
Q1 (0.25)	0.26	0.31	0.20
Min	0.23	0.18	0.16
Median	0.32	0.33	0.23
Max	0.55	0.48	0.31
Q3 (0.75)	0.53	0.41	0.27

Tab. 14 – Analysis of MMP-12 signals by groups

[10] Early: 6-7 wks.; middle: 8-10wks.; late: 11-12 wks.

If only the mean values were regarded a steady decrease from 0.38 over 0.35 down to 0.23 became apparent as shown in Fig. 53. The foundation for the calculation of these mean values was given in Tab. 15. Where the early and middle stages were based on five and eight individuals, the late stage only rested on two.

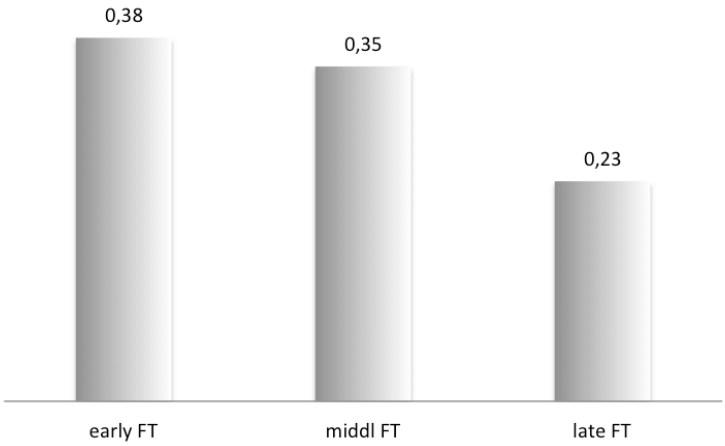

Fig. 53 – MMP-12 signals: mean value based on individuals by groups
Early FT: 6 to 7 wks.; **middle FT:** 8 to 10 wks.; **late FT:** 11 to 12 wks.

Weeks	**6 to 7**	**8 to 10**	**11 to 12**
	early FT	***middle FT***	***late FT***
	0,23	0,48	0,16
	0,26	0,35	0,31
	0,32	0,30	
	0,57	0,31	
	0,53	0,41	
		0,18	
		0,32	
		0,41	
Mean value	**0,38**	**0,34**	**0,23**

Tab. 15 – MMP-12 signals: individuals by groups

If these groups were then split further into seven groups by the weeks from six to twelve, the last four ones each comprised a single case only. This leads to discordant values in the decreasing middle and late first trimester as against the observations made previously as well as compared to the increase from the 6th to the 7th week in the early stage (contrasted in Fig. 54 and Tab. 16).

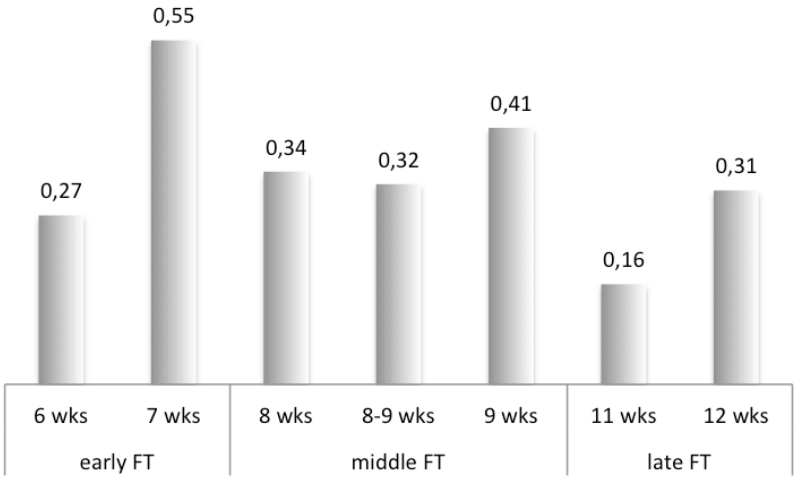

Fig. 54 – MMP-12 signals: mean value based on individual by weeks

Weeks	6 wks	7 wks	8 wks	8-9 wks	9 wks	11 wks	12 wks
	0,23	0,57	0,48	0,32	0,41	0,16	0,31
	0,26	0,53	0,35				
	0,32		0,30				
			0,31				
			0,41				
			0,18				
Mean value	**0,27**	**0,55**	**0,34**	**0,32**	**0,41**	**0,16**	**0,31**

Tab. 16 – MMP-12 signals: individuals by weeks

E Discussion

To obtain a better understanding of the developing human placenta and also to get helpful hints on the basic biology of malignant tumours in the second line, we started our investigation, performing an mRNA full gene transcript comparing isolated trophoblast cells, known to be highly invasive in the first trimester versus a low invasive population gained from term placentas. This led us to a wide range of 220 significantly up- or down-regulated genes (155). One of those genes was macrophage elastase (MMP-12) being significantly higher expressed in the first trimester and – at the time, when the chip was performed – not previously described in the human placenta. A subsequently performed semiquantitative reverse transcriptase PCR of first trimester and term placental tissue samples confirmed the earlier findings and encouraged us to investigate MMP-12 expression in situ. The highly sensitive method of radioactive in-situ hybridisation utilizing S35-labelled riboprobes brought promising results after eight weeks of exposure. But unfortunately, in the meantime Aplin and coworkers (133) published their results on MMP-12 expression in early stages of placental development and spiral artery remodelling. Scrutinising his results critically, we were able to notice some differences, regarding the spatial localisation, when comparing it to our first results. So we decided not do abandon our research but in contrary to intensify it.

Based on the results exposed in 'Chapter D' we were able to draw the following conclusions.

MMP-12 exhibits a limited spatial expression

Starting with the fact, that MMP-12 was 89.58 fold higher expressed in first trimester than in term placenta we proposed the question where precisely in the placenta this gene is expressed.

On the level of RNA we were able to show congruent data for S35- as well as Dig-labelled in-situ hybridisation. Both featured a random pattern of single or grouped MMP-12 positive cells within the cell columns. Almost a mirror image of this picture was found on the protein level were we could show that these cells were all a sub-population of HLA-G positive extravillous cytotrophoblast cells.

From the previously published literature we already knew that Aplin et al had found MMP-12-positivity within villous as well as the entirety of the extravillous cytotrophoblast population (compare Fig. 55) (133).

The difference between this data and our new findings might be explained as Aplin's group was only using antibodies in the course of standard immunohistochemistry as single instance in their line of argumentation. As we knew from our own research, antibodies can be a very insecure method to detect complicated targets such as MMP-12. Both clones we used against human MMP-12 (hinge region and carboxyterminal end) displayed cross-reactions leading to false positive signals e.g in placental site giant cells or the villous cytotrophoblast, and a generally high background, especially pronounced with the CE-clone. Knowing this fact, it was a vital step to validate the obtained data on the RNA-level, using in-situ hybridisation. Comparing the results of those two methods we were able to differentiate the correct findings we obtained in some evCTB from false-positive signals in the vCTB or the PSGC.

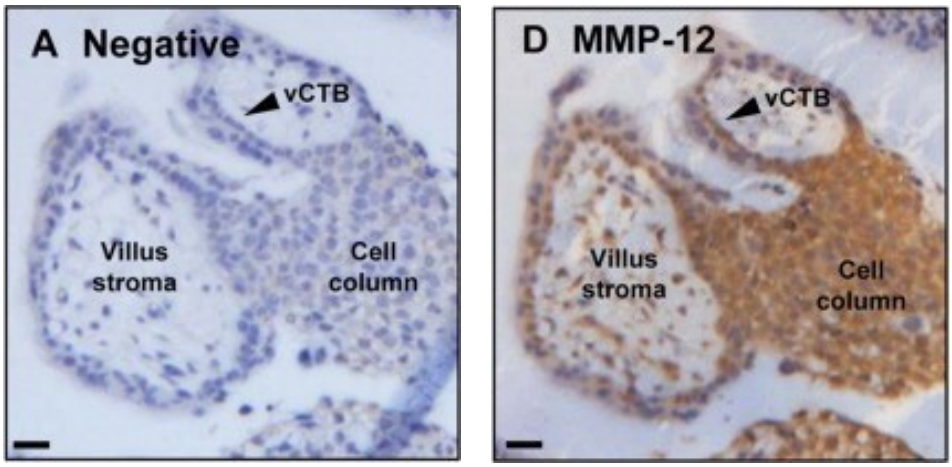

Fig. 55 – IHC on MMP-12 expression in sections of first trimester placenta [excerpted from (133)]

A: placental villus and cell column, negative control; **D:** placental villus and cell column, monoclonal rabbit anti-human MMP-12 antibody (carboxyterminal end, EP1261Y); **Legend:** villous cytotrophoblast (vCTB); **counterstain (haematoxylin), MMP-12 (brown)**

MMP-12 is expressed in a subpopulation of evCTB

To analyse the origin of the MMP-12 positive cells we performed double-label immunofluorescent assays using HLA-G, CK-7, CD34 and CD68.

From the literature it was well known that macrophages, in which macrophage elastase was first detected (56) are often found within the placenta and close to utero-placental vessels within the decidua (156).

We could show that the MMP-12 positive cells within the cell columns as well as in the decidua, where they were detected within or close to vessel-like structures, were simultaneously positive for HLA-G. This suggests the assumption that those cells might be

a subpopulation of the extravillous trophoblast cells. Regarding the strong positivity for the HLA-G within the vessel-like structures, validity could be proven by detection on the level of RNA or by antibodies against further markers for invasive trophoblast cells, decidual glands or specific for vascular endothelium.

The expression pattern is random within the cell columns

Recognising that only some of the extravillous trophoblasts were positive for macrophage elastase put up the question whether there might be a pattern within the spatial distribution. No valid data on this topic was available of previous literature, as the distribution found by Aplin et al (133) might be based on false positive signals.

Only detected within the extravillous trophoblast population of the cell columns we spotted no well-defined expression pattern within these boundaries.

The signal density of MMP-12 decreases throughout the first trimester

The similarity between the semiquantitative reverse transcriptase polymerase chain reaction and the GeneChip microarray regarding the mRNA expression led to the investigation of the signal density for MMP-12 over the course of the first trimester of pregnancy.

With an objectified, computer aided analysis we were able to collect data grouped by early, middle and late first trimester based on ratios of the total cell population. In view of the median a decrease from 0.32 to 0.33 in early and middle compared to 0.23 at FT was noticed. Disregarding the influence of statistical outliers in the mean value, this decrease was even more pronounced going down from 0.38 to 0.23, thus the change of the signal density was between 9 resp. 39 per cent (median – absolute/relative) and 15 resp. 65 per cent (mean value – absolute/relative) higher in the early than in the late first trimester.

These results would have been impressive unless the significance might not have been diminished by some potential biases.

First of all a methodical bias had to be quoted as the case numbers, especially for the later stages were too low. Exemplary therefore the weeks 11 and 12 should be regarded, were only two samples had been collected and used. This derived its origin in the fact that placental tissue samples were only able to be obtained from legal abortions, which normally were conducted at an earlier stage of pregnancy.

The second bias originated from the tissue itself featuring a broad variety of qualitative levels from perfectly preserved to almost degenerated. As already characterised in the

methods part – the latter generally showed poor response to immunofluorescence. Most of the tissues quality was settled in between the two extremities.
Finally the observer bias might have had an influence on the result, as only one, non-blinded observer conducted all studies.
Because of these three potential biases, the aforementioned results should not be regarded as absolute values but instead rather as a tendency. Due to the minimal number of cases, no p-value was pointed out.

Expression of MMP-12 was shown within vessels and glands in the decidua

Subsequently to the investigation of MMP-12 expression patterns in cell columns the attention was turned to the decidua where further positive signals had been noticed. Here we were able to demonstrate the expression of macrophage elastase on the RNA- and protein-level, located in the stroma of the decidua as well as at the level of the endothelial lining of utero-placental vessels and glandular ducts.
Previously literature, published by Aplin & Harris, already had demonstrated MMP-12 expression within vascular smooth muscles and endovascular trophoblast cells in the context of spiral artery invasion and remodelling (133). Endoglandular trophoblast invasion, but not the upregulation of MMP-12, was shown by Huppertz & Moser as a possible new invasion path or an opening and connecting mechanism of the uterine glands for histiotrophic nutrition (see Fig. 56) (17).
The results demonstrated in this thesis undergird the previously published findings, however, with minor distinctions. In smaller, non-remodelled utero-placental arteries high levels of MMP-12 positivity have been found at the endothelial level as well as some signals within the media. Highly positive endovascular trophoblasts accumulated in these vessels and occluded the lumen almost entirely. As a result of the low signal-to-background ratio for the carboxyterminal end clone of the MMP-12 antibodies – positive cells were hard to differentiate from background in some of the images (but additionally proven on the level of RNA).
Data obtained from expression in larger vessels was harder to interpret as the differentiation between remodelled spiral arteries, larger utero-placental veins and angular cut glands is generally know to be complicated (15,17). The used markers HLA-G and CK-7 were only partly helpful for this issue, as the latter was positive within both – vessels and glands – and the endovascular HLA-G positive cells were able to replace the endothelium respectively the epithelium in both structures (3,17,133). Erythrocytes were

only a clear sign for vessels if they occurred in large quantities. Single erythrocytes had to be interpreted as artefacts, which were carried in afterwards during washing steps or flattening in the water bath after cutting. Close to the intervillous space the remodelled spiral arteries furthermore had lost their muscular media, appearing alike venous vessels or wide glandular orifices.

With these limitations in mind, a final and concluding interpretation of the given data on a reliable base is not possible. Further studies will have to be performed to investigate the relevance and impact of MMP-12 expression within vessels and glands. In addition, regarding the density of the expression at the early gestational age of 6 weeks post conception, it raises the question whether this alteration might not be influenced by extravillous trophoblast cells. Furthermore it might be a part of the trophoblast-independent first step as compared to the three-stage alterations that have previously been described in the introduction. If so, not only vessels at the implantation pole should be affected. What speaks against this hypothesis is the aforementioned significant signal for HLA-G. But having its basement on immunohistochemistry only - the necessity of further validation (by other markers or on the RNA-level) is present to exclude the eventuality of false positivity.

It was assumed by Aplin that the involvement of MMP-12 only bears upon its elastolytic capabilities, needed for the remodelling of the spiral arteries containing huge amounts of elastic fibres within the media as well as in their internal elastic lamina. For the remodelling and enlargement of the glandular orifices by trophoblast cells, as postulated by Huppertz, this would not make much sense as not many elastic fibres would have to be anticipated in this area. Therefore we assume that trophoblast or endometrial cells expressing MMP-12 might use different features of this protein. Either degradation of structural proteins such as laminin or even influencing cell regulation as already proofed for malignant tumour progression (7).

Presumptive trophoblast plugging within decidual glands

The accumulation of trophoblast plugs in utero-placental arteries, occluding maternal blood flow until the end of the first trimester is widely described in the literature (157,158). As expected, we found occluding trophoblast plugs within clearly outlined, un-remodelled spiral arteries of the 6^{th} and 9-10^{th} week of pregnancy. Inside the lumen of the presumptive

decidual glands, a scattered pattern of detached ‘endoglandular’ trophoblast cells, as well as massive trophoblast accumulations were noticed.

With reservation, regarding the fact that differentiation between remodelled arteries and glands was complicated and not yet entirely validated for our data, this was to our best knowledge (and except for the single trophoblast cells shown by Huppertz et al) (17) the first hint for large-sized trophoblast plugs within the lumen of decidual glands in situ.

Other interpretations would include protruding placental villi, as already described for utero-placental veins (159) or fibrinoid respectively secretory plugs with an exceptional high amount of concentrated detached ‘endoglandular’ trophoblast cells.

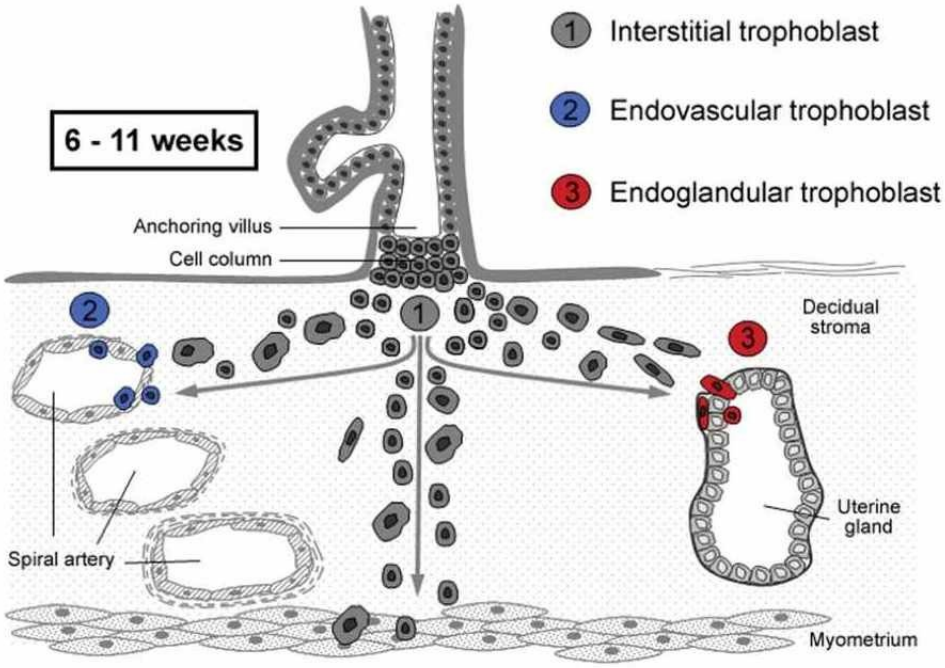

Fig. 56 – Endoglandular trophoblast in the context of trophoblast invasion [taken from (17)]

Prospect and applicability of the research findings

Summarising this work briefly, we have been able to extend the knowledge on MMP-12 regarding its expression in the extravillous trophoblast cells from the cell columns down to utero-placental vessels and glands. In contradistinction to Aplin and co-workers we were able to present congruent data on the base of two different levels of detection, providing a high level of certainty for the shown findings. Notwithstanding the fact that some of the data needs further investigation to gain final validity, it lays the foundation for further basic research on this amazing and versatile research area. Not only a better understanding

regarding the development of the human placenta might be reasonably expected – but also a transfer of knowledge into other fields of medicine, and perhaps a future building block for the comprehension of tumour progression and invasion.

F References

1. Soundararajan R, Rao AJ. Trophoblast "pseudo-tumorigenesis": Significance and contributory factors. Reprod Biol Endocrinol. 2004 Mar 25;2:15.
2. Cohen M, Bischof P. Factors Regulating Trophoblast Invasion. Gynecologic and Obstetric Investigation. 2007;64(3):126–30.
3. Kaufmann P, Black S, Huppertz B. Endovascular Trophoblast Invasion: Implications for the Pathogenesis of Intrauterine Growth Retardation and Preeclampsia. Biol Reprod. 2003 Jan 7;69(1):1–7.
4. Ball E, Bulmer JN, Ayis S, Lyall F, Robson SC. Late sporadic miscarriage is associated with abnormalities in spiral artery transformation and trophoblast invasion. The Journal of Pathology. 2006 Jan 9;208(4):535–42.
5. Kim Y. Failure of physiologic transformation of the spiral arteries in patients with preterm labor and intact membranes. American Journal of Obstetrics and Gynecology. 2003 Oct;189(4):1063–9.
6. Liotta LA, Tryggvason K, Garbisa S, Hart I, Foltz CM, Shafie S. Metastatic potential correlates with enzymatic degradation of basement membrane collagen. Nature. 1980 Mar 6;284(5751):67–8.
7. Martin MD, Matrisian LM. The other side of MMPs: Protective roles in tumor progression. Cancer and Metastasis Reviews. 2007 Aug 24;26(3-4):717–24.
8. Benirschke K, Kaufmann P, Baergen RN. 4. Placental Types. Pathology of the Human Placenta, 5th Edition. 5th ed. Springer; 2006.
9. Benirschke K, Kaufmann P, Baergen RN. 2. Macroscopic Features of the delivered Placenta. Pathology of the Human Placenta, 5th Edition. 5th ed. Springer; 2006.
10. Schultze BS. Ueber velamentale und placentale Insertion der Nabelschnur. Archives of Gynecology and Obstetrics. 1887 Feb 1;30(1):47–56.
11. MD HK, PSE HK PSE, MD DMN, MD YW. The Placenta: From Development to Disease. John Wiley & Sons; 2011.
12. Kraus FT, (U.S.) AFI of P. Placental pathology. American Registry of Pathology in collaboration with the Armed Forces Institute of Pathology; 2004.
13. Development of the placental villi [Internet]. [cited 2012 Apr 1]. Available from: http://embryology.ch/anglais/fplacenta/villosite01.html
14. Benirschke K, Kaufmann P, Baergen RN. 3. Microscopic Survey. Pathology of the Human Placenta, 5th Edition. 5th ed. Springer; 2006.

15. Benirschke K, Kaufmann P, Baergen RN. 9. Nonvillous Parts and Trophoblast Invasion. Pathology of the Human Placenta, 5th Edition. 5th ed. Springer; 2006.
16. Hartmann M, Pabst MA, Schmied R. Zytologie, Histologie und Mikroskopische Anatomie: Licht- und elektronenmikroskopischer Bildatlas. 3. A. Facultas Universitätsverlag; 2005.
17. Moser G, Gauster M, Orendi K, Glasner A, Theuerkauf R, Huppertz B. Endoglandular trophoblast, an alternative route of trophoblast invasion? Analysis with novel confrontation co-culture models. Human Reproduction. 2010 Feb 22;25(5):1127–36.
18. Burton GJ, Jauniaux E, Charnock-Jones DS. Human Early Placental Development: Potential Roles of the Endometrial Glands. Placenta. 2007 Apr;28:S64–S69.
19. Benirschke K, Kaufmann P, Baergen RN. 7. Architecture of Normal Villous Trees. Pathology of the Human Placenta, 5th Edition. 5th ed. Springer; 2006.
20. Fox H. Aging of the Placenta. Arch Dis Child Fetal Neonatal Ed. 1997 Jan 11;77(3):F171–F175.
21. The physiology of the placenta [Internet]. [cited 2012 Apr 2]. Available from: http://embryology.ch/anglais/fplacenta/physio01.html
22. Early development [Internet]. [cited 2012 Apr 3]. Available from: http://embryology.ch/anglais/fplacenta/fecond01.html
23. Sadler TW, Langman J. Medizinische Embryologie. Die normale menschliche Entwicklung und ihre Fehlbildungen. 10., korrigierte A. Thieme, Stuttgart; 2003.
24. Implantation [Internet]. [cited 2012 Apr 3]. Available from: http://embryology.ch/anglais/fplacenta/fecond02.html
25. The trophoblast [Internet]. [cited 2012 Apr 4]. Available from: http://embryology.ch/anglais/fplacenta/fecond03.html
26. Benirschke K, Kaufmann P, Baergen RN. 5. Early Development of the Human Placenta. Pathology of the Human Placenta, 5th Edition. 5th ed. Springer; 2006.
27. Luckett WP. Origin and differentiation of the yolk sac and extraembryonic mesoderm in presomite human and rhesus monkey embryos. Am. J. Anat. 1978 May;152(1):59–97.
28. Enders AC, King BF. Formation and differentiation of extraembryonic mesoderm in the rhesus monkey. Am. J. Anat. 1988 Apr;181(4):327–40.
29. Early villous stages [Internet]. [cited 2012 Jul 2]. Available from: http://embryology.ch/anglais/fplacenta/villosite02.html

30. Nanaev A, Chwalisz K, Frank HG, Kohnen G, Hegele-Hartung C, Kaufmann P. Physiological dilation of uteroplacental arteries in the guinea pig depends on nitric oxide synthase activity of extravillous trophoblast. Cell Tissue Res. 1995 Dec;282(3):407–21.
31. Kam EPY, Gardner L, Loke YW, King A. The role of trophoblast in the physiological change in decidual spiral arteries. Hum. Reprod. 1999 Jan 8;14(8):2131–8.
32. Bischof P, Irminger-Finger I. The human cytotrophoblastic cell, a mononuclear chameleon. Int. J. Biochem. Cell Biol. 2005 Jan;37(1):1–16.
33. Genbacev O, Jensen KD, Powlin SS, Miller RK. In vitro differentiation and ultrastructure of human extravillous trophoblast (EVT) cells. Placenta. 1993 Aug;14(4):463–75.
34. Damsky CH, Fitzgerald ML, Fisher SJ. Distribution patterns of extracellular matrix components and adhesion receptors are intricately modulated during first trimester cytotrophoblast differentiation along the invasive pathway, in vivo. J Clin Invest. 1992 Jan;89(1):210–22.
35. Sasagawa M, Yamazaki T, Endo M, Kanazawa K, Takeuchi S. Immunohistochemical localization of HLA antigens and placental proteins (alpha hCG, beta hCG CTP, hPL and SP1 in villous and extravillous trophoblast in normal human pregnancy: a distinctive pathway of differentiation of extravillous trophoblast. Placenta. 1987 Oct;8(5):515–28.
36. Huppertz B, Kertschanska S, Demir AY, Frank HG, Kaufmann P. Immunohistochemistry of matrix metalloproteinases (MMP), their substrates, and their inhibitors (TIMP) during trophoblast invasion in the human placenta. Cell Tissue Res. 1998 Jan;291(1):133–48.
37. Damsky CH, Librach C, Lim KH, Fitzgerald ML, McMaster MT, Janatpour M, et al. Integrin switching regulates normal trophoblast invasion. Development. 1994 Dec;120(12):3657–66.
38. Ferretti C, Bruni L, Dangles-Marie V, Pecking AP, Bellet D. Molecular circuits shared by placental and cancer cells, and their implications in the proliferative, invasive and migratory capacities of trophoblasts. Hum. Reprod. Update. 2007 Apr;13(2):121–41.
39. Eble JA, Haier J. Integrins in cancer treatment. Curr Cancer Drug Targets. 2006 Mar;6(2):89–105.

40. Craven CM, Morgan T, Ward K. Decidual spiral artery remodelling begins before cellular interaction with cytotrophoblasts. Placenta. 1998 May;19(4):241–52.
41. Hees H, Moll W, Wrobel KH, Hees I. Pregnancy-induced structural changes and trophoblastic invasion in the segmental mesometrial arteries of the guinea pig (Cavia porcellus L.). Placenta. 1987 Dec;8(6):609–26.
42. Earl U, Morrison L, Gray C, Bulmer JN. Proteinase and proteinase inhibitor localization in the human placenta. Int. J. Gynecol. Pathol. 1989;8(2):114–24.
43. Nanaev AK, Kosanke G, Reister F, Kemp B, Frank HG, Kaufmann P. Pregnancy-induced de-differentiation of media smooth muscle cells in uteroplacental arteries of the guinea pig is reversible after delivery. Placenta. 2000 May;21(4):306–12.
44. Tuttle SE, O'Toole RV, O'Shaughnessy RW, Zuspan FP. Immunohistochemical evaluation of human placental implantation: an initial study. Am. J. Obstet. Gynecol. 1985 Oct 1;153(3):239–44.
45. Chakraborti S, Mandal M, Das S, Mandal A, Chakraborti T. Regulation of matrix metalloproteinases: an overview. Molecular and cellular biochemistry. 2003;253(1):269–85.
46. Massova I, Kotra LP, Fridman R, Mobashery S. Matrix metalloproteinases: structures, evolution, and diversification. The FASEB journal. 1998;12(12):1075.
47. Herron GS, Unemori E, Wong M, Rapp JH, Hibbs MH, Stoney RJ. Connective tissue proteinases and inhibitors in abdominal aortic aneurysms. Involvement of the vasa vasorum in the pathogenesis of aortic aneurysms. Arteriosclerosis, Thrombosis, and Vascular Biology. 1991 Nov 1;11(6):1667–77.
48. Denhardt DT, Feng B, Edwards DR, Cocuzzi ET, Malyankar UM. Tissue inhibitor of metalloproteinases (TIMP, aka EPA): structure, control of expression and biological functions. Pharmacol. Ther. 1993 Sep;59(3):329–41.
49. Woessner JF. MMPs and TIMPs—an historical perspective. Molecular biotechnology. 2002;22(1):33–49.
50. Gross J, Lapiere CM. COLLAGENOLYTIC ACTIVITY IN AMPHIBIAN TISSUES: A TISSUE CULTURE ASSAY*. Proc Natl Acad Sci U S A. 1962 Jun;48(6):1014–22.
51. Eisen AZ, Jeffrey JJ, Gross J. Human skin collagenase. Isolation and mechanism of attack on the collagen molecule. Biochim. Biophys. Acta. 1968 Mar 25;151(3):637–45.
52. Sternlicht MD, Werb Z. How matrix metalloproteinases regulate cell behavior.

Annual review of cell and developmental biology. 2001;17:463.

53. Stöcker W, Grams F, Baumann U, Reinemer P, Gomis-Rüth FX, McKay DB, et al. The metzincins--topological and sequential relations between the astacins, adamalysins, serralysins, and matrixins (collagenases) define a superfamily of zinc-peptidases. Protein Sci. 1995 May;4(5):823–40.

54. Stöcker W, Bode W. Structural features of a superfamily of zinc-endopeptidases: the metzincins. Curr. Opin. Struct. Biol. 1995 Jun;5(3):383–90.

55. Van Wart HE, Birkedal-Hansen H. The cysteine switch: a principle of regulation of metalloproteinase activity with potential applicability to the entire matrix metalloproteinase gene family. Proc Natl Acad Sci U S A. 1990 Jul;87(14):5578–82.

56. Banda MJ, Werb Z. Mouse macrophage elastase. Purification and characterization as a metalloproteinase. Biochemical Journal. 1981 Feb 1;193(2):589.

57. Limited proteolysis by macrophage elastase inactivates human alpha 1- proteinase inhibitor. The Journal of Experimental Medicine. 1980 Dec 1;152(6):1563.

58. Gronski TJ, Martin RL, Kobayashi DK, Walsh BC, Holman MC, Huber M, et al. Hydrolysis of a Broad Spectrum of Extracellular Matrix Proteins by Human Macrophage Elastase. Journal of Biological Chemistry. 1997 May 2;272(18):12189–94.

59. Nagase H, Woessner JF. Matrix Metalloproteinases. Journal of Biological Chemistry. 1999 Jul 30;274(31):21491 –21494.

60. Lang R, Kocourek A, Braun M, Tschesche H, Huber R, Bode W, et al. Substrate specificity determinants of human macrophage elastase (MMP-12) based on the 1.1 Å crystal structure1. Journal of Molecular Biology. 2001 Sep 28;312(4):731–42.

61. Woessner JF Jr. Matrix metalloproteinases and their inhibitors in connective tissue remodeling. FASEB J. 1991 May;5(8):2145–54.

62. Springman EB, Angleton EL, Birkedal-Hansen H, Van Wart HE. Multiple modes of activation of latent human fibroblast collagenase: evidence for the role of a Cys73 active-site zinc complex in latency and a“ cysteine switch” mechanism for activation. Proceedings of the National Academy of Sciences. 1990;87(1):364.

63. Parks WC, Shapiro SD. Matrix metalloproteinases in lung biology. Respiratory research. 2000;2(1):10.

64. Saarialho-Kere UK, Kovacs SO, Pentland AP, Olerud JE, Welgus HG, Parks WC. Cell-matrix interactions modulate interstitial collagenase expression by human

keratinocytes actively involved in wound healing. Journal of Clinical Investigation. 1993;92(6):2858.

65. Wang Z. TIMP-2 Is Required for Efficient Activation of proMMP-2 in Vivo. Journal of Biological Chemistry. 2000 May 25;275(34):26411–5.
66. Sottrup-Jensen L. Alpha-macroglobulins: structure, shape, and mechanism of proteinase complex formation. J. Biol. Chem. 1989 Jul 15;264(20):11539–42.
67. Birkedal-Hansen H, Moore W, Bodden M, Windsor L, Birkedal-Hansen B, DeCarlo A, et al. Matrix metalloproteinases: a review. Critical Reviews in Oral Biology & Medicine. 1993;4(2):197–250.
68. Yang Z, Kyriakides TR, Bornstein P. Matricellular Proteins as Modulators of Cell–Matrix Interactions: Adhesive Defect in Thrombospondin 2-null Fibroblasts is a Consequence of Increased Levels of Matrix Metalloproteinase-2. Molecular Biology of the Cell. 2000 Oct;11(10):3353.
69. Yang Z. Extracellular Matrix Metalloproteinase 2 Levels Are Regulated by the Low Density Lipoprotein-related Scavenger Receptor and Thrombospondin 2. Journal of Biological Chemistry. 2000 Dec 11;276(11):8403–8.
70. Mammalian MMPs and Substrates [Internet]. [cited 2012 Jun 15]. Available from: http://www.clip.ubc.ca/mmp_timp_folder/mmp_substrates.shtm
71. MEROPS - clan MA- the Peptidase Database [Internet]. [cited 2012 Aug 29]. Available from: http://merops.sanger.ac.uk/cgi-bin/clansum?clan=MA
72. MEROPS - family M10- the Peptidase Database [Internet]. [cited 2012 Aug 29]. Available from: http://merops.sanger.ac.uk/cgi-bin/famsum?family=M10
73. Ng KTP, Qi X, Kong KL, Cheung BYY, Lo CM, Poon RTP, et al. Overexpression of matrix metalloproteinase-12 (MMP-12) correlates with poor prognosis of hepatocellular carcinoma. European Journal of Cancer. 2011;
74. Basset P, Bellocq JP, Wolf C, Stoll I, Hutin P, Limacher JM, et al. A novel metalloproteinase gene specifically expressed in stromal cells of breast carcinomas. Nature. 1990 Dec 27;348(6303):699–704.
75. Heppner KJ, Matrisian LM, Jensen RA, Rodgers WH. Expression of most matrix metalloproteinase family members in breast cancer represents a tumor-induced host response. The American journal of pathology. 1996;149(1):273.
76. Egeblad M, Werb Z. New functions for the matrix metalloproteinases in cancer progression. Nature Reviews Cancer. 2002 Mar;2(3):161–74.
77. Lynch CC, Matrisian LM. Matrix metalloproteinases in tumor-host cell

communication. Differentiation. 2002 Dec;70(9-10):561–73.

78. Koop S, Khokha R, Schmidt EE, MacDonald IC, Morris VL, Chambers AF, et al. Overexpression of metalloproteinase inhibitor in B16F10 cells does not affect extravasation but reduces tumor growth. Cancer Res. 1994 Sep 1;54(17):4791–7.

79. Whitelock JM, Murdoch AD, Iozzo RV, Underwood PA. The degradation of human endothelial cell-derived perlecan and release of bound basic fibroblast growth factor by stromelysin, collagenase, plasmin, and heparanases. J. Biol. Chem. 1996 Apr 26;271(17):10079–86.

80. Imai K, Hiramatsu A, Fukushima D, Pierschbacher MD, Okada Y. Degradation of decorin by matrix metalloproteinases: identification of the cleavage sites, kinetic analyses and transforming growth factor-beta1 release. Biochem. J. 1997 Mar 15;322 (Pt 3):809–14.

81. Mañes S, Mira E, Barbacid MM, Ciprés A, Fernández-Resa P, Buesa JM, et al. Identification of insulin-like growth factor-binding protein-1 as a potential physiological substrate for human stromelysin-3. J. Biol. Chem. 1997 Oct 10;272(41):25706–12.

82. Mañes S, Llorente M, Lacalle RA, Gómez-Moutón C, Kremer L, Mira E, et al. The matrix metalloproteinase-9 regulates the insulin-like growth factor-triggered autocrine response in DU-145 carcinoma cells. J. Biol. Chem. 1999 Mar 12;274(11):6935–45.

83. Agrez M, Chen A, Cone RI, Pytela R, Sheppard D. The alpha v beta 6 integrin promotes proliferation of colon carcinoma cells through a unique region of the beta 6 cytoplasmic domain. J. Cell Biol. 1994 Oct;127(2):547–56.

84. Powell WC, Fingleton B, Wilson CL, Boothby M, Matrisian LM. The metalloproteinase matrilysin proteolytically generates active soluble Fas ligand and potentiates epithelial cell apoptosis. Curr. Biol. 1999 Dec 16;9(24):1441–7.

85. Vargo-Gogola T, Crawford HC, Fingleton B, Matrisian LM. Identification of novel matrix metalloproteinase-7 (matrilysin) cleavage sites in murine and human Fas ligand. Arch. Biochem. Biophys. 2002 Dec 15;408(2):155–61.

86. Vargo-Gogola T, Fingleton B, Crawford HC, Matrisian LM. Matrilysin (matrix metalloproteinase-7) selects for apoptosis-resistant mammary cells in vivo. Cancer Res. 2002 Oct 1;62(19):5559–63.

87. Fingleton B, Vargo-Gogola T, Crawford HC, Matrisian LM. Matrilysin [MMP-7] expression selects for cells with reduced sensitivity to apoptosis. Neoplasia. 2001

Dec;3(6):459–68.

88. Balbín M, Fueyo A, Tester AM, Pendás AM, Pitiot AS, Astudillo A, et al. Loss of collagenase-2 confers increased skin tumor susceptibility to male mice. Nat. Genet. 2003 Nov;35(3):252–7.
89. D'Armiento J, DiColandrea T, Dalal SS, Okada Y, Huang MT, Conney AH, et al. Collagenase expression in transgenic mouse skin causes hyperkeratosis and acanthosis and increases susceptibility to tumorigenesis. Mol. Cell. Biol. 1995 Oct;15(10):5732–9.
90. McCawley LJ, Crawford HC, King LE Jr, Mudgett J, Matrisian LM. A protective role for matrix metalloproteinase-3 in squamous cell carcinoma. Cancer Res. 2004 Oct 1;64(19):6965–72.
91. Witty JP, Lempka T, Coffey RJ Jr, Matrisian LM. Decreased tumor formation in 7,12-dimethylbenzanthracene-treated stromelysin-1 transgenic mice is associated with alterations in mammary epithelial cell apoptosis. Cancer Res. 1995 Apr 1;55(7):1401–6.
92. McCawley LJ, Wright J, LaFleur BJ, Crawford HC, Matrisian LM. Keratinocyte expression of MMP3 enhances differentiation and prevents tumor establishment. Am. J. Pathol. 2008 Nov;173(5):1528–39.
93. Sternlicht MD, Lochter A, Sympson CJ, Huey B, Rougier JP, Gray JW, et al. The stromal proteinase MMP3/stromelysin-1 promotes mammary carcinogenesis. Cell. 1999 Jul 23;98(2):137–46.
94. Radisky DC, Levy DD, Littlepage LE, Liu H, Nelson CM, Fata JE, et al. Rac1b and reactive oxygen species mediate MMP-3-induced EMT and genomic instability. Nature. 2005 Jul 7;436(7047):123–7.
95. Kerkelä E, Ala-aho R, Klemi P, Grénman S, Shapiro SD, Kähäri V-M, et al. Metalloelastase (MMP-12) expression by tumour cells in squamous cell carcinoma of the vulva correlates with invasiveness, while that by macrophages predicts better outcome. J. Pathol. 2002 Oct;198(2):258–69.
96. Folkman J. Endogenous angiogenesis inhibitors. Apmis. 2004;112(7-8):496–507.
97. Patterson BC, Sang QA. Angiostatin-converting enzyme activities of human matrilysin (MMP-7) and gelatinase B/type IV collagenase (MMP-9). J. Biol. Chem. 1997 Nov 14;272(46):28823–5.
98. Lijnen HR, Ugwu F, Bini A, Collen D. Generation of an angiostatin-like fragment from plasminogen by stromelysin-1 (MMP-3). Biochemistry. 1998 Apr

7;37(14):4699–702.

99. Dong Z, Kumar R, Yang X, Fidler IJ. Macrophage-derived metalloelastase is responsible for the generation of angiostatin in Lewis lung carcinoma. Cell. 1997 Mar 21;88(6):801–10.

100. Westermarck J, Kähäri VM. Regulation of matrix metalloproteinase expression in tumor invasion. FASEB J. 1999 May;13(8):781–92.

101. Hamano Y, Zeisberg M, Sugimoto H, Lively JC, Maeshima Y, Yang C, et al. Physiological levels of tumstatin, a fragment of collagen IV alpha3 chain, are generated by MMP-9 proteolysis and suppress angiogenesis via alphaV beta3 integrin. Cancer Cell. 2003 Jun;3(6):589–601.

102. Pozzi A, Moberg PE, Miles LA, Wagner S, Soloway P, Gardner HA. Elevated matrix metalloprotease and angiostatin levels in integrin alpha 1 knockout mice cause reduced tumor vascularization. Proc. Natl. Acad. Sci. U.S.A. 2000 Feb 29;97(5):2202–7.

103. Chantrain CF, Shimada H, Jodele S, Groshen S, Ye W, Shalinsky DR, et al. Stromal matrix metalloproteinase-9 regulates the vascular architecture in neuroblastoma by promoting pericyte recruitment. Cancer Res. 2004 Mar 1;64(5):1675–86.

104. Bergers G, Brekken R, McMahon G, Vu TH, Itoh T, Tamaki K, et al. Matrix metalloproteinase-9 triggers the angiogenic switch during carcinogenesis. Nat. Cell Biol. 2000 Oct;2(10):737–44.

105. Houghton AM, Grisolano JL, Baumann ML, Kobayashi DK, Hautamaki RD, Nehring LC, et al. Macrophage elastase (matrix metalloproteinase-12) suppresses growth of lung metastases. Cancer Res. 2006 Jun 15;66(12):6149–55.

106. Acuff HB, Sinnamon M, Fingleton B, Boone B, Levy SE, Chen X, et al. Analysis of host- and tumor-derived proteinases using a custom dual species microarray reveals a protective role for stromal matrix metalloproteinase-12 in non-small cell lung cancer. Cancer Res. 2006 Aug 15;66(16):7968–75.

107. Hofmann H-S, Hansen G, Richter G, Taege C, Simm A, Silber R-E, et al. Matrix metalloproteinase-12 expression correlates with local recurrence and metastatic disease in non-small cell lung cancer patients. Clin. Cancer Res. 2005 Feb 1;11(3):1086–92.

108. Kerkelä E, Ala-Aho R, Jeskanen L, Rechardt O, Grénman R, Shapiro SD, et al. Expression of human macrophage metalloelastase (MMP-12) by tumor cells in skin

cancer. J. Invest. Dermatol. 2000 Jun;114(6):1113–9.

109. Deryugina EI, Quigley JP. Matrix metalloproteinases and tumor metastasis. Cancer Metastasis Rev. 2006 Mar;25(1):9–34.

110. Schultz RM, Silberman S, Persky B, Bajkowski AS, Carmichael DF. Inhibition by human recombinant tissue inhibitor of metalloproteinases of human amnion invasion and lung colonization by murine B16-F10 melanoma cells. Cancer Res. 1988 Oct 1;48(19):5539–45.

111. Khokha R. Suppression of the tumorigenic and metastatic abilities of murine B16-F10 melanoma cells in vivo by the overexpression of the tissue inhibitor of the metalloproteinases-1. J. Natl. Cancer Inst. 1994 Feb 16;86(4):299–304.

112. Watanabe M, Takahashi Y, Ohta T, Mai M, Sasaki T, Seiki M. Inhibition of metastasis in human gastric cancer cells transfected with tissue inhibitor of metalloproteinase 1 gene in nude mice. Cancer. 1996 Apr 15;77(8 Suppl):1676–80.

113. Itoh T, Tanioka M, Yoshida H, Yoshioka T, Nishimoto H, Itohara S. Reduced angiogenesis and tumor progression in gelatinase A-deficient mice. Cancer Res. 1998 Mar 1;58(5):1048–51.

114. Itoh T, Tanioka M, Matsuda H, Nishimoto H, Yoshioka T, Suzuki R, et al. Experimental metastasis is suppressed in MMP-9-deficient mice. Clin. Exp. Metastasis. 1999 Mar;17(2):177–81.

115. Agarwal D, Goodison S, Nicholson B, Tarin D, Urquidi V. Expression of matrix metalloproteinase 8 (MMP-8) and tyrosinase-related protein-1 (TYRP-1) correlates with the absence of metastasis in an isogenic human breast cancer model. Differentiation. 2003 Mar;71(2):114–25.

116. Montel V, Kleeman J, Agarwal D, Spinella D, Kawai K, Tarin D. Altered Metastatic Behavior of Human Breast Cancer Cells After Experimental Manipulation of Matrix Metalloproteinase 8 Gene Expression. Cancer Res. 2004 Jan 3;64(5):1687–94.

117. Hotary KB, Allen ED, Brooks PC, Datta NS, Long MW, Weiss SJ. Membrane type I matrix metalloproteinase usurps tumor growth control imposed by the three-dimensional extracellular matrix. Cell. 2003 Jul 11;114(1):33–45.

118. Sabeh F, Ota I, Holmbeck K, Birkedal-Hansen H, Soloway P, Balbin M, et al. Tumor cell traffic through the extracellular matrix is controlled by the membrane-anchored collagenase MT1-MMP. J. Cell Biol. 2004 Nov 22;167(4):769–81.

119. Zhai Y, Hotary KB, Nan B, Bosch FX, Muñoz N, Weiss SJ, et al. Expression of

membrane type 1 matrix metalloproteinase is associated with cervical carcinoma progression and invasion. Cancer Res. 2005 Aug 1;65(15):6543–50.

120. Coussens LM, Tinkle CL, Hanahan D, Werb Z. MMP-9 supplied by bone marrow-derived cells contributes to skin carcinogenesis. Cell. 2000 Oct 27;103(3):481–90.

121. Acuff HB, Carter KJ, Fingleton B, Gorden DL, Matrisian LM. Matrix metalloproteinase-9 from bone marrow-derived cells contributes to survival but not growth of tumor cells in the lung microenvironment. Cancer Res. 2006 Jan 1;66(1):259–66.

122. Fisher SJ, Cui TY, Zhang L, Hartman L, Grahl K, Zhang GY, et al. Adhesive and degradative properties of human placental cytotrophoblast cells in vitro. J. Cell Biol. 1989 Aug;109(2):891–902.

123. Bischof P, Friedli E, Martelli M, Campana A. Expression of extracellular matrix-degrading metalloproteinases by cultured human cytotrophoblast cells: effects of cell adhesion and immunopurification. Am. J. Obstet. Gynecol. 1991 Dec;165(6 Pt 1):1791–801.

124. Martelli M, Campana A, Bischof P. Secretion of matrix metalloproteinases by human endometrial cells in vitro. J. Reprod. Fertil. 1993 May;98(1):67–76.

125. Emonard H, Christiane Y, Smet M, Grimaud JA, Foidart JM. Type IV and interstitial collagenolytic activities in normal and malignant trophoblast cells are specifically regulated by the extracellular matrix. Invasion Metastasis. 1990;10(3):170–7.

126. Blankenship TN, King BF. Identification of 72-kilodalton type IV collagenase at sites of trophoblastic invasion of macaque spiral arteries. Placenta. 1994 Mar;15(2):177–87.

127. Autio-Harmainen H, Hurskainen T, Niskasaari K, Höyhtyä M, Tryggvason K. Simultaneous expression of 70 kilodalton type IV collagenase and type IV collagen alpha 1 (IV) chain genes by cells of early human placenta and gestational endometrium. Lab. Invest. 1992 Aug;67(2):191–200.

128. Polette M, Nawrocki B, Pintiaux A, Massenat C, Maquoi E, Volders L, et al. Expression of gelatinases A and B and their tissue inhibitors by cells of early and term human placenta and gestational endometrium. Lab. Invest. 1994 Dec;71(6):838–46.

129. Xu P, Wang YL, Zhu SJ, Luo SY, Piao YS, Zhuang LZ. Expression of matrix metalloproteinase-2, -9, and -14, tissue inhibitors of metalloproteinase-1, and

matrix proteins in human placenta during the first trimester. Biol. Reprod. 2000 Apr;62(4):988–94.

130. 92-kD type IV collagenase mediates invasion of human cytotrophoblasts. The Journal of Cell Biology. 1991 Apr 2;113(2):437.

131. Vettraino IM, Roby J, Tolley T, Parks WC. Collagenase-I, stromelysin-I, and matrilysin are expressed within the placenta during multiple stages of human pregnancy. Placenta. 1996 Nov;17(8):557–63.

132. Maquoi E, Polette M, Nawrocki B, Bischof P, Noël A, Pintiaux A, et al. Expression of stromelysin-3 in the human placenta and placental bed. Placenta. 1997 May;18(4):277–85.

133. Harris LK, Smith SD, Keogh RJ, Jones RL, Baker PN, Knöfler M, et al. Trophoblast- and Vascular Smooth Muscle Cell-Derived MMP-12 Mediates Elastolysis during Uterine Spiral Artery Remodeling. The American Journal of Pathology. 2010 Oct;177(4):2103–15.

134. Staun-Ram E, Goldman S, Gabarin D, Shalev E. Expression and importance of matrix metalloproteinase 2 and 9 (MMP-2 and -9) in human trophoblast invasion. Reprod. Biol. Endocrinol. 2004 Aug 4;2:59.

135. Hurskainen T, Seiki M, Apte SS, Syrjakallio-Ylitalo M, Sorsa T, Oikarinen A, et al. Production of Membrane-type Matrix Metalloproteinase-1 (MT-MMP-1) in Early Human Placenta: A Possible Role in Placental Implantation? Journal of Histochemistry & Cytochemistry. 1998 Feb 1;46(2):221–9.

136. Nawrocki B, Polette M, Marchand V, Maquoi E, Beorchia A, Tournier JM, et al. Membrane-type matrix metalloproteinase-1 expression at the site of human placentation. Placenta. 1996 Nov;17(8):565–72.

137. Marzusch K, Ruck P, Dietl JA, Horny H-P, Kaiserling E. Immunohistochemical localization of tissue inhibitor of metalloproteinases-2 (TIMP-2) in first trimester human placental decidua. European Journal of Obstetrics & Gynecology and Reproductive Biology. 1996 Sep;68:105–7.

138. Bass KE, Li H, Hawkes SP, Howard E, Bullen E, Vu TK, et al. Tissue inhibitor of metalloproteinase-3 expression is upregulated during human cytotrophoblast invasion in vitro. Dev. Genet. 1997;21(1):61–7.

139. Kliman HJ, Feinberg RF. Human trophoblast-extracellular matrix (ECM) interactions in vitro: ECM thickness modulates morphology and proteolytic activity. Proceedings of the National Academy of Sciences of the United States of

America. 1990 Apr;87(8):3057.

140. Shimonovitz S, Hurwitz A, Hochner-Celnikier D, Dushnik M, Anteby E, Yagel S. Expression of gelatinase B by trophoblast cells: Down-regulation by progesterone. American Journal of Obstetrics and Gynecology. 1998 Mar;178(3):457–61.
141. Bischof P. Endocrine, paracrine and autocrine regulation of trophoblastic metalloproteinases. Early Pregnancy. 2001 Jan;5(1):30–1.
142. Qiu X, Xie Y, Chen L, Gemzell-Danielsson K. Expression of matrix metalloproteinases and their inhibitors at the feto-maternal interface in unruptured ectopic tubal pregnancy. Acta Obstetricia et Gynecologica Scandinavica. 2011 Sep;90(9):966–71.
143. RNA quality control [Internet]. [cited 2012 Aug 29]. Available from: http://biomedicalgenomics.org/RNA_quality_control.html
144. DNA Array Core Facility [Internet]. [cited 2012 Aug 30]. Available from: http://www.scripps.edu/california/research/dna-array/index.html
145. GeneChip Human Genome U95 Set | Affymetrix - Manuals [Internet]. [cited 2012 Aug 30]. Available from: http://www.affymetrix.com/estore/browse/products.jsp?navMode=34000&productId=131538&navAction=jump&aId=productsNav#1_3
146. Chuang Lab / UCSF [Internet]. [cited 2012 Aug 29]. Available from: http://www.cvri.ucsf.edu/~chuang/resources.html
147. In situ hybridization genedetect.com [Internet]. [cited 2012 Aug 30]. Available from: http://www.genedetect.com/insitu.htm
148. Wilkinson DG. In Situ Hybridization. Oxford University Press; 1992.
149. Roche - Application Manual: Nonradioactive ISH [Internet]. [cited 2012 Aug 30]. Available from: http://www.roche-applied-science.com/PROD_INF/index.jsp?id=techMan&pageid=/PROD_INF/MANUALS/InSitu/InSi_toc.htm
150. Ino H. Application of Antigen Retrieval by Heating for Double-label Fluorescent Immunohistochemistry with Identical Species-derived Primary Antibodies. Journal of Histochemistry and Cytochemistry. 2004 Sep 1;52(9):1209–17.
151. Buchwalow IB, Böcker W. Immunohistochemistry: Basics and Methods. Springer; 2010.
152. Tsurui H, Nishimura H, Hattori S, Hirose S, Okumura K, Shirai T. Seven-color Fluorescence Imaging of Tissue Samples Based on Fourier Spectroscopy and

Singular Value Decomposition. Journal of Histochemistry & Cytochemistry. 2000 May 1;48(5):653–62.

153. Renshaw S. Immunohistochemistry: Methods Express. 1st ed. Renshaw S, editor. Scion Publishing Ltd; 2006.

154. Shi S-R, Cote RJ, Taylor CR. Antigen Retrieval Immunohistochemistry: Past, Present, and Future. J Histochem Cytochem. 1997 Mar 1;45(3):327–43.

155. Bilban M, Ghaffari-Tabrizi N, Hintermann E, Bauer S, Molzer S, Zoratti C, et al. Kisspeptin-10, a KiSS-1/metastin-derived decapeptide, is a physiological invasion inhibitor of primary human trophoblasts. J. Cell. Sci. 2004 Mar 15;117(Pt 8):1319–28.

156. Reister F, Frank HG, Heyl W, Kosanke G, Huppertz B, Schröder W, et al. The distribution of macrophages in spiral arteries of the placental bed in pre-eclampsia differs from that in healthy patients. Placenta. 1999 Apr;20(2-3):229–33.

157. Jaffe R, Jauniaux E, Hustin J. Maternal circulation in the first-trimester human placenta—Myth or reality? American Journal of Obstetrics and Gynecology. 1997 Mar;176(3):695–705.

158. Kliman HJ. Uteroplacental Blood Flow□: The Story of Decidualization, Menstruation, and Trophoblast Invasion. The American Journal of Pathology. 2000 Dec;157(6):1759.

159. The Openings of Uteroplacental Vessels With Villous Infiltration at Different Gestational Ages [Internet]. Archives of Pathology & Laboratory Medicine Online. [cited 2012 Sep 6]. Available from: /han/pubmed/www.archivesofpathology.org/doi/abs/10.1043/1543-2165%282005%29129%3C382%3ATOOUVW%3E2.0.CO%3B2

G List of abbreviations

Ab	Antibody
acc. to	According to
ADAM	A-disintegrin-and-metalloproteinase
AP	Alkaline phosphatase
AP-1	Activator protein 1
APMA	Aminophenyl mercuric acetate
BCP	Bromchlorpropan
BCPI	5-bromo-4-chloro-3-indolyl phosphate
bFGF	Basic fibroblast growth factor
bp	Base pair
[c]	Concentration
CAM	Chorioallantoic membrane
CD34	Cluster of differentiation 34
CD68	Cluster of differentiation 68
cDNA	Complementary deoxyribonucleic acid
CE	Carboxyterminal end
[Ci]	Curie
CK-7	Cytokeratin-7
COMP	Cartilage oligomeric matrix protein
[cpm]	Counts per minute
GSPG	Chondroitin sulphate proteoglycan
CTB	Cytotrophoblast cells
vCTB	Villous cytotrophoblast cells
evCTB	Extra-villous cytotrophoblast cells
inCTB	Interstitial cytotrophoblast cells
enCTB	Endovascular cytotrophoblast cells
D	Decidua
DAPI	4’,6-diamidino-2-phenylindole

DEPC	Diethylpyrocarbonat
dH_2O	Deionized water
DHEA	Dehydroepiandrosterone
DIG	Digoxigenin
dl	Double lable
DMBA	7,12-Dimethylbenz(a)anthracene
DNA	Deoxyribonucleic acid
dNTP	Desoxynucleoside triphosphate
DTT	Dithiothreitol
DSPG2	Decorin
E	Erythrocyte(s)
e.g.	Exempli gratia
ECM	Extra-cellular matrix
ECN	Enzyme commission numbers
EDP	Elastin-derived peptides
EDTA	Ethylenediaminetetraacetic acid
EGF	Epidermal growth factor
EM	Extraembryonic mesenchyme
em.	Emission
et al	Et aliae; and others
etc.	Et cetera
EtOH	Ethyl alcohol
ETS	E-twenty six
ex.	Excitation
Fab	Fragment antigen-binding
Fig.	Figure
FFPE	Formalin-fixed paraffin-embedded
fw	Forward
FTP	First trimester placenta
[g]	Gram
g	Acceleration factor in times of earth's gravity
G	Goat

GSSG	Oxidized glutathione
gtt	Guttae, drops
[h]	Hour
H	Human
^{3}H	^{3}Hydroxygen, Tritium
hCG	Human chorion-gonadotropin
hCS	Human chorionic somatotropine
HCl	Hydrogen chloride
HIER	Heat-induced epitope retrieval
HLA-G	Human leukocyte antigen G
H_2O_2	Hydrogen peroxide
HOCl	Hypochlorous acid
hPL	Human placental lactogen
HR	Hinge region
i.e.	Idem est
IEL	Internal elastic lamina
IF	Immunofluorescence
IGF	Insulin-like growth factor
IgG	Immunoglobulin G
IGFBP-1	Insulin-like growth factor-binding protein 1
IHC	Immunohistochemistry
IL	Interleukin
IMP	(Smaller) inhibitor of metalloproteinase
ISH	In-situ hybridization
K	Kilo, 1000
kb	Kilo-base (pair)
KCl	Potassium chloride
[L]	Liter
LIMP	Larger inhibitor of metalloproteinase
LIF	Leukemia inhibitory factor
LLC	Lewis lung carcinoma
LRP	Lipoprotein receptor-related protein

[M]	Mol
M	Mouse
[min]	Minute
[ml]	Millilitre
[mM]	Millimol
[mm]	Millimetre
$MgCl_2$	Magnesium chloride
MMP	Matrix metalloproteinases
NaCl	Sodium chloride
NaOH	Sodium hydroxide
NBT	Nitro blue tetrazolium
NEM	N-ethylmaleimide
NGF	Nerve growth factor
[nm]	Nanometre
NO	Nitrogen monoxide
^{32}P	^{32}Phosphate
PBS	Phosphate buffered saline
p.c.	Post conception
PCR	Polymerase chain reaction
PDGF	Platelet-derived growth factor
PEA3	Ets transcription factor
PFA	Paraformaldehyde
pH	Potentia hydrogenii
PIER	Proteolytic-induced epitope retrieval
pos.	Positive
PSGC	Placenta site giant cells
Rb	Rabbit
RefSeq	Reference sequence
resp	Respectively
rHB2	Riboprobe hybridisation buffer 2???
RNA	Ribonucleic acid
mRNA	Messenger ribonucleic acid

tRNA	Transfer ribonucleic acid
RNAse	Ribonuclease
ROI	Region of interest
ROS	Reactive oxygen species
rt	Reverse transcriptase
RT	Room temperature
rv	Reverse
^{35}S	^{35}Sulfur
sFasL	Soluble Fas-ligand, CD95L
[sec]	Second
sq	Semi-quantitative
SDS	Sodium dodecyl sulfate
SSC	Saline sodium citrate
Tab.	Table
TAE	Tris base, acetic acid and EDTA
TBST	Tris-buffered saline and Tween 20
TGF	Transforming growth factor
TIMP	Tissue inhibitors of metalloproteinases
TNF	Tumour necrosis factor
TP	Term placenta
tPA	Tissue-type plasminogen activator
TPA	12-O-tetradecanoylphorbol-13-acetate
Tris	Tris(hydroxymethyl)aminomethane
TSP	Thrombospondin
UCLA	University of California, Los Angeles
uPA	Urokinase-type plasminogen activator
[V]	Volt
VEGF	Vascular endothelial growth factor
VL	Vessel lumen
vs.	Versus
VSMCs	Vascular smooth muscle cells
vWF	Von Willebrand Factor

wks	Weeks
WOP	Week of pregnancy
x	Times of magnification
[µl]	Microliter
[µm]	Micrometre
[µg]	Microgram

H List of figures

I List of tables

J List of buffers and protocols

Additional protocols

Step	Procedure
Heating	Fill 80 ml of DEPC water in a 100 ml beaker Heat to 60°C with a hot plate with stirring in a fume hood
Solvation	Add 20 g PFA to the heated water while stirring
Filling up	When particles are in an opaque suspension, fill up close to 100 ml with DEPC water.
Titration	Add diluted NaOH drop wise (HCl if overcorrected); target pH: 7.4
Finish	When solution is clear – fill up to 100 ml and filter. Test pH-value again. Store stock at -20°C and dilute it down to 4 % for use.

Protocol 8 – Preparation of 20 % PFA-stock

Buffer and solutions

Anti-digoxigenin solution

Reagent	Specification	Quantity
Buffer #1		6 ml
Triton-X-100		18 µl
Normal sheep serum		60 µl
Anti-digoxigenin	Dilution: 1:500	12 µl
Total		**96 ml**

Box buffer

Reagent	Specification	Quantity
SSC	4 x	50 ml
Formamide	50 %	125 ml
dH_2O		75 ml
Total		**250 ml**

Buffer #1

Reagent	Specification	Quantity
Tris-HCl	2M, pH 7.5	10 ml
NaCl	5M	6 ml
dH_2O		184 ml
Total		**200 ml**

Buffer stock solution (for buffer #2)

Reagent	Specification	Quantity
Blocking reagent		10 g
Buffer #1		100 ml
For mixing: stir and heat. Store at 4°C		
Final concentration (of blocking reagent)		**10 %**

Buffer #2

Reagent	Specification	Quantity
Blocking stock solution		10 ml
Buffer #1		90 ml
Final concentration (of blocking reagent)		**1 %**

Buffer #3

Reagent	Specification	Quantity
Tris-HCl	2M, pH 9.5	10 ml
NaCl	5M	4 ml
$MgCl_2$		6 ml
dH_2O		180
Total		**200 ml**

Buffer #4

Reagent	Specification	Quantity
Tris-HCl	2M, pH 8.0	250 µl
EDTA	0.5M, pH 8.0	200 µl
dH_2O		49.55 ml
Total		**50 ml**

Dehydration solution for S35 ISH

Final c(EtOH)	50 %	70 %	90 %
EtOH	125 ml	175 ml	225 ml
NA_4AC	25 ml	25 ml	25 ml
dH_2O	100 ml	50 ml	-
Total	**250 ml**	**250 ml**	**250 ml**

Denhardt's solution 50 x stock

Reagent	Specification	Quantity
Ficoll		5 g
Polyvinylpyrrolidone		5 g
Bovine serum albumin		5 g
Fill up to 500 ml, filter and store at -20°C		
Total		**500 ml**

Dextran sulphate 10 %

Reagent	Specification	Quantity
Dextran sulphate		25 g
DEPC H_2O	Fill up to approximately 40 ml	
In 37°C water bath over-night to go into a very viscous solution		
When in solution, bring up to 50 ml		
Total		**50 ml**

EDTA 0.5 M

Reagent	Specification	Quantity
Disodium ethylenediaminetetraacetate		186.1 g
H_2O		800 ml
Stir vigorously and adjust pH to 8.0 (as the salt would not go into solution before close to target pH value) Adjust to 1000 ml and autoclave. Store at RT.		
Total		**1000 ml**

Hybridisation solution

Reagent	Specification	Quantity
SDS	10 %	2 ml
SSC	20 x	2 ml
TRNA	10 mg/ml	1 ml
Dextransulfate	50 %	4 ml
Formamide	100 %	10 ml
DEPC H_2O		1 ml
Denatured Herring Salmon Serum DNA	10 µg/ml	1 ml
Total		**21 ml**

Normal sheep serum block

Reagent	Specification	Quantity
Buffer #1		2 ml
Triton-X-100		6 µl
Normal sheep serum	Dilution: 1:50	40 µl

PBS 10 x stock

Reagent	Specification	Quantity
NaCl		80.0 g
KCl		2.0 g
Na_2HPO_4 -H_2O		14.4 g
NaH_2PO_4 -H_2O	30 mM	2.4 g
dH_2O		900 ml
Mix to dissolve, adjust pH to 7.4 and bring volume up to 1000 ml. Store at RT.		
Total		**1000 ml**

rHB2 buffer

Reagent	Specification	Quantity
Formamide	50 %	15.0 ml
NaCl	0.3 M	1.8 ml
Tris	20 mM, pH 8.0	600 µl
EDTA	5 mM	600 µl
Denhardt's	1 x	300 µl
Dextrane sulphate	10 %	6.0 ml
DTT	10 mM	46.26 mg
DEPC H_2O		5.7 ml
Total		**30 ml**

RNAse buffer

Reagent	Specification	Quantity
NaCl	500 nM	100 ml
Tris	10 mM; pH 8.01	10 ml
DEPC H_2O		890 ml
Total		**1000 ml**

SCC 20 x stock

Reagent	Specification	Quantity
NaCl		175.3 g
Sodium citrate		88.2 g
H_2O		800 ml
Adjust pH to 7.0 and bring volume up to 1000 ml. Treat with DEPC and autoclave.		
Total		**1000 ml**

SDS 10 %

Reagent	Specification	Quantity
SDS		100 g
dH_2O		900 ml
Heat to 68°C to dissolve and adjust pH to 7.2 with HCl. Adjust volume to 1000 ml with dH_2O.		
Total		**1000 ml**

TAE 10 x stock

Reagent	Specification	Quantity
Tris base		48.4 g
Glacial acetic acid	17.4 M	11.4 ml
EDTA disodium salt		3.7 g
dH_2O		800 ml
Mix to dissolve and bring volume up to 1000 ml. Store at RT.		
Total		**1000 ml**

TBS 1 x

Reagent	Specification	Quantity
Tris		6.05 g
NaCl		8.76 g
dH_2O		800 ml
Mix to dissolve, adjust pH to 7.5 with HCl and bring volume up to 1000 ml. Store at 4°C.		
Total		**1000 ml**

TBST 1 x

Reagent	Specification	Quantity
Tween-20		1 ml
TBS	1 x	999 ml
Mix and store at 4°C.		
Total		**1000 ml**

TE buffer

Reagent	Specification	Quantity
Tris	1 M	0.5 ml
EDTA	0.5 mM	0.1 ml
DEPC H_2O		49.40 ml
Adjust pH to 8.0.		
Total		**50 ml**

Tris 1.0 M

Reagent	Specification	Quantity
Tris base		121.1 g
DEPC dH_2O		800 ml
Adjust pH with concentrated HCl when solution is at RT. Bring up to 1000 ml and filtrate.		
Total		**1000 ml**

Curriculum vitae

Name	Eyth, Christian Peter
Nationality	German
Date of birth	16.01.1985
Place of birth	Tübingen / Germany

Education

Date	10/2005 – present
Institute	Medical University of Graz / Austria
Major subject	Doctor of Medicine – Expected graduation date 10/2012
Date	08/1995 – 06/2004
Grammar School	Albeck Gymnasium in Sulz am Neckar / Germany

Medical training

Elective period

04/2012 – 06/2012	Imperial College London – Chelsea and Westminster Hospital, London / UK Department of Burns, Reconstructive and Plastic Surgery
02/2012 – 03/2012	Brighton and Sussex Medical School – Royal Sussex County Hospital, Brighton / UK Department of Otorhinolaryngology, Head and Neck Surgery
12/2011 – 01/2012	GP surgery Dr. H.R. Biedermann, Kalsdorf b. Graz / Austria Teaching practice for general medicine
10/2011 – 12/2011	University Medical Centre of Graz / Austria Department of Oncology, University Palliative Medicine Unit

Study assistant

03/2009 – present — Medical University of Graz / Austria
Institute for Pathophysiology and Immunology

- Assistant in teaching an laboratory research
- Supervising laboratory courses for students and summer school projects
- Teaching elective students
- Molecular biology – Performance and analysis of novelty gene on DNA and RNA levels
- Histology – Tissue processing for paraffin embedding, standard- as well as special stains further Immunohistochemistry, Double-label Immunofluorescence and In-situ hybridization

Medical clerkships

08/2011	Friedrich-Alexander-University Erlangen-Nürnberg / Germany University Medical Centre for Otorhinolaryngology, Head and Neck Surgery
02/2010	University Medical Centre of Graz / Austria Department of Otorhinolaryngology, Head and Neck Surgery
07/2009 – 08/2009	Institute for Pathophysiology and Immunology Graz / Austria Laboratory – advanced techniques in molecular biology and histology
08/2008	Robert-Bosch-Hospital in Stuttgart / Germany Department of Anaesthesiology and Critical Care Medicine / ICU
07/2008	State Hospital Graz-West / Austria Department of Internal Medicine
02/2008	State Hospital Feldbach / Austria Department of Internal Medicine
07/2007 – 08/2007	State Hospital Graz-West / Austria Department of General Surgery

Publications and Presentations

09/2012	*„Unusual cases of cyanoacrylate burn injuries: a report of two cases and a review of the literature“* ISBI 2012 – 16th Congress of the International Society for Burn Injuries: Poster presentation Edinburgh / Scotland
09/2011	*„Temporal and spatial localization of Matrix Metalloprotease 12 in the human placenta“* 3rd Annual Meeting of the Austrian Association of Molecular Life Sciences and Biotechnology (ÖGMBT): Poster presentation Puch by Salzburg / Austria
02/2008	*„Diabetes mellitus – Pathophysiology and Pharmacotherapy”* Advanced education for state qualified nurses Health and Advice Centre – Sulz am Neckar / Germany
02/2007	*„An Introduction to Emergency Medicine and Basic Life Support“* Advanced education for state qualified nurses Health and Advice Centre – Sulz am Neckar / Germany

Congresses and Workshops

09/2012	16th Congress of the International Society for Burn Injuries (ISBI) Edinburgh / Scotland
10/2010	48th Annual Meeting of the Austrian Society of Plastic, Reconstructive and Aesthetic Surgery Graz / Austria
05/2010	81st Annual Meeting of the German Society of Otorhinolaryngology, Head and Neck Surgery Wiesbaden / Germany
09/2007	Training of surgical stitches, "pig-foot workshop" by Tyco-Healthcare Kaiserin-Elisabeth-Hospital Vienna / Austria
06/2007	48th Annual Meeting of the Austrian Society of Surgery Graz / Austria

Community service

09/2004 – 05/2005	German Red Cross in Tübingen / Germany Area of responsibility: ambulance officer

Personnel skills and competences

Languages	German	Native tongue	French	Good
	English	Business fluent	Latin	Basic knowledge

IT-Skills	Office applications: Microsoft Office, Open Office Microsoft and Macintosh operating systems Medical and scientific data bases like PUBMED Scientific applications: ChemBioDraw, Motic Images Advanced, Leica Application Suite
Driving license	Class B
Hobbies	Sport: Running, swimming (DLRG – live saving badge in silver), snowboarding Sailing: Austrian Sailing Federation – Yacht master license A and FB2